



Vaasan yliopisto
UNIVERSITY OF VAASA

Roope Arikka

**Evaluation of the Impact of Hybrid Solar Modules
on Energy Production and Economic Viability in
Finnish Industrial-Level Power Plants**

School of Technology and Innovations
Master's thesis in Smart Grids
Master Programme in Smart Energy

Vaasa 2024

UNIVERSITY OF VAASA
School of Technology and Innovations

Author: Roope Arikka
Title of the Thesis: Evaluation of the Impact of Hybrid Solar Modules on Energy Production and Economic Viability in Finnish Industrial-Level Power Plants
Degree: Master of Science in Technology
Program: Smart Energy
Supervisor: Anne Mäkiranta
Instructor: Birgitta Martinkauppi & Julius Vilppo
Year: 2024 **Pages:** 113

ABSTRACT:

This master's thesis presents an evaluation of photovoltaic-thermal (PVT) technology and its applicability in the Finnish energy sector. PVT technology, which combines photovoltaic and thermal systems, offers the potential to improve the efficiency of solar modules by cooling the solar cells and generating thermal energy concurrently. The research, conducted in collaboration with Sweco Finland Oy, aims to enhance the understanding of PVT modules' feasibility and their role in the transition to renewable energy.

The thesis is divided into a theoretical framework, which provides a background on the principles of PV cells and solar collectors, and a methodological framework, which involves the development of a simulation model for an industrial-scale PVT power plant. The study investigates the performance of PVT modules in Finland's climate, with a focus on the technical and economic viability of such systems.

The findings from the simulation model, applied to a typical Finnish location, suggest that PVT systems can produce slightly more electrical energy annually than comparable PV systems and have the potential to produce significant thermal energy. However, the economic analysis indicates that the cost of both electrical and thermal energy from PVT systems is currently higher than conventional energy sources in Finland, highlighting the need for substantial investment support or higher tariffs for the energy produced to make PVT technology economically viable.

The study also discusses the challenges associated with PVT systems, such as the need for continuous use of the thermal energy to prevent stagnation, the potential for more significant power degradation due to environmental conditions, and the limitations imposed by regional temperature thresholds. Despite these challenges, PVT technology demonstrates the capability of producing more energy per unit area compared to conventional PV systems. The thesis concludes that while PVT systems show promise for higher-efficiency solar energy conversion, their economic and practical implementation in Finland will require careful consideration of local conditions, additional optimizations, and possibly financial incentives to become competitive with existing energy production methods.

KEYWORDS: Hybrid Solar Modules, Energy Production, Economic Viability, PVT, Renewable Energy, Efficiency

VAASAN YLIOPISTO**Tekniikan ja innovaatiojohtamisen akateeminen yksikkö**

Tekijä:	Roope Arikka
Tutkielman nimi:	Hybridiaurinkomodulien vaikutuksen arviointi energiantuotantoon ja taloudelliseen kannattavuuteen teollisen mittakaavan aurinkovoimalaitoksissa Suomessa
Tutkinto:	Diplomi-insinööri
Oppiaine:	Sähkötekniikka
Työn valvoja:	Anne Mäkiranta
Työn ohjaaja:	Birgitta Martinkauppi & Julius Vilppo
Valmistumisvuosi:	2024 Sivumäärä: 113

TIIVISTELMÄ:

Tämä diplomityö käsittelee hybridiaurinkoenergia (PVT) teknologian soveltuvuutta Suomen energiasektorille. PVT-teknologiaan perustuvat moduulit yhdistävät yleisesti käytössä olevan valosähköisen (PV) moduulin ja lämpöä tuottavan aurinkokeräimen ominaisuudet. PVT hybridimoduulit tarjoavat mahdollisuuden parantaa aurinkoenergiomodulien tehokkuutta jäähdyttämällä aurinkokennoja ja tuottamalla samanaikaisesti lämpöenergiaa. Tutkimus, joka toteutettiin yhteistyössä Sweco Finland Oy:n kanssa, pyrkii parantamaan ymmärrystä PVT-modulien toteuttavuudesta ja niiden roolista uusiutuvan energian siirtymässä.

Diplomityö jakautuu teoreettiseen viitekehykseen, joka tarjoaa taustatietoa PV-kennojen periaatteista ja aurinkokeräimistä, sekä metodologiseen viitekehykseen, joka sisältää teollisen mittakaavan PVT-voimalaitoksen simulaatiomallin kehittämisen. Tutkimus käsittelee PVT-modulien suorituskykyä Suomen ilmastossa, keskittyen kyseisten järjestelmien tekniseen ja taloudelliseen toteutettavuuteen.

Simulaation tulokset viittaavat siihen, että PVT-järjestelmät voivat tuottaa marginaalisesti enemmän sähköenergiaa vuosittain verrattuna vastaaviin PV-järjestelmiin ja niillä on potentiaalia tuottaa merkittävästi lämpöenergiaa. Taloudellinen analyysi kuitenkin osoittaa, että PVT-järjestelmien sähkö- ja lämpöenergian kustannukset ovat tällä hetkellä korkeammat kuin perinteisillä energialähteillä Suomessa, mikä korostaa tarvetta merkittäväälle investointituelle tai korkeammille energiantuotantotariffeille PVT-teknologian taloudellisen kannattavuuden saavuttamiseksi.

Tutkimus käsittelee myös PVT-järjestelmien haasteita, kuten tarvetta lämpöenergian jatkuvalle käytölle stagnaation ehkäisemiseksi, suuremman tehoaleneman mahdollisuutta ympäristöolosuhteiden takia ja alueellisten lämpötilaerojen asettamia rajoituksia. Huolimatta näistä haasteista, PVT-teknologia osoittaa kykyä tuottaa enemmän energiaa yksikköpinta-alaa kohden verrattuna perinteisiin PV-järjestelmiin. Johtopäätöksissä todetaan, että vaikka PVT-järjestelmillä on lupaavia näyttöjä korkean tehokkuuden saavuttamiseksi aurinkoenergian muuntamisessa, niiden taloudellinen ja käytännön toteutus Suomessa vaatii huolellista harkintaa huomioiden paikalliset olosuhteet, lisäoptimoinnit ja mahdolliset taloudelliset kannustimet kilpailukyvyyn saavuttamiseksi.

AVAINSANAT: hybridi aurinkomodulit, energiantuotanto, taloudellinen kannattavuus, uusiutuva energia, hyötysuhde

Contents

Preface	9
1 Introduction	10
1.1 Background	11
1.2 Research Objective	12
1.3 Scope of Study	12
1.4 Structure of Thesis	13
2 Theoretical Framework	15
2.1 Basic Principle of PV Cell and Module	15
2.1.1 Efficiency of PV Cell and Module	16
2.1.2 Temperature's Effect on the PV Cell and Module Efficiency	20
2.2 Thermal Collector Operation Principle and Efficiency	22
2.2.1 Operational Temperature of the Thermal Collectors	23
2.2.2 Energy Conversion Efficiency of the Thermal Collectors	23
2.3 Hybrid Solar Modules	27
2.3.1 Liquid-Circulating Hybrid Solar Module	28
2.3.2 Air-Circulating Hybrid Solar Module	41
2.3.3 Evacuated Hybrid Solar Module	43
2.4 Technical Characteristics of Various Hybrid Modules	44
2.5 Examination of Existing PVT Power System Operations	46
2.5.1 PVT Power System Case 1	47
2.5.2 PVT Power System Case 2	48
3 Methodological Framework	51
3.1 Simulation of PVT Power Plant	51
3.1.1 Simulation of PVT Power Plant at the Location 1	53
3.1.2 Simulation of PVT Power Plant at the Location 2	56
3.1.3 Simulation of PVT Power Plant at the Location 3	58
3.2 Simulation of PV Power Plant	59
3.2.1 Simulation of PV Power Plant at the Location 1	60
3.2.2 Simulation of PV Power Plant at the Location 2	61

3.2.3	Simulation of PV Power Plant at the Location 3	62
4	Review and Analysis of Technical Results	63
4.1	General Review and Evaluation of Simulation Results	63
4.2	Evaluation and Validation of the Reliability of Simulation Results	65
5	Economic Review and Analysis	68
5.1	PV Power Plants LCOE Analysis	72
5.2	PVT Power Plants LCOE Analysis	74
5.3	Comparison of the Analysis Results	80
6	Discussion	83
7	Conclusions	86
7.1	Theoretical Section Findings and Conclusions	86
7.2	Methodological Section Findings and Conclusions	87
8	Summary	89
	References	91
	Appendices	110
	Appendix 1. PV Simulation Model	110
	Appendix 2. PVT Simulation Model	111
	Appendix 3. PVT Simulation Electrical Power Test Results	112
	Appendix 4. PVT Simulation Thermal Power and Quantities Test Results	113

Figures

Figure 1. Solar cell double diode equivalent circuit model.	17
Figure 2. Temperature effect on the c-Si solar cell's current-voltage and power-voltage graphs.	21
Figure 3. Structure of the conventional liquid-circulating PVT module.	29
Figure 4. Multiple PVT module thermal flow channel designs: a) serial, b) parallel, c) web, d) spiral, e) combined parallel-serial, and f) bionic.	30
Figure 5. The schematics double serpentine channel absorbers.	31
Figure 6. Different fluid channel patterns of PVT module.	32
Figure 7. Thermographic study of PVT and PV modules.	33
Figure 8. Electrical efficiency of PVT system with different cooling medium.	34
Figure 9. Electrical efficiency of PVT system with different cooling medium.	35
Figure 10. Comparison of electrical, thermal and hybrid efficiencies of PV module and PVT-PCM.	36
Figure 11. PVT power plant electrical parameters simulation results at location 1.	55
Figure 12. PVT power plant thermal parameters simulation results at location 1.	56
Figure 13. PVT power plant electrical parameters simulation results at location 2.	57
Figure 14. PVT power plant thermal parameters simulation results at location 2.	57
Figure 15. PVT power plant electrical parameters simulation results at location 3.	58
Figure 16. PVT power plant thermal parameters simulation results at location 3.	59
Figure 17. PV power plant simulation results at location 1.	61
Figure 18. PV power plant simulation results at location 2.	62
Figure 19. PV power plant simulation results at location 3.	62
Figure 20. Simulated PV power plant annual energy output at different locations.	63
Figure 21. Simulated PVT power plant annual energy output at different locations.	64
Figure 22. Cost components of large-scale PV installations.	69
Figure 23. PVT & PV module power degradation over time.	71
Figure 24. Energy output of simulated PV power plants over a life cycle period.	73
Figure 25. LCOE of simulated PV power plants.	74
Figure 26. Energy output of the simulated PVT power plant at location 1 over a life cycle period.	75
Figure 27. Energy output of the simulated PVT power plant at location 2 over a life cycle period.	76
Figure 28. Energy output of the simulated PVT power plant at location 3 over a life cycle period.	77
Figure 29. Electrical energy based LCOE of simulated PVT power plants.	77
Figure 30. Thermal energy based LCOE of simulated PVT power plants.	78
Figure 31. Total energy based LCOE of simulated PVT power plants.	79
Figure 32. Comparison of simulated PVT & PV power plant LCOE based on electrical energy.	80
Figure 33. Comparison of simulated PVT & PV power plant LCOE based on total energy.	81

Tables

Table 1. Liquid-circulating PVT modules characteristics.	39
Table 2. Air-Circulating PVT modules characteristics.	42
Table 3. Evacuated PVT module characteristics.	44
Table 4. PVT modules characteristics comparison.	45

Nomenclature

A	area
Amt	amount
a-Si	amorphous silicon
BOS	balance of system
CAPEX	capital expenditures
C_p	specific heat capacity
c-Si	crystalline silicon
D	solar irradiation
DIM	dimension
EFPC	evacuated flat plate collector
EG	ethylene glycol
EG-PW	ethylene glycol-pure water
EG-PW	ethylene glycol-pure water mixture
EROI	energy return on investment
FF	fill factor
FPC	flat plate collectors
FPSAC	flat plate solar air collector
G	irradiance
I	terminal current
I'_{sc}	ideal current source
I_d	saturation current
I_{mpp}	current at maximum power point
I_{ph}	photo-current
I_{sc}	short-circuit current
k	Boltzmann's constant
K_1	temperature coefficient
kWh	kilowatt-hour
kWp	kilowatt-peak
LCOE	levelized costs of energy
LeTID	light and elevated temperature induced degradation
MCLT	minority carrier lifetime
MJ	multi-junction

MMP	maximum power point
MW	megawatt
MW _e	megawatt electrical
MWh	megawatt-hour
NOCT	nominal operating cell temperature
N_s	quantity of PV cells connected in series
OPEX	operating expenses
PCM	phase change material
PERC	passivated emitter and rear solar cells
p-n	positive-negative
PSC	perovskite solar cells
PV	photovoltaic
PVT	photovoltaic thermal
PW	pure water
PWh	petawatt-hour
P_{MPP}	power in maximum power point
P_{max}	maximum power
q	electron charge
Re	Reynolds number
R_S	series resistance
R_{Sh}	shunt resistance
SA	surface area
Sh	sunlight duration
STC	standard test conditions
T	temperature
TE	thermal energy
T_r	reference value of solar cell temperature
V	terminal voltage
VAT	value-added tax
V_{mpp}	voltage at maximum power point
V_{oc}	open-circuit voltage
V_t	thermal voltage
Wt	weight
η	efficiency

Preface

First and foremost, I would like to express my deepest gratitude to Sweco Finland Oy for providing me with the opportunity to carry out my master's thesis as a commission for their esteemed company. The support and resources offered by Sweco have been invaluable throughout this journey, and I am truly appreciative of the trust they have placed in me to contribute to their body of work.

I would also like to extend my heartfelt thanks to my company supervisor, whose guidance and expertise have been instrumental in shaping this thesis. Your dedication and commitment to excellence have not only aided in the completion of this work but have also enriched my learning experience.

My sincere appreciation goes to the University of Vaasa, particularly the School of Technology and Innovations, for their exceptional guidance and the educational foundation they have provided. The knowledge and skills I have acquired during my studies have been crucial in the preparation and execution of this research.

To my family, friends, and all my loved ones, I am eternally grateful for your unwavering support, encouragement, and the countless discussions we have had about the subject matter and the challenges encountered during my research. Your presence and belief in my abilities have been a source of strength and motivation.

Lastly, I would like to extend a special thank you to Sweco Belgium for their comprehensive economic study on PVT modules and for granting me permission to utilize their research findings. Your contribution has significantly enhanced the quality and depth of my thesis.

Thank you all for being a part of this academic endeavor. Your collective support has been the cornerstone of my success.

1 Introduction

The global demand for energy on Earth has increased nearly linearly since the 20th century (Ahmad & Zhang, 2020). Although scenario studies indicate that, compared to past trends, the overall global energy consumption is projected to increase more moderately in the coming decades, the share of electrical energy in final consumption is expected to continue growing (Kober, et al., 2020). The initial worldwide assessment acknowledges scientific findings suggesting a necessary 43 % reduction in global greenhouse gas emissions by 2030, relative to 2019 levels, to constrain global warming to 1.5 °C. This recognition took place during the conference of the parties held in the United Arab Emirates in 2023. The assessment urges participating nations to pursue measures aimed at tripling global renewable energy capacity and doubling advancements in energy efficiency by the year 2030 (United Nations, 2023).

Apart from nuclear fission energy, almost all energy consumed by humans originates from the sun, making solar energy a vital renewable energy source (Corkish, et al., 2016, pp. 1-29). The total amount of solar energy that reaches the Earth and can potentially be captured globally ranges from 4 375 to 13 843 PWh per year (Belyakov, 2019, pp. 417-438). In 2022, the estimated global primary energy consumption was approximately 167 788 TWh (U.S. Energy Information Administration, 2023). In theory, solar energy has the potential to meet the entire world's energy demand if the necessary technology were widely and readily available (Kabir, et al., 2018). However, it is quite unlikely that the global energy demand could practically be met solely through solar energy, primarily because there is significant variety and uncertainty in the energy output, which is constrained by natural circumstances (Zongxiang, et al., 2024). A less unrealistic estimation would consider the possibility of the solar energy sector rising to the position of the second most important production source globally over the next three decades. This scenario requires strategical support and implementation of the establishment of new solar power plants, battery energy storage systems to offer a consistent and trustworthy power source for electricity at night or on overcast days, and thermal energy storage systems for seasonal storage purposes (Maka & Chaudhary, 2024; Ma et al., 2024;

Pourasl, et al., 2023). Estimates indicate that such a development could theoretically enable approximately 25 % of the world's electricity demand to be generated by solar power by the year 2050 (Pourasl, et al., 2023).

Photovoltaic (PV), solar thermal collectors, and photovoltaic-thermal (PVT) are examples of common solar energy technologies (Gorjian, et al., 2021). PV modules that generate electricity through the use of photovoltaic effect phenomena are generally inefficient both in test conditions and in real-world applications. For instance, a monocrystalline PV module's laboratory efficiency is usually approximately 24 %, but its real-world efficiency is only about 11 % (Peng, et al., 2017). Shadow, air pollution and dust, varying radiation intensity, spectral variability, among other atmospheric conditions, and the temperature of solar cells are typically acknowledged as significant factors affecting the performance of PV modules (Venkateswari & Sreejith, 2019; Al-Dousari, et al., 2019; Paudyal & Imenes, 2021). Research and development focused on improving the efficiency of PV modules by cooling the cells and harnessing the waste heat have contributed to the advancement of a novel technique known as PVT technology. In PVT systems, both electricity and heat can be generated simultaneously (Paudyal & Imenes, 2021).

The aim of this master's thesis is to analyze the utilization of hybrid solar modules, or in other words PVT modules, in industrial-scale solar power plants under Finnish conditions, considering both technical and economic perspectives. The study is conducted as qualitative research, incorporating existing research knowledge on the topic, and utilizing a simulation model-based assessment of the plants' production potential in the climatic conditions of Finland.

1.1 Background

This master's thesis has been conducted as a commission for Sweco Finland Oy, a subsidiary of the international Sweco AB corporation. Sweco is a globally listed engineering consulting company, specializing in areas such as consulting engineering, environmental

technology, and architecture. The company employs around 21 000 professionals from various fields and has offices in at least 15 different countries (Sweco AB, 2024).

1.2 Research Objective

One of the primary objectives of the study is to provide a thorough and pertinent theoretical overview of hybrid solar modules, with a specific focus on PVT modules, from a technological standpoint. A second objective is to develop a simulation model for an industrial-scale solar power plant comprised of PVT modules. In this context, the term 'industrial-scale solar power plant' refers to facilities with a capacity of 1 megawatt (MW) and over. The research aims to undertake a techno-economic analysis, leveraging both existing research findings and simulation results, with the goal of assessing the viability of deploying an industrial-scale solar power plant incorporating PVT modules.

The research objectives specified by the company are as follows: improving the company's understanding of the feasibility of hybrid solar modules as a part of the green transition. The goal is to determine a reasonable benefit that will allow the use of research findings in project sales efforts and, eventually, new design commissions. Another objective is to create a simulation model, which can be prospectively utilized in the design of solar power plants and the assessment of their profitability.

1.3 Scope of Study

In literature and research, the term commonly used is 'PVT collector.' In this study, the term 'PVT module' has been chosen, which refers to the same technical solution. In the research, the term 'hybrid solar module' specifically refers to the flat plate PVT module. The research is limited to focus on flat plate PVT modules, excluding solutions that concentrate solar radiation, for example. The theoretical part of the study addresses and compares both air-circulating and liquid-circulating PVT modules. However, the

simulation section of the research specifically examines modules based on liquid-circulating PVT technology. The study concentrates on PVT modules composed of crystalline silicon (c-Si) and multi-junction (MJ) cells, including passivated emitter and rear solar cells (PERC).

The research focuses on examining the electrical properties of PVT modules and their differences compared to conventional PV technology. The study briefly touches upon factors affecting the productivity and efficiency of a power plant consisting of PVT modules, such as the topology of the solar power plant and losses due to power electronics. However, in-depth analysis of these aspects is beyond the scope of the research. The study also addresses the heat production characteristics of PVT modules, but the examination of technical solutions related to heat transfer, utilization, and storage is excluded from this research.

The most current academic publications on the topic serve as the research's primary sources. The primary sources are scientific articles and conference proceedings; pertinent standards related to the subject matter are also acknowledged.

1.4 Structure of Thesis

The study is divided into two parts: the theoretical framework and the methodological framework. The theoretical section of the thesis begins by examining the impact of temperature on the efficiency of a solar cell. Subsequently, the operation of traditional solar collectors is discussed, followed by an exploration of the technical characteristics of hybrid solar modules, encompassing both liquid-circulating and air-circulating modules, as well as evacuated hybrid modules. The last section of the theoretical framework examines two different case studies in which PVT modules are used in power plants or in which specific modules function in practical applications.

The second section of the thesis comprises the methodological framework, where the simulation model for a power plant consisting of PVT modules, and the model's functionality are examined. This is followed by an examination of the simulation model of a power plant consisting of conventional PV modules. The next step involves scrutinizing and comparing the results obtained from both simulation models from a technical perspective. In the last chapter of the methodological section, the production of simulated power plants is analyzed from an economic standpoint. The discussion chapter follows at the end of the thesis, after which the results of the research are summarized, and conclusions are drawn on the topic.

2 Theoretical Framework

This chapter provides an overview of the theoretical framework for the study. Initially, the basic operational principles of c-Si solar cells, and c-Si PV modules, as well as factors affecting efficiency, are discussed. A primary focus is placed on the impact of temperature on the efficiency of solar cells. The goal is to answer the questions of why and how temperature influences the efficiency of both solar cells and solar modules. Subsequently, the operational principles of solar collectors are examined. In the theoretical section, the principles of solar cells and solar collectors are specifically addressed separately, because the structure and operation of hybrid modules, namely PVT modules, are deeply based on the physical laws governing these components (Ramos, et al., 2019). Following this, the study moves on to discuss the operational principles, structure, and differences of PVT modules utilizing various technologies. In the final section of the theoretical part, the operation and output of existing PVT modules and power plants composed of PVT modules are examined.

2.1 Basic Principle of PV Cell and Module

The process of converting solar electromagnetic radiation into electrical energy relies heavily on solar cells. Semiconductor materials are the most typical material for solar cells (Soga, 2006). A wide variety of materials and their compounds can be used in the production of solar cells, but one of the most often used materials is technology based on c-Si wafers (Lunardi, et al., 2018).

The conversion of solar energy into electrical energy in solar cells can be divided into two stages. In the first stage, the absorption of energy carried in the form of electromagnetic radiation caused by motion of photons, commonly referred to as light, generates an electron-hole pair (Markvart & Castañer, 2003; Saleh, et al., 2018). This is followed by the separation of the electron and hole by the device's structure; electrons are directed to the negative terminal and holes to the positive terminal, in other words, the

semiconductor diode separates and collects the charge carriers between different structural parts of the cell and directs the resulting electrical current in a specific direction (Markvart & Castañer, 2003; Gray, 2011, p. 82). To reflect this, a perfect solar cell is said to function similarly to a current source that is connected in parallel to a diode (Pindado, et al., 2014).

2.1.1 Efficiency of PV Cell and Module

The electrical characteristics of a simplified ideal solar cell can be represented using a circuit model where a current source is connected in parallel with a forward-biased diode, as well as with resistors that are connected both in series and in parallel (Pindado, et al., 2014). For modelling solar cells, single-diode and double-diode models are commonly used. The double-diode equivalent circuit has a more complex structure and exhibits more nonlinear characteristics than the single-diode equivalent circuit. Single-diode models are more commonly used because they achieve the required accuracy while also being sufficiently simple to implement (Yağın, et al., 2018). Instead of using the single-diode model, the double-diode model can yield more accurate results because it considers factors such as temperature and variations in solar radiation that can affect the energy gap, sub-cell parameters, and the double-diode dark intensities currents for both diodes (Hamed, et al., 2022). Figure 1 illustrates the double-diode equivalent circuit model of a solar cell, which consists of a current source with two diodes connected in parallel, alongside a resistor connected in parallel with them, and another resistor connected in series with these components.

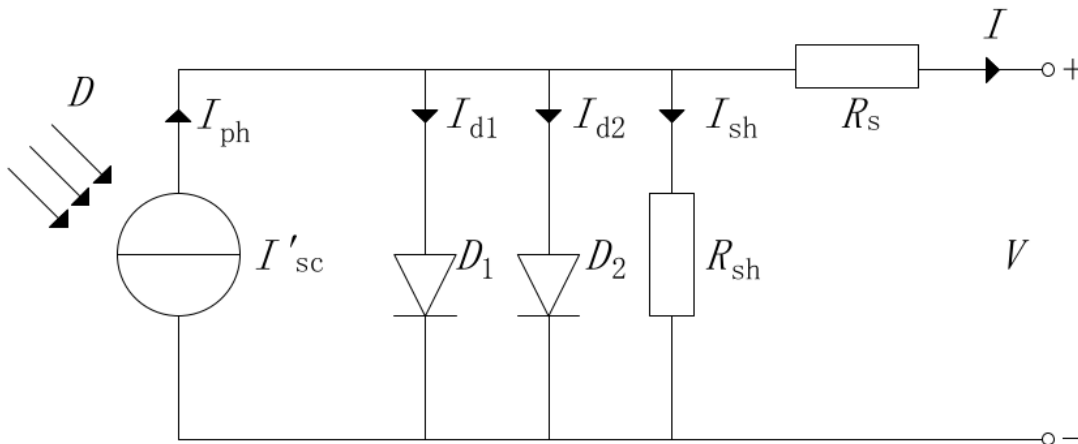


Figure 1. Solar cell double diode equivalent circuit model (adapted from Gray, 2011, p. 120; El-Ahmar, et al., 2016).

In the Figure 1, the ideal current source I'_{sc} represents the solar cell short circuit current in nominal operation conditions when parasitic resistance of the cell does not affect the operation of the circuit (Gray, 2011, p. 120). R_s is the series resistance of the cell, shunt resistance is represented by R_{sh} , and the intensity of the incident light (solar irradiation) is represented by D (El-Ahmar, et al., 2016). It should be noted that for the purpose of streamlining the analysis, the resistance values are sometimes omitted, as the R_{sh} is characteristically high and the R_s is correspondingly low. This simplification is commonly applied within the context of employing a single-diode circuit model (Zainal, et al., 2016). In the circuit model, I_{d1} and I_{d2} are the saturation currents resulting from the diffusion mechanism and the charge region of space (Abbassi, et al., 2022). Diodes D_1 and D_2 represent the diffusions and recombination at the positive and negative interfaces of the solar cell's p-n junction (Navarro, et al., 2023; Mintairov, et al., 2024). The voltage reduction that happens in the transfer resistances, primarily due to the increase in temperature of the solar cell's contacts, is represented by R_s in the electrical circuit model. The influence of both the shunt resistance across the solar cell's surface and the leakage current at the diode's p-n junction interface is represented by the shunt resistance R_{sh} .

(Nguyen-Duc, et al., 2020). In the circuit model, I represents the actual terminal current of the solar cell, and V represents the terminal voltage of the cell. In the circuit model, the photo-current I_{ph} produced by the solar cell is primarily dependent on the solar radiation intensity G and the cell temperature, according to Eq. 1 (El-Ahmar, et al., 2016):

$$I_{ph} = \{I'_{sc} + K_1(T - T_r)\} \frac{G}{1000}, \quad (1)$$

where I'_{sc} represents solar cell short circuit current in nominal operation conditions, K_1 is temperature coefficient constant of the solar cell short circuit current, T is the real temperature value, T_r is the reference value of the cell temperature, and G is irradiation value (El-Ahmar, et al., 2016). Based on Kirchhoff's first law, the terminal current I of the solar cell circuit model depicted in Figure 1 can be expressed as follows (Abbassi, et al., 2022):

$$\begin{aligned} I &= I_{ph} - I_{d1} - I_{d2} - I_{sh} \\ &= I_{ph} - I_{01} \left(\exp\left(\frac{V+R_s I}{a_1 V_t}\right) - 1 \right) - I_{02} \left(\exp\left(\frac{V+R_s I}{a_2 V_t}\right) - 1 \right) - \frac{V+R_s I}{R_{sh}}, \end{aligned} \quad (2)$$

where I_{01} and I_{02} represents saturation current of the solar cell. Parameters a_1 and a_2 are the ideal factors that determine the characteristics of diffusion and recombination currents of the solar cell (Abbassi, et al., 2022). The parameter V_t is the thermal voltage of the diode, and it can define as follows (Sharma, 2014):

$$V_t = \frac{N_s \cdot k \cdot T}{q}, \quad (3)$$

where N_s specifies the quantity of PV cells connected in series, k is the Boltzmann's constant ($1.38 \cdot 10^{-23} \text{ J K}^{-1}$), and q means an electron charge, which is around ($1.60 \cdot 10^{-19} \text{ C}$) (Ocaya, 2006). Upon examining Eqs. 1-3, it can be observed that with constant radiation intensity, cell's temperature T has a significant effect on the solar cell's terminal current I and, consequently, also on the cell's terminal voltage V .

Solar cell manufacturers provide three main electrical characteristics that allow for the examination of the solar cell's efficiency, as well as the temperature dependence of the efficiency. These parameters are the cell's open-circuit voltage V_{oc} , the cell short-circuit current I_{sc} , and the maximum power point (MPP) P_{max} (Abbassi, et al., 2022; Nieto, et al., 2024). With the parameters, the efficiency η of the solar cell can be expressed as follows (Nieto, et al., 2024):

$$\eta = \frac{I_{sc} \cdot V_{oc} \cdot FF}{G \cdot A}, \quad (4)$$

where A is the cell area, G is the irradiance onto the cell, and FF is the fill factor. This can be represented as (Markvart & Castañer, 2003):

$$FF = \frac{P_{max}}{I_{sc} \cdot V_{oc}} = \frac{I_{mpp} \cdot V_{mpp}}{I_{sc} \cdot V_{oc}}, \quad (5)$$

where P_{max} represent MPP of the cell which is the product of current I_{mpp} and voltage V_{mpp} at the MPP, I_{sc} is the short-circuit current and V_{oc} is the open-circuit voltage of the cell. Besides the factors already cited, the inferior performance of solar cells can also be attributed to a low minority carrier lifetime (MCLT) value. Dangling bonds, which can serve as defects on the wafer's surface particularly in c-Si solar cells, contribute to a reduction in the MCLT value via a defect-assisted recombination process. Furthermore, the MCLT is compromised by process-induced imperfections on the wafer surface, including dislocations, chemical residues, and metal contaminations (Jang, et al., 2024). To address these challenges, one strategy involves the use of the passivated emitter and rear contact (PERC) cell technology, which diminishes recombination at the cell's rear side by introducing a patterned dielectric layer between the silicon substrate and the aluminum back contact. This configuration ensures that the aluminum contacts only a minimal portion of the cell area, thereby enhancing overall cell efficiency (Benda, 2018). PERC solar cells have become predominant within the PV market, leading to considerable research efforts aimed at enhancing their power conversion efficiency and further minimizing the

costs associated with productions (Jang, et al., 2024). Consequently, the PERC cell is progressively emerging as the most economically viable option for the large-scale manufacturing of c-Si solar cells (Huang, et al., 2017).

Research indicates that within a PV module, an estimated 60 % of the incident solar energy is consumed during the generation of charge carriers. The residual energy is further lost through processes such as charge carrier transport, recombination, and during the conversion from individual cells to the collective module structure. As a result, approximately 70 % of the solar irradiance is transformed into thermal energy, which results in an increase in the temperature of the cells. In addition, almost 12 % of solar energy is not harnessed due to multilayer reflection. Further research has established that an escalation in temperature of the solar cells and module correlates with a decrease in energy conversion efficiency, predominantly attributable to augmented recombination losses within the PV cell. This underscores the critical importance of understanding the optoelectronic and transport properties of semiconductors in the development and fabrication of high-efficiency PV cells and modules (Shen, et al., 2020; Segev, et al., 2018).

2.1.2 Temperature's Effect on the PV Cell and Module Efficiency

Companies that manufacture PV modules typically specify the MPP of solar cells and modules under hypothetical operating conditions, which means standard test conditions (STC) or the nominal operating cell temperature (NOCT) (Odeh, 2018; Sun, et al., 2020). International Electrotechnical Commission (IEC) defines properties for STC as follows: Solar cell temperature during test is 25 °C, irradiance level is 1 000 W·m⁻², and air mass (AM) 1.5 global (G) spectrum (International Electrotechnical Commission IEC, 2016). A bit closer to the actual usage conditions of solar panels, the NOCT conditions are defined as follows: irradiance on cell surface is 800 W·m⁻², air temperature is 20 °C, wind velocity is 1 m/s, and mounting should be open on the back side (International Electrotechnical Commission IEC, 2022).

In a real operating environment, when the radiation intensity is at its highest, the operating temperature of the PV module can rise to 70 °C, especially in warm countries where the ambient temperature can also be high (Sun, et al., 2020, p. 1029). In actual operation, when the temperature of the solar cell is significantly higher than the conditions defined by STC or NOCT the MPP, and consequently the efficiency of the solar cells and solar modules are also significantly lower. Figure 2 illustrates the characteristics of the c-Si solar cell's current-voltage and power-voltage with constant radiation intensity level ($515 \text{ W} \cdot \text{m}^{-2}$) and with varied cell temperature (Chander, et al., 2015).

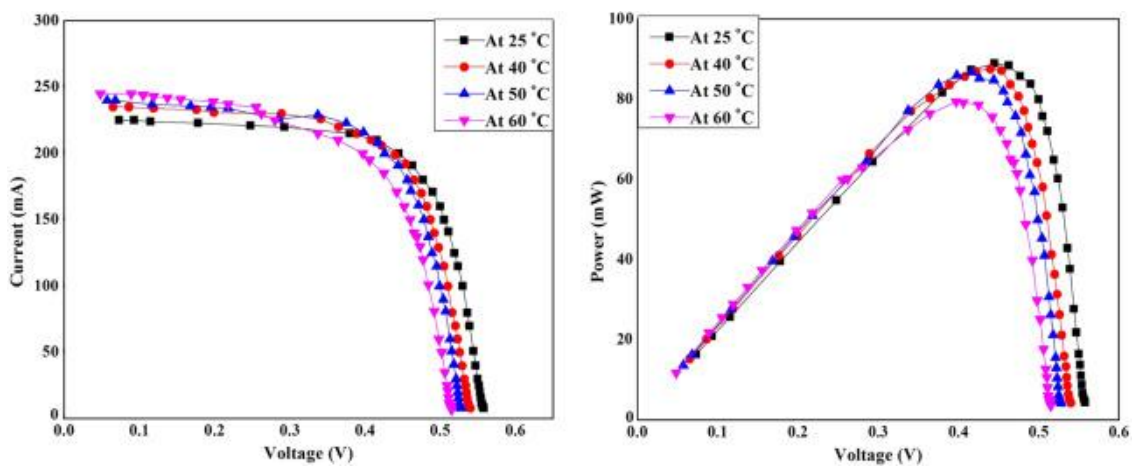


Figure 2. Temperature effect on the c-Si solar cell's current-voltage and power-voltage graphs (Chander, et al., 2015).

Figure 2 shows that at a solar cell temperature of 60 °C, as opposed to 25 °C, the cell's MPP is considerably lower. PV modules are composed of several connected solar cells, the MPP of the module decreases as the MPP of an individual cell does, mostly caused by the ascending series resistance of the connections between cells with temperature (Bounouar, et al., 2020).

The temperature coefficient, which varies with the different types of solar cell technologies used in modules, determines the output reduction caused by temperature. PV manufacturing companies usually provide values for the voltage temperature coefficient, the current temperature coefficient, and the power temperature coefficient. One study

shows that the measured average temperature coefficient of power for typical poly-c-Si and mono-c-Si-based PV modules ranges from $-0.387\%/^{\circ}\text{C}$ to $-0.446\%/^{\circ}\text{C}$ (Dash & Gupta, 2015). In other words, this means that when the temperature of a solar cell increases by 1°C , the power output of PV modules reduces by $0.387\text{--}0.446\%$. The average efficiency of commercial PV modules ranges from 17% to 20% (Centre for Sustainable Systems, University of Michigan, 2023). For example, if the PV module energy conversion efficiency at a temperature of 25°C is 20% and the operation temperature of the module increases to 60°C , the energy conversion efficiency would decrease to 16.88% .

According to studies, a single-junction c-Si solar cell may achieve a maximum efficiency of 33.3% at room temperature (26.85°C), and the efficiency can be optimized up to 48.48% by cooling, or to 40% by increasing the optical concentration (Alharbi & Kais, 2015). Currently available single-junction c-Si solar cells have a maximum efficiency of about 26% at STC (Ouédraogo, et al., 2021). Nevertheless, as already mentioned in the introductory section, the practical efficiency of solar cells and the whole PV module can be up to half of what the efficiency is under laboratory conditions. Solar cells can be cooled to retain an efficiency that is comparable to that of a laboratory or, in the best scenario, to reach even greater efficiency levels.

2.2 Thermal Collector Operation Principle and Efficiency

In this subchapter basic principles and features of solar thermal collectors, particularly variety of flat plate collectors (FPC) are reviewed. FPC can be classified as a non-concentrating solar thermal collector technology (Summ, et al., 2024). A solar thermal energy collector, such as the FPC, is a device of which the basic principle involves the conversion of solar radiation energy into thermal energy through a medium, which is typically a liquid such as water or a glycol-water mixture (Karki, et al., 2019). Besides using water or a water-based mixture as a heat transfer carrier, a thermal collector can also employ air or oil to serve as the internal energy transport medium (Rosen & Farsi, 2022). In addition to the traditional low-pressure liquid-based technology, FPC modules can also utilize

technology based on vacuum tubes, those solar collectors are known as the evacuated flat plate collector (EFPC) (Carrión-Chamba, et al., 2022). Apart from the two previously described technologies, there is a third technology. This third technology involves the transfer of thermal energy with air as a medium, and this type of technology is defined as a flat plate solar air collector (FPSAC) (Zhang & Zhu, 2022).

2.2.1 Operational Temperature of the Thermal Collectors

Collectors operating with non-concentrating technologies, such as the FPC, typically have a higher efficiency at low operational temperatures (30 – 80 °C) (Rosales-Pérez, et al., 2024; Karki, et al., 2019). In particular, the heat loss coefficients of the FPC based on low-pressure liquid-circulation technology increase with rising temperature, which significantly reduces their efficiency as the operational temperature exceeds medium levels (more than 100 °C) (Rosales-Pérez, et al., 2024). On the contrary, the EFPC may function very effectively at medium temperatures (100 – 200 °C) (Bellos & Tzivanidis, 2023). Compared to liquid-based thermal collectors, the FPSACs are less widespread. The fact that air has a lower thermal capacity than water is one of the causes (Charvat, et al., 2012). However, the development and study of FPSACs has always aimed for high efficiency, minimal heat loss, and a simple structure, and ultimately cheaper investment and operating costs (Zhang & Zhu, 2022).

2.2.2 Energy Conversion Efficiency of the Thermal Collectors

Efficiency of solar collectors, which typically refers to the thermal efficiency of the collector, means the amount of radiant energy received by the collector surface area in relation to the amount of usable thermal energy it produces (Kalogirou, 2009). The energy conversion efficiency of flat-plate solar collectors is strongly dependent on the collector's optical properties and thermal losses. The thermal losses of the collectors result from conduction, convection, and radiation heat transfer processes to the surroundings. In

addition to these factors, the conversion efficiency also depends on the local radiation conditions (Rodríguez-Hidalgo, et al., 2011). Research also indicates that the specific heat capacity and heat transfer capabilities of the working fluid or other substance used as the medium in a solar collector affect the efficiency of the solar collector (Vutukuru, et al., 2019). For instance, the thermal conductivity of water is around $0.6 \frac{W}{m} \cdot K$ at $20 \text{ }^\circ\text{C}$, and the thermal conductivity of mixture, where 50 % is ethylene glycol and 50 % is pure water (EG-PW), is around $0.4 \frac{W}{m} \cdot K$, and compared to earlier the thermal conductivity of air is around $0.03 \frac{W}{m} \cdot K$ at $26.85 \text{ }^\circ\text{C}$ (Mao, et al., 2023; Kaya, et al., 2018; Wu, et al., 2009).

Theoretical studies show that the thermal conductivity and other properties of the heat transfer fluids used in the FPSC can be significantly improved by adding nanofluids to base fluids such as water or water-glycol mixtures (Al-Sulttani, et al., 2022). Nanofluid is a mixture consisting of solid nanoparticles (less than 100 nm) and a base fluid, where the nanoparticles are dispersed in specific proportions (Liu, et al., 2022). These nanoparticles are produced using nanotechnology, which allows for the creation of various types, including metallic nanoparticles such as silver, chromium, copper, iron, metal oxides (e.g., CuO, FeO, CeO₂, SiO₂, TiO₂), carbides (such as SiC, TiC), nitrides (like AlN, SiN), and carbon-based nanoparticles (Gupta & Prasad, 2020). In one experimental study comparing the use of an EG-PW as the working fluid for a solar collector's heat transfer medium with a zinc oxide-ethylene glycol and water (ZnO/EG-PW) nanofluid mixture as the heat transfer medium, it was demonstrated that thermal conductivity increases with the volumetric concentration of nanoparticles that have a diameter of 30 nm. The study proved that by using a ZnO/EG-PW nanofluid mixture containing 3.0 % by volume of ZnO nanoparticles, the solar collector achieved approximately 26 % better efficiency compared to the scenario where pure EG-PW was used as the working fluid (Kaya, et al., 2018). When considering the benefits of nanofluids and the nanoparticles they contain in enhancing the efficiency of various thermal energy devices and applications, such as solar collectors, it is imperative to acknowledge the substantial environmental and health risks associated with nanofluids. Concerns about the potential environmental and health hazards of nanofluids have been highlighted in numerous studies addressing the topic (Elsaid, et al.,

2021; López, et al., 2019). Additionally, these issues have been raised in discussions with companies importing solar collectors and hybrid solar modules. Representatives from these companies have noted that one factor impeding the wider adoption of solar collectors and hybrid modules is the possible environmental and health risks linked to nanofluids.

The energy conversion efficiency η_{en} of a solar thermal collector can be expressed mathematically in a simple form as follows (Lupu, et al., 2018):

$$\eta_{en} = \frac{Q_u}{G \cdot A_c}, \quad (6)$$

where G represent the solar radiation intensity, and A_c is the surface area of the collector. In the Eq. 6, the Q_u express the useful heat rate absorbed by the working fluid, or other form of medium, of the collector, which can be expressed as follows:

$$Q_u = m \cdot C_p \cdot (T_{fl,out} - T_{fl,in}), \quad (7)$$

where m is the mass of the working fluid, C_p is the thermal capacity of the fluid, or other form of a medium, of the collector, and T represents the temperature of the medium.

A conventional FPC utilizing a water/glycol mixture as a heat transfer medium can provide heat at temperatures up to 80 °C, achieving energy conversion efficiencies as high as 60 % (Dincer & Bicer, 2018). Studies indicate that FPC operating at low temperatures can achieve considerably higher efficiencies by using nanofluids as the heat transfer medium instead of water or water/glycol mixtures. By employing multi-walled carbon nanotube (MWCNT) nanofluids, the conventional efficiency of the FPC can increase to 87 % (Alam, et al., 2021). It is challenging to determine a precise mean efficiency figure when evaluating the normal energy conversion efficiency of an FPSAC since the efficiencies reported in different studies might vary considerably. However, experimental studies show that the FPSAC average energy conversion efficiency ranges from 28 % to 78.6 %

at low operational temperatures (30 – 80 °C) (Xi, et al., 2021; Prakash, et al., 2022; Bakari, 2018). When examining the energy conversion efficiencies of FPC modules, it can be observed that the efficiency of thermal energy-producing FPC modules is significantly higher when compared to the average energy conversion efficiency of electricity-producing PV modules.

The terms "stagnation temperature" and "stagnation point" are frequently brought up when analyzing the operating temperature range of solar collectors. Simply defined, the temperature of a solar thermal system during times when there is no flow of the medium is known as the stagnation temperature. The stagnation temperature refers to the medium temperature in a solar collector that arises from the given irradiance and ambient temperature during times when no useful energy is extracted from the solar thermal collector (Luzzi & Lovegrove, 2004). In chemical geodynamics, stagnation point typically is defined as a specific location in a fluid flow where the velocity is zero, and the fluid is at rest. This point is characterized by pure shear and potential for exponential stretching of material, contrasting with laminar regions where the flow is uninterrupted, and stretching is linear. The long-term impact on materials within the flow is determined by their interaction with these stagnation points versus the more common laminar areas, with steady-state and two-dimensional flows typically resulting in predominantly linear stretching due to the infrequency of stagnation point encounters (Tackley, 2015).

Comprehending both the stagnation temperature and the locations of stagnation points within a solar thermal system is crucial for optimizing energy conversion efficiency and ensuring the system's protection (Sforza, 2016). Stagnation in solar thermal systems often results from reduced power consumption, fluid flow drops, or interruptions in energy supply. This can cause the medium temperature in solar thermal collectors to increase rapidly, leading to increased operating pressure and potential phase changes that further elevate pressure risking component damage. System energy-saturation, where the system overheats and enters stagnation upon reaching its energy capacity, can occur at saturation temperatures around 100 °C initiating steam formation within the collector

(Rimar, et al., 2020). Studies show that the stagnation situation of flat plate solar collector systems, lasting about 10 minutes at the stagnation temperature, is typically due to system oversizing and can significantly damage the system or its parts, especially collectors, by accelerating material and heat-transfer fluid degradation. This degradation can cause corrosion, clogging, and insulation material degradation, negatively affecting the collectors' heat loss performance (Streicher, 2001). Although the process of stagnation is difficult to regulate and control, it is imperative that this factor is considered in the system design to prevent efficiency losses, deterioration, and potential system failure. The two fundamental strategies for managing collector stagnation temperature involve either reducing the solar energy absorbed by the collector or dissipating excess heat from the collector (Hussain & Harrison, 2015).

2.3 Hybrid Solar Modules

In this subsection, hybrid solar modules, namely PVT modules, are discussed. As previously mentioned, the technology of PVT modules is based on the combination of flat-plate solar collectors and PV modules. Therefore, it is essential to understand the operating principles, physical properties, and laws of both types of devices, as well as the efficiency limits that were examined in the two previous subsections. This section will examine PVT modules based on three different technologies: liquid-circulating, air-circulating, and evacuated PVT modules. In this section, various PVT technologies are examined, with the goal of analyzing aspects such as their basic structure, operational temperature ranges, overall efficiency ratio, electrical efficiency, investment costs, as well as the durability of materials and their expected lifespan. In Section 2.4, the technical parameters, and characteristics of three distinct PVT technologies are combined to facilitate a comparative analysis of their salient features.

2.3.1 Liquid-Circulating Hybrid Solar Module

As was previously noted, the initial purpose of PVT modules was to use waste heat to cool PV cells and preserve their efficiency. The medium in liquid-based PVT module is usually water or a glycol-water combination. Though they can't transport heat as well as water, combinations of glycol are recommended in colder climates to avoid freezing (Kazemian, et al., 2018). Adding nanofluids, which are made of tiny metal particles like zinc, can increase the glycol mixes' specific heat capacity (Al-Sulttani, et al., 2022). As has already been stated, a recurring concern highlighted in both scientific research and dialogues with PVT module importers revolves around the environmental implications of heat transfer fluids, especially nanofluids. The potential for environmental detriment is significant if highly concentrated nanofluids were to escape from containment systems. Additionally, the methods employed in the production of nanofluids may result in the generation of chemicals that pose risks to both environmental integrity and human health. (Said, et al., 2023). However, research indicates that it is possible to develop and utilize nanofluids that are less harmful to the environment, which achieve nearly similar efficiency ratios as conventional nanofluids (Kumar, et al., 2021).

Liquid-circulating PVT modules are essentially just combinations of FPC and typical PV module schemes. In Figure 3, one of the typical structures of a liquid-based PVT module is presented (Ramos, et al., 2019). In Figure 3, it is readily apparent that the thermal absorber flow channels of the PVT module, constructed from copper pipes, are arranged in parallel, a common design approach for thermal medium channels.

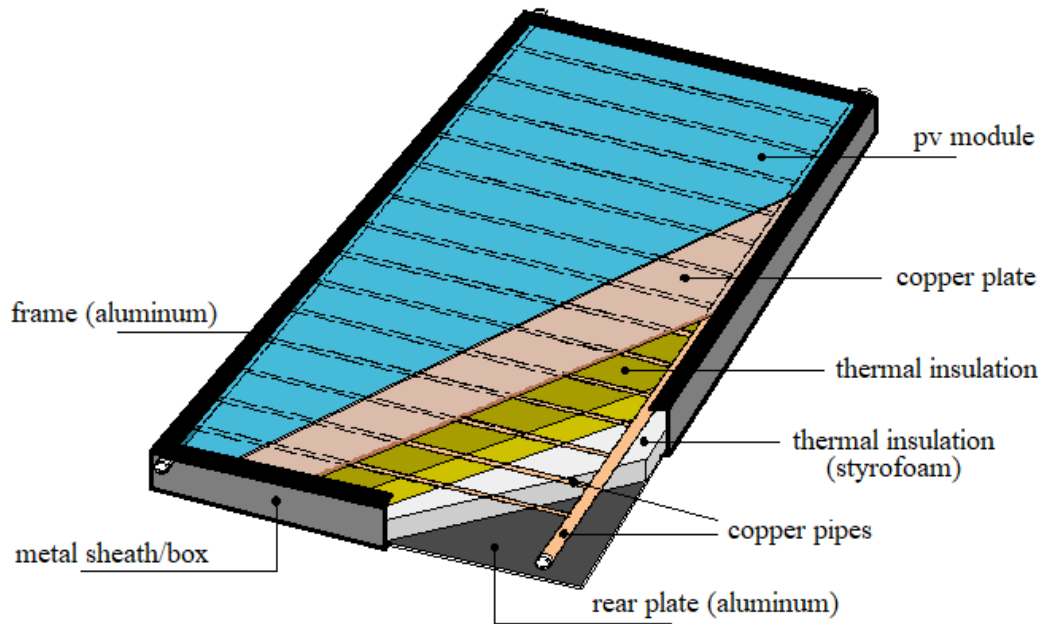


Figure 3. Structure of the conventional liquid-circulating PVT module (Ramos, et al., 2019).

Thermal fluid flow channels, functioning as heat exchangers, are key to the thermal and electrical efficiency of PVT modules. Heat transfer efficiency from PV cells to the fluid depends on factors like material properties, design, thermal resistance, and component integration. Different absorbers and medium flow channels affect PVT system performance (Emmanuel, et al., 2021). Figure 4 illustrates six flow channel designs : a) serial, b) parallel, c) web, d) spiral, e) combined parallel-serial, and f) bionic (Poredoš, et al., 2020). Research indicates that the design of flow channels plays a pivotal role in enhancing temperature uniformity, as well as the thermal and electrical efficiencies, of PVT modules. Moreover, the hydraulic performance of these modules is significantly influenced by the flow channel configuration (Yao, et al., 2021). Studies show that single spiral flow-channel designs are particularly beneficial for reaching optimal thermal and electrical efficiency. The header-riser and serial configurations are the two most common flow channel designs seen in the scientific literature that study different design techniques for PVT absorber plates (Poredoš, et al., 2020). PVT modules may feature a dual flow channel structure in addition to single flow channel configurations. According to the findings of one study on the subject, the flow velocity of nanofluid at the inlet of a double serpentine channel is half that of a single channel when the Reynolds number

(Re) is constant, resulting in a longer duration of heat transfer between the fluid and solid surfaces (Ali, et al., 2023).

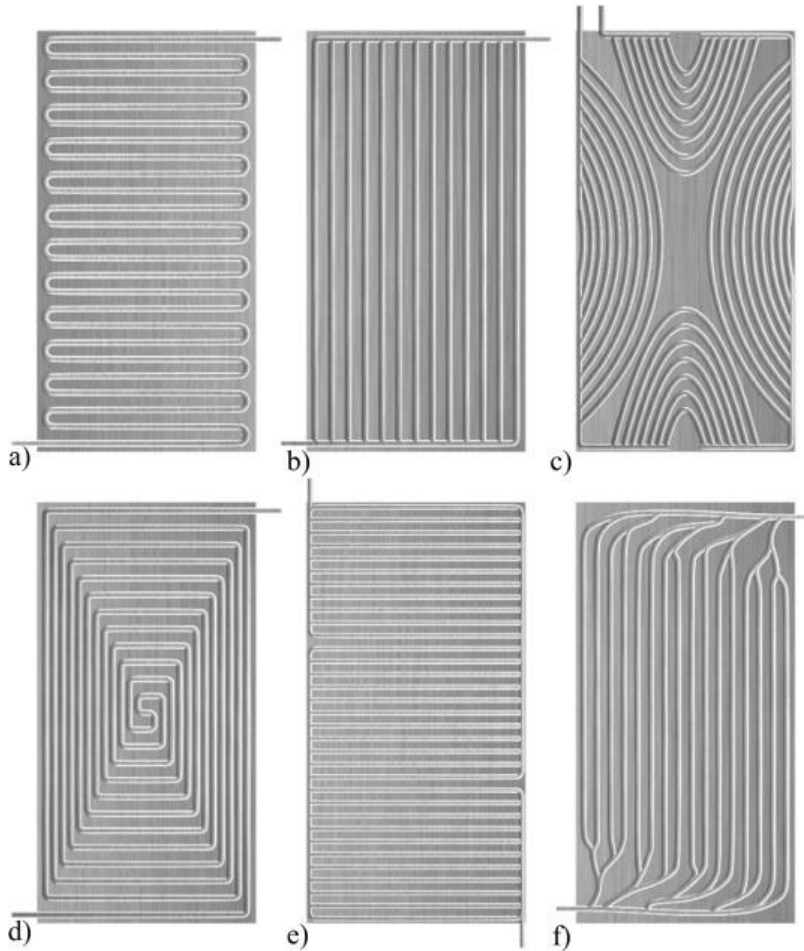


Figure 4. Multiple PVT module thermal flow channel designs: a) serial, b) parallel, c) web, d) spiral, e) combined parallel-serial, and f) bionic (Poredoš, et al., 2020).

In addition, compared to a single serpentine tube, the double serpentine channel offers a greater contact surface area between the channel walls and the nanofluid coolant. In comparison to a single serpentine channel, the double serpentine configuration's increased contact area results in an improved heat transfer coefficient (Ali, et al., 2023). A typical schematic of the double serpentine channel structure of a PVT module is presented in Figure 5.

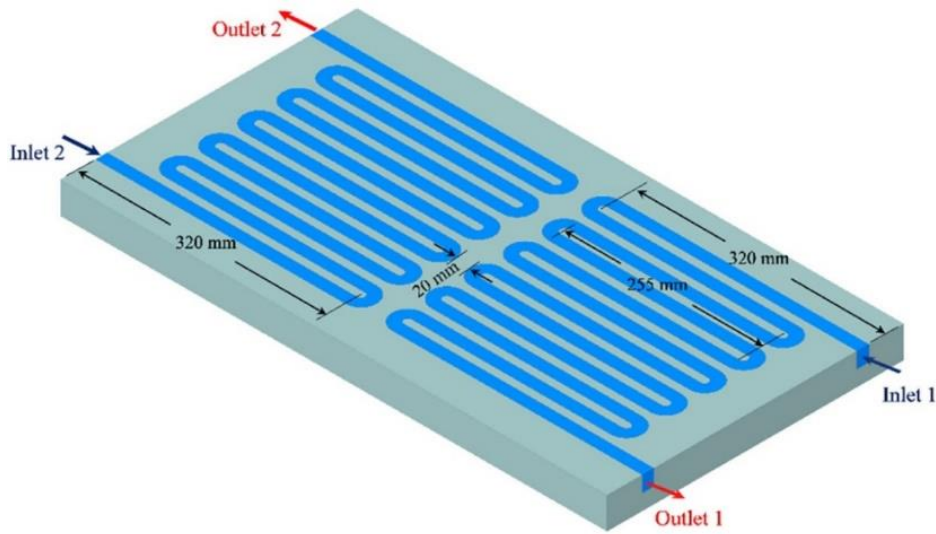


Figure 5. The schematics double serpentine channel absorbers (Ali, et al., 2023).

In addition to the fluid channel patterns for PVT modules previously discussed, certain studies advocate for a hexagon-grid coupled fluid channel pattern structure, as depicted in Figure 6. A feasibility analysis conducted by one study determined that an optimized hexagon-grid coupled fluid channel pattern has the potential to markedly reduce the operating temperature of solar cells within PVT modules. Furthermore, this optimized design could enhance the electrical efficiency of the modules by nearly 50 % on a typical summer day compared to PVT modules employing conventional commercial flow channel patterns (Yao, et al., 2021).

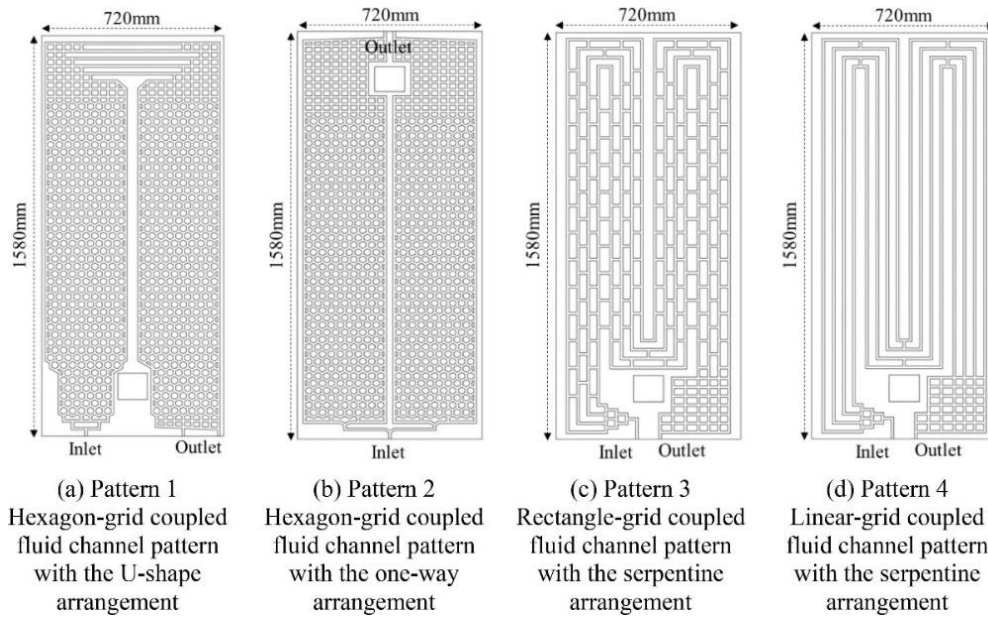


Figure 6. Different fluid channel patterns of PVT module (Yao, et al., 2021).

It is essential to recognize that although the cell temperatures in liquid-based PVT modules remain significantly lower than those of standard PV modules, there are still variations in temperature across different cells within PVT modules. These temperature discrepancies can result in differential cell efficiencies. This phenomenon is illustrated in Figure 7, which presents the results of a thermographic analysis comparing PVT and PV modules, highlighting the temperature differences in question (Baiceanu, et al., 2020). Each thermographic image presented in Figure 7 clearly illustrates a comparison between two types of modules: the PVT module on the left and the PV module on the right. It is immediately apparent from these images that the solar cells at the top and bottom of the PVT modules consistently show much higher temperatures than those in the module's central area. Each image captures a distinct scenario, characterized by varying average ambient temperatures and PV module temperature levels.

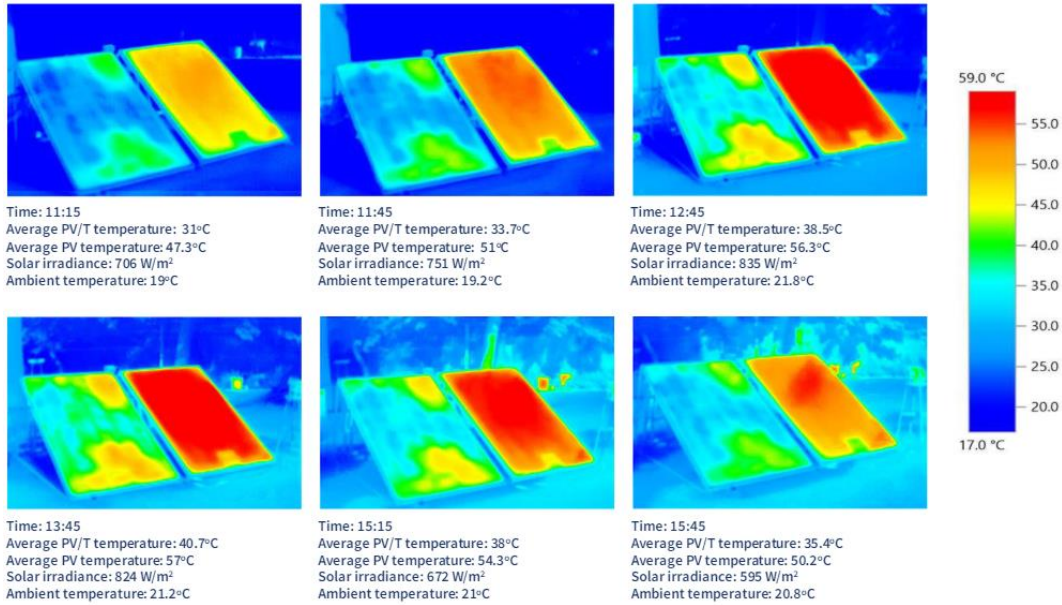


Figure 7. Thermographic study of PVT and PV modules (Baiceanu, et al., 2020).

The optimal energy conversion efficiency in liquid-based PVT systems is reached at low operational temperatures, meaning when the temperature of the heat transfer fluid stays below 100 °C (Rosales-Pérez, et al., 2024). In one theoretical study investigating the impact of temperature on the electrical efficiency of PVT modules utilizing water as a thermal medium, it was observed that there is an increase of up to 4.17 % in average electrical efficiency compared to conventional PV modules without cooling (Mishra, et al., 2021). Another theoretical study suggests that increasing nanofluid volume concentration in a PVT module from 0 % to 0.25 % boosts electrical efficiency by up to 2 % compared to PVT module that utilizes only water as a medium. According to the same study, the thermal efficiency of the PVT module configurations varies between 32 % and 43 % in single and double serpentine channels. The fluid systems where viscosity has a significant impact on flow patterns and velocity are classified between 500 and 2000 by their Re value, according to the study. Optimal overall energy conversion efficiencies of 84.30 % for single and 90.47 % for double serpentine designs were recorded with Re value of 1000 and nanoparticle concentration level of 1 % (Ali, et al., 2023; Rehm, et al., 2008). One experimental analysis investigated the impact of employing a copper oxide nanofluid on the performance of an unglazed PVT system. Findings indicate that cooling

with nanofluid and water decreased the panel's temperature by as much as 23.7 °C and 15.0 °C, respectively, relative to an uncooled PVT setup. Moreover, the application of nanofluid cooling notably augmented the overall efficiency of the PVT system, outperforming the water-cooled counterpart by 21 %, attributable to the enhanced thermal conductivity offered by the nanoparticles (Menon, et al., 2022). Figure 8 is observed to illustrate the influence of different heat transfer fluid compositions on the electrical efficiency of a PVT module. Figure 8 compares three variations of the PVT system: one without any heat transfer fluid for cell cooling, effectively mirroring a conventional PV system; a second utilizing only pure water for cell cooling; and a third employing a nanofluid mixture. Conversely, Figure 9 examines the thermal efficiency of the PVT system when either pure water or a nanofluid mixture is used as the heat transfer fluid. It is readily discernible from both graphs that the system exhibits significantly enhanced electrical and thermal efficiency when nanofluid-based heat transfer mediums are utilized in lieu of pure water.

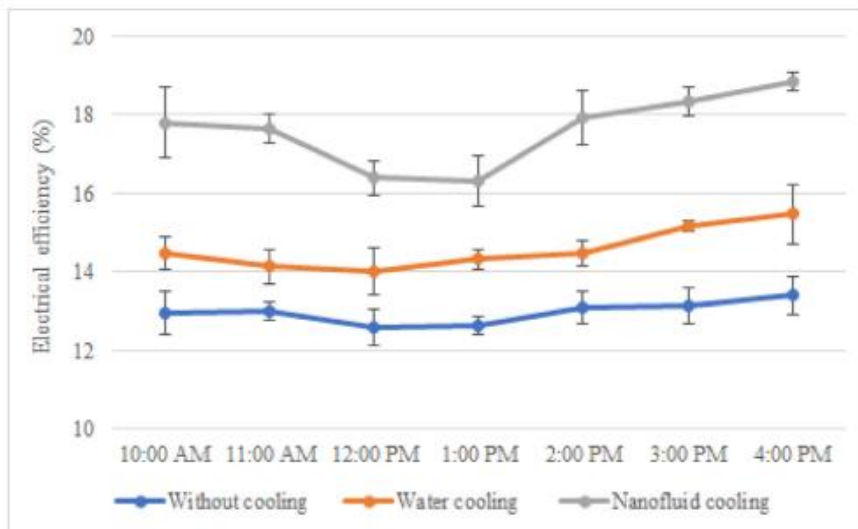


Figure 8. Electrical efficiency of PVT system with different cooling medium (Menon, et al., 2022).

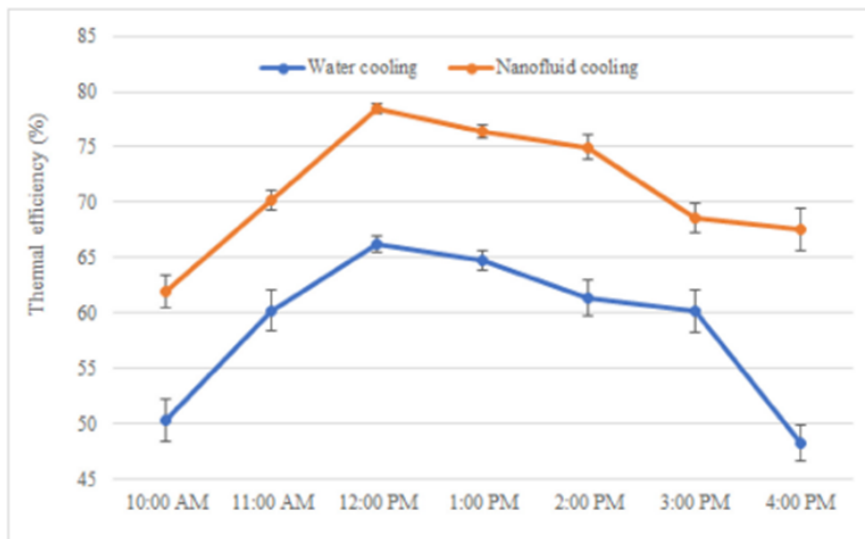


Figure 9. Electrical efficiency of PVT system with different cooling medium (Menon, et al., 2022).

Incorporating phase change materials (PCM) into the structural design of both traditional PV and PVT modules presents a potential solution to regulate their temperature. Numerous studies have been conducted to evaluate the efficiency of cooling techniques that integrate PCMs with PV panels. These investigations have examined the effects of PCM physical properties, ambient environmental conditions, and the design of PCM encapsulation, utilizing both numerical simulations and experimental methods (Sharma, et al., 2021). Fundamentally, the operational principles of PCMs are predicated on their capacity to absorb thermal energy during the phase transition from solid to liquid, as well as their ability to release energy upon reverting from liquid to solid (Hu & babu, 2009). An experimental investigation contrasting a conventional PV module with a hybrid PVT module augmented with PVT-PCM revealed that the hybridization yields a significant enhancement in the daily cumulative electrical efficiency by 0.54 %, with a potential peak increase of 0.98 %. This improvement equates to an overall elevation in the PV system's efficiency by as much as 7.43 % per day. This efficiency gain primarily stems from the hybrid module's ability to maintain the operating temperature of the PVT-PCM's photovoltaic cells between 10 and 17 °C lower than that of a standard PV module. Given the extended operational lifespan of contemporary solar panels, the integration of PVT-PCM technology exhibits considerable promise for application within conventional PV systems,

suggesting a pathway for substantial performance optimization (Joo, et al., 2023). Figure 10 graphically presents a comparative analysis of the daily electrical, thermal, and combined efficiencies of a standard PV module and a PVT module integrated with phase change materials (Carmona, et al., 2021).

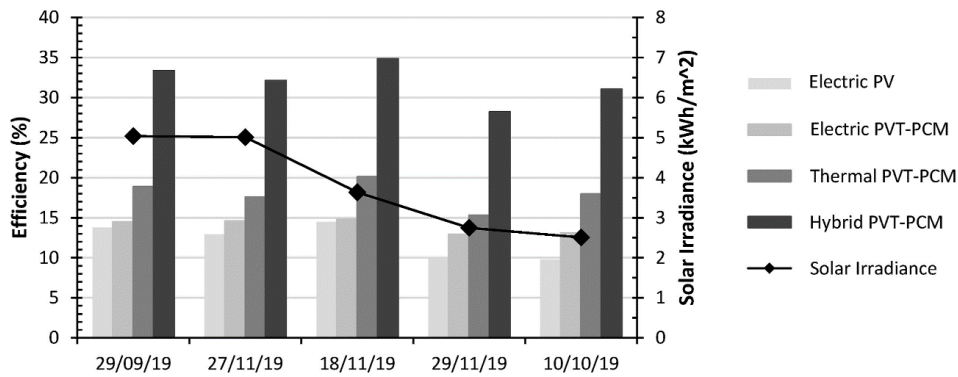


Figure 10. Comparison of electrical, thermal and hybrid efficiencies of PV module and PVT-PCM (Carmona, et al., 2021).

Similarly, to conventional PV modules, PVT modules might also employ an effective method to mitigate the recombination of electrons and holes on the solar cell surface and to hinder the diffusion of extraneous materials—this is achieved by incorporating a PERC layer. The rear surface of the solar cell is coated with an insulating film referred to as the passivating layer, which serves to improve the flow of current. By eliminating defects caused by inadequate passivation, the solar cell's capacity to generate energy is significantly enhanced (Jang, et al., 2024; Satpathy & Pamuru, 2021). Research demonstrates that PERC technology exhibits superior performance in solar cells, primarily due to its extended diffusion length relative to traditional mono- and multi-crystalline silicon cells, coupled with a thinner inactive layer. The enhanced diffusion length in PERC cells is particularly notable at low surface recombination velocities, suggesting why these cells outperform their conventional counterparts (Singh, et al., 2023). Additionally, the diminished impact of resistive losses under conditions of low light intensity contributes to the high efficiency of PERC cells (Krügener & Harder, 2013). This attribute is critical, especially since PERC cells maintain functionality under diffuse solar radiation, a common

scenario in regions like Finland where the majority of annual solar irradiation is diffuse (Motiva Oy, 2024). Although research demonstrates that incorporating PERC technology in solar cells can positively influence their energy conversion efficiency, there are stability concerns associated with PERC technology as well. Studies have identified that solar cells experience degradation when exposed to light and high temperatures, conditions typical of field operations. This phenomenon, known as light and elevated temperature induced degradation (LeTID), poses a significant challenge to the reliability and long-term performance of passivated emitter and PERC devices (Niewelt, et al., 2024).

Research delineates the deleterious effects of aging factors—including dust, discoloration, delamination, temperature variation, humidity, fractures, and hotspots—on the performance and longevity of PV and PVT modules. Over time, these elements variably diminish solar PV efficiency and service life. Dust is associated with a relatively modest impact, whereas cracks and hotspots markedly compromise both efficiency and durability. Temperature and humidity-induced delamination and discoloration are also of notable concern (Dhimish & Tyrrell, 2022; Rahman, et al., 2023). One study indicates that a mean annual efficiency declines 0.93 % in mono-crystalline PV modules, with distinct rates of degradation across different components (Atia, et al., 2023). Furthermore, the empirical evidence suggests that the operational lifespan of PV systems may be significantly less than projected, with a marked uptick in severe malfunctions emerging after a decade of use (Libra, et al., 2023). Contrary to the linear degradation model often posited by manufacturers, field data implies that power loss may exhibit non-linearity, contingent upon the technology of the module and the pattern of degradation. Additional findings reveal that once cellular degradation begins, the rate of overall module deterioration tends to accelerate (Kaaya, et al., 2020). Recent research has introduced and delineated an algorithm designed to assess the trajectory of degradation trends, incorporating an innovative approach that accounts for multiple degradation factors which are time- and pattern-dependent. This methodology appears to offer enhanced precision over previously established methods used for forecasting long-term PV performance degradation, which frequently yields implausible degradation scenarios.

Nonetheless, it is prudent to acknowledge that the formulation of a degradation model that fully encapsulates real-world conditions remains an elusive goal. This challenge arises due to the degradation of PV and PVT modules contingent upon a myriad of factors and variables (Aghaei, et al., 2022; Kaaya, et al., 2020).

Research suggests that PV systems located in colder climates, such as Finland, exhibit a heightened vulnerability to the development of hotspots, which refer to areas of localized overheating within a PV cell or module (Dhimish, et al., 2024; Rahman, et al., 2023). Fluctuations in ambient temperature may precipitate the fracturing of PV module glass, a consequence of thermomechanical stress (Rahman, et al., 2023). It is noteworthy that within the annual cycle in Finland, significant temperature fluctuations are characteristic, with the temperature difference between winter and summer potentially approaching 90 °C (FMI, 2018). Studies indicate that over time, the prevalence of these microfractures escalates, culminating in an increased count of compromised cells and hastening the degradation of the PV module, leading to a lifespan shorter than anticipated. Furthermore, the degradation process is exacerbated by a decline in light reflectance and transmittance owing to phenomena such as discoloration and delamination, both of which can induce immediate and progressive decline in cell integrity and peak power performance (Rahman, et al., 2023). Consequently, a comprehensive understanding of the genesis of thermomechanical stress within solar cells is imperative for enhancing the durability of both PV and PVT modules (Beinert, et al., 2019).

Table 1 delineates the technical specifications of liquid-based PVT modules from four different manufacturers, detailing parameters such as maximum electrical power, peak thermal power, stagnation temperature, module dimensions, and weight. Employing this information, the requisite number of modules to generate 1 MW of peak electrical power and the associated total surface area were computed. The table further presents cost evaluations, reflecting the capital expenditure (CAPEX) per module for 1 MW power production. These specifications originate from manufacturers' reports (Dualsun, n.d; Aora Energy S.L., n.d; Crane Ltd, n.d). Cost projections for the modules are based on

market research conducted by Sweco Belgium in collaboration with doctoral student Peere Wouter from KU Leuven University in 2021. Except for the last module's pricing, which is derived from reseller listed price, after excluding Spain's standard value-added tax (VAT) of 21 % (Salcantay OU, n.d). The research conducted by Sweco Belgium is not available to the public. It is designed specifically for the use of engineering and consulting companies, as well as for academic research within the university. It's important to note that all prices mentioned are provided as approximate reference points and are subject to change.

Table 1. Liquid-circulating PVT modules characteristics.

Manufacturer	P_{MPP} (W)	P_{TE} (W)	T_{sat} (°C)	DIM (m ²)	Wt (kg)	Amt/MW_e	SA/MW_e (m ²)	$CAPEX$ (€/MW _e)
DualSun	425	869	80	2.08	34.4	2353	4894	1 300 000
Solimpeks	330	855	70	1.67	34.0	3030	5148	1 500 000
Abora	350	1372	126	1.96	50.0	2857	5600	2 000 000
Crane	250	890	85	1.72	31.0	4000	6864	2 100 000
Mean	339	997	90	1.86	37.4	3060	5607	1 700 000
Deviation	72	251	25	0.19	8.6	689	890	400 000

From Table 1, it can be observed that the average electrical MPP of commercially available liquid-based PVT modules under STC is approximately 340 W. In contrast, the maximum thermal power value is about 1000 W, nearly three times the electrical peak power. It should be noted that there is a relatively large standard deviation in the maximum thermal power, due primarily to an anomalously high value reported by one manufacturer. Similarly, the average stagnation temperature reported by another manufacturer appears to be excessively high, particularly in scenarios where pure water is used as the heat transfer fluid in the system. On the other hand, the same manufacturer reports the module's maximum pressure resistance as 10 bar, at which the boiling and steam formation point increases relative to the boiling point at normal atmospheric pressure. Table 1 also reveals that the average weight of a commercially available PVT module is around 37 kg, which is approximately twice the mass of a standard PV module, generally

around 18 kg (Farrell, et al., 2019). This factor warrants careful consideration during the installation of modules atop roof structures or other structural supports bearing load. Furthermore, the table indicates significant variability in both the number of modules required to generate 1 MW of power and their total surface area. It is important to consider that the actual required surface area for a power plant composed of these modules, when installed on a field or flat roof, will be considerably larger than the total surface area of the modules alone. For example, if the modules are installed at 28°, a gap of about 4 meters in width should be left between rows of modules (Jamil, et al., 2017). It must be acknowledged that the cost estimates delineated in the table predominantly derive from pricing information as of the year 2021 and have not been adjusted to reflect subsequent inflationary trends or escalations in material and production costs that would affect the contemporary pricing landscape.

Research suggests that while liquid-based PVT modules are operationally cost-effective and ostensibly straightforward, their adoption in the market is hindered by steep initial investment and performance challenges, even though they typically incur low ongoing costs after installation (Emmanuel, et al., 2021). For example, according to a survey study conducted by Sweco Belgium in 2021, which targeted manufacturers, the findings indicate that the annual average operational and maintenance expenses for the liquid-circulating PVT module are approximately 3 €/m² in power plants with a total area exceeding 2000 m². In other terms, this signifies that the annual operating expenses (OPEX) constitute roughly 1.1 % of the CAPEX. It must be acknowledged that the numerical value is based solely on the figure reported by a single manufacturer. Therefore, the value may not necessarily reflect an accurate statistical average. Consequently, the actual OPEX value can exceed the presented value. On the other hand, research indicates that the OPEX of conventional PV plants are typically calculated as a fixed percentage of the total plant cost, ranging between 0.8 % and 1.2 % annually (Shimura et al., 2016).

One research that compares the annual total energy production of PV and PVT systems in Republic of Ghana, indicates that the estimated annual average total energy output

from the PV systems is 159.42 kWh/m², and 330.15 kWh/m² from the PVT system (Abdul-Ganiyu, et al., 2021). In other words, a freestanding PV system can only provide half of the yearly total energy output that a standard liquid-based PVT system of the same size can. This indicates that a surface area twice as large would be needed if the objective is to create the same quantity of heat energy and electricity using PV modules and conventional solar collectors. The investigation further reveals that the levelized cost of energy (LCOE) derived from basic PV stands at 410 €/MWh in electrical energy production and PVT systems 300 €/MWh in total energy production, respectively, based on an average peak sunlight duration (*Sh*) of 4.6 hours (Abdul-Ganiyu, et al., 2021). It is imperative to acknowledge that the original studies presented the LCOE values in dollars per kWh, and these figures have been converted to the currency value corresponding to the reference date, utilizing the exchange rate index provided by the European Central Bank. Additionally, it must be recognized that the energy production attributed to the PVT system encompasses the aggregate energy yield, signifying the combined total of electrical and thermal energy outputs.

2.3.2 Air-Circulating Hybrid Solar Module

Liquid-based and air-based PVT systems have a similar core operational basis. Warm or hot air must be drawn out of the PV module to lower its temperature and improve the performance of air-based PVT modules. One possible use for the warm air collected from the PVT module is to provide the building with external thermal energy (Kim, et al., 2014). The duct medium and fluid flow behavior have been the main topics of PVT study, with water being preferred because of its higher heat transfer coefficient. But air-based systems are flexible and inexpensive in a variety of settings, which makes them suited for promoting solar energy throughout the globe. To maximize the performance of air-based PVT systems, it is essential to investigate several design elements (Dunne, et al., 2023).

An experimental study revealed average thermal and electrical efficiencies for the air-based PVT module at 22 % and 15 %, respectively. Electrical efficiency benefited from optimal output with the PVT air collector, as forced ventilation curbed the temperature

increase in the PV cells (Kim, et al., 2014). Research on air-based PVT modules for drying agricultural crops has shown that the annualized cost of energy gain per unit is more than the cost of thermal energy gain (Nazri, et al., 2018). Research suggests that air-based PVT systems are emerging as a cost-effective and efficient advancement in the harnessing of solar energy, potentially making them especially well-suited for a vast array of agricultural drying processes. Nevertheless, the technology pertaining to air-circulating PVT systems is still in the developmental phase. Consequently, most of the studies discourse on this subject remains theoretical, and, to date, there are virtually no commercially available implementations of this technology (Chaibi, et al., 202; Nazri, et al., 2018).

Table 2 delineates the technical specifications of air-based PVT modules derived from empirical research. These modules, custom-designed and constructed for investigative purposes, are not yet accessible on the commercial market. It is apparent that the efficiency and power output of these prototypes are comparatively modest. Notably, the electrical energy conversion efficiency is significantly lower than that of commercially available PV cells, likely attributable to the budgetary constraints of the research, resulting in the selection of less costly components. Consequently, the attributes presented in Table 2 may not fully reflect the prospective capabilities of air-based PVT technology.

Table 2. Air-Circulating PVT modules characteristics.

Manufacturer	P_{MPP} (W)	P_{TE} (W)	T_{sat} (°C)	DIM (m ²)	Wt (kg)	Amt/MW_e	SA/MW_e (m ²)	$CAPEX$ (€/MW _e)
Experimental	250	352	50	1.6	N.A.	4000	6400	N.A.
Experimental	65	605	54	1.6	N.A.	15477	25228	N.A.
Experimental	100	592	50	0.8	N.A.	10000	8450	N.A.
Experimental	40	181	55	0.3	N.A.	25000	8033	N.A.
Mean	114	432	52	1.1	N.A.	13619	12028	N.A.
Deviation	94	204	3	0.6	N.A.	8918	8844	N.A.

2.3.3 Evacuated Hybrid Solar Module

The evacuated PVT modules technology is based on the same principles as liquid-based PVT technology, refer to Chapter 2.3.1. The key difference lies in the fact that in evacuated PVT modules, the metal tubes of the liquid-circulating heat exchanger are insulated within a closed vacuum chamber. By utilizing vacuum insulation, heat leaks are prevented in evacuated PVT modules, allowing for the exploitation of higher temperatures compared to traditional liquid-based PVT technologies (Hu, et al., 2021). For effective thermal energy conversion in the temperature range of 100 to 200 °C, which is also the temperature range for EFPC are usually designed (Bellos & Tzivanidis, 2023). Research has demonstrated that, in theory, PVT modules are capable of functioning within the same temperature ranges as conventional EFPC. Nevertheless, it has been observed that the electrical efficiency of evacuated PVT modules utilizing poly-C-Si tends to diminish rapidly once temperatures exceed 98 °C. The same investigation suggests that amorphous silicon (a-Si) cells may exhibit enhanced electrical efficiency at elevated operational temperatures, a phenomenon potentially attributable to the effect of thermal annealing. Moreover, these cells are anticipated to exhibit extended durability without the need for encapsulation when situated within the vacuum environment of evacuated PVT module (Kutlu et al., 2020).

A theoretical investigation posits that the efficiency of both electrical and thermal energy production within PVT modules can be significantly enhanced by housing the PV cell within a vacuum glass chamber. Utilization of materials with high bandgap properties enables the PV cell to maintain a temperature close to ambient levels, which in turn allows a greater portion of the solar spectrum to impinge upon the selective solar absorber. Such an arrangement facilitates the generation of thermal energy, even at temperatures reaching 150 °C (Luca, et al., 2023). Even though the majority of research primarily focuses on theoretical analyses of evacuated PVT modules and their capacity to function at elevated temperatures while generating thermal energy with an efficiency comparable to that of conventional EFPC, empirical studies have suggested that utilizing autonomous systems integrating PV and commercially available EFPC would necessitate

nearly 50 % more collector surface area than the projected evacuated PVT modules to attain an equivalent annual total energy yield (Luca, et al., 2023). A case study conducted on a dairy farm in Germany provided an analysis that demonstrated concentrating PVT systems exhibit greater efficiency at elevated operating temperatures compared to flat plate PVT systems. Consequently, this makes concentrating PVT systems more appropriate for farm energy systems where there is a demand for high-temperature thermal energy (Hosouli, et al., 2023).

Vacuum technology in PVT modules is presently available on the market, albeit to a limited extent. Table 3 showcases the characteristics of one such commercially available evacuated PVT module. The table includes a cost evaluation, detailing the CAPEX per module for producing 1 MW of electrical power. These specifications are sourced from the manufacturers' data (Naked Energy, n.d.). The cost estimates for these modules are derived from market research conducted by Sweco Belgium in collaboration with KU Leuven University in 2021. It's important to note that all prices mentioned are provided as approximate reference points and are subject to change. From Table 3, it is readily apparent that the stagnation temperature of the commercially available evacuated PVT module is markedly lower than the operating temperature range suggested by theoretical studies for optimal PVT thermal energy production.

Table 3. Evacuated PVT module characteristics.

Manu- facturer	P_{MPP} (W)	P_{TE} (W)	T_{sat} (°C)	DIM (m ²)	Wt (kg)	$Amt/$ MW_e	$SA/$ MW_e (m ²)	CAPEX (€/MW _e)
Naked Energy	350	1375	80	1.7	41	2857	4714	800 000

2.4 Technical Characteristics of Various Hybrid Modules

In this section, the technical parameters, and characteristics of three different PVT technologies are reviewed to enable a comparative analysis of their prominent features. The

examination extends beyond mere technical specifications to include an evaluation of both capital and operational costs inherent to these technologies. Additionally, the section scrutinizes and contrasts the commercial availability of each technology, offering an extensive overview. The objective of this discourse is to furnish a concise summary and accentuate the distinguishing attributes of the various methodologies, delineating, in essence, their respective advantages and disadvantages.

Table 4 presents the aggregated technical specifications for the three distinct PVT technologies discussed in the preceding chapter. It enumerates average values for key parameters such as maximum electrical and peak thermal power outputs, stagnation temperature, module dimensions, weight, and the commercial availability of each technology. The table's lowermost rows display the mean, median, and standard deviation of the collected dataset. Notably, the table reveals that, contrary to what might be inferred from theoretical studies and statistical expectations, the CAPEX of evacuated PVT modules exceeds that of liquid-circulating PVT modules by more than double.

Table 4. PVT modules characteristics comparison.

PVT type	P_{MPP} (W)	P_{TE} (W)	T_{sat} (°C)	DIM (m ²)	$Amt/$ MW_e	Wt (kg)	$SA/$ MW_e (m ²)	CAPEX (€/MW _e)	Available
Liquid	339	997	90	1.9	3060	37	5607	1 700 000	yes
Air	114	432	52	1.1	13619	N.A.	12028	N.A.	no
Evacuated	350	1375	80	1.7	2857	41	4714	800 000	limited extent
Mean	240	788	72	1.5	7731	38	8361	1 500 000	
Median	250	855	70	1.7	4000	34	6400	1 500 000	
Deviation	140	409	25	0.6	7824	8	6466	500 000	

In summary, the advantages and challenges of different PVT technologies can be encapsulated as follows:

Liquid-based PVT modules benefit from being the most readily commercially available technology. However, their principal challenges include higher costs and a theoretically

lower operational temperature for thermal energy production compared to the theoretical operational temperature of evacuated PVT modules.

The simplicity and potential cost-effectiveness of air-based PVT modules stand out as their main advantages over other technologies. The primary obstacle for this technology is that it is still in the research and development phase and not yet commercially accessible.

Contrary to expectations from research and statistical probabilities, the price level of evacuated PVT modules is significantly lower compared to liquid-based PVT modules. The challenge facing evacuated PVT modules lies in their very limited commercial availability.

2.5 Examination of Existing PVT Power System Operations

This subsection examines two separate case studies where PVT modules are implemented in power systems or individual modules performed in practical conditions. The first case study is in Yokohama, Japan. This research investigates the operation of a single water-based PVT module and compares its performance to that of a similar mono-c-Si PV module (Terashima, et al., 2020). The second case study examined is conducted in Forlì, Italy. In this case, the annual energy output of a small power system consisting of four commercially available water-based PVT modules is compared to the energy output of eight different PV systems (Bianchini, et al., 2017).

Both case studies are briefly reviewed in their main aspects. Subsequently, a concise analysis is presented on what can be observed from the case study and what must be considered when keeping in mind the premises and objectives of this research, namely, the intention to evaluate the use of PVT modules specifically in Finnish conditions.

2.5.1 PVT Power System Case 1

The study investigates an eco-friendly PVT solar module capable of confining high-temperature radiation within its structure, as confirmed through experimental evidence. The module incorporates a decompression-boiling heat collector that effectively absorbs heat from the PV components, maintaining low temperatures for the air and cover glass inside the module due to the reduced boiling point of the working fluid under vacuum (Terashima, et al., 2020).

The module features an innovative emboss-processed cover glass that reflects heat radiation from the PV module back into the module at high temperatures. Experimental results from a single PVT system demonstrate the ability to sustain the module's surface radiation temperature at around 45 °C in summer while providing hot water exceeding 60 °C by managing the flow rate of the heat-transfer fluid. The system was proven to convert 71.3 % of solar energy into electricity and heat at 40 °C during a summer day in Yokohama, Japan (Terashima, et al., 2020). For colder climates, an EG-PW mixture solution with a low freezing point can serve as the working fluid, ensuring energy conversion efficiency remains above 50 % in the colder conditions (Terashima, et al., 2020).

The study shows that in essence, the utilization of the proposed PVT solar modules could lead to a significant reduction in electricity usage for thermal applications and a corresponding decrease in environmental thermal load (Terashima, et al., 2020).

The study under review details the development and experimental validation of a novel PVT solar module designed to confine high-temperature radiation within its structure. Upon examining the key aspects of the case study, it becomes evident that the module's innovative decompression-boiling heat collector and emboss-processed cover glass contribute significantly to its thermal management capabilities. The experimental data demonstrate the module's ability to maintain lower surface radiation temperatures and produce hot water efficiently, even in the peak of summer in Yokohama, Japan (Terashima, et al., 2020).

Analyzing these findings, one can observe the module's potential for high-efficiency solar energy conversion, a crucial aspect for consideration in the Finnish context. Finland's climate poses unique challenges due to its colder temperatures and varying daylight conditions. The demonstrated capability of the module to operate effectively with an EG-PW mixture as the heat transfer fluid indicates its adaptability to colder environments, which aligns with the Finnish climate.

However, when considering the adoption of PVT modules in Finnish conditions, several factors must be considered. Additionally, the local environmental regulations, architectural integration possibilities, and the potential need for system modifications to optimize performance for Finland's specific seasonal and weather patterns should be acknowledged.

2.5.2 PVT Power System Case 2

In a comprehensive study of PVT solar systems in Central Italy, two methodologies were employed to assess the systems' performance. Initially, an in-depth monitoring phase was conducted on a PVT system in Forlì, Italy, to collect data on its operation under various environmental conditions. The research indicated that when PVT systems are exclusively configured for hot water production, the addition of active cooling results in a negligible enhancement, approximately 2 %, in photovoltaic electricity generation. Conversely, significant improvements in electrical output are attainable by lowering the temperature of the cooling fluid, provided the flow rate remains unchanged. However, this method results in water temperatures below 40 °C, which are impractical for use without the application of external heat pumps, a process that would compromise the system's overall efficiency. The PVT system demonstrated the ability to concurrently generate significant levels of electricity (835 kWh/m²) and heat (1600 kWh/m²), with thermal output reaching mean outlet temperatures over 40 °C (Bianchini, et al., 2017).

These findings were further supported by employing the ISO 9806:2013 model to estimate the system's monthly and annual thermal performance under the observed climatic conditions. The study highlights several key observations (Bianchini, et al., 2017):

1. Active cooling does not significantly enhance PV efficiency or yield due to the relatively high temperature of the cooling water, allowing for reliable predictions of the electric performance of the PVT system throughout the year without factoring in cooling effects.
2. The thermal performance is relatively unaffected by changes in the cooling fluid flow rate.
3. The produced hot water temperature is suitable for domestic use, albeit the heat production is seasonally skewed, peaking from May to September, which suggests that PVT systems are more suited to applications with seasonal hot water demands rather than consistent, year-round use.
4. An economic evaluation, including LCOE analysis, revealed that PVT systems can achieve cost parity with an investment of approximately 3700–4700 €/kWp, making them a viable option for the combined production of electricity and thermal energy when space is limited.
5. The study also notes that, in contrast to flat plate solar thermal collectors, which distribute heat production more evenly across the year, PVT systems tend to concentrate heat production within a shorter timeframe. This characteristic suggests that traditional solar thermal collectors may be more suitable for households with steady hot water needs throughout the year.

When considering the application of these findings within the Finnish context, numerous critical factors must be taken into consideration. The markedly colder climate and varying patterns of solar irradiance in Finland could significantly influence the performance and cost-effectiveness of PVT systems. The distinct seasonal variation in thermal energy generation, observed in the Italian study, could introduce complexities in providing a stable year-round supply of hot water in Finnish buildings or across other energy-

dependent sectors. Moreover, in Finland, reliance on solar energy for thermal needs all year round would not be feasible without incorporating thermal storage solutions. Therefore, it is essential to conduct a customized evaluation of PVT technology in Finland, considering the unique local energy consumption patterns, infrastructural challenges, and the vital commitment to sustainable energy initiatives.

3 Methodological Framework

In this section, the methodological perspective of the research is focused upon. Two simulation models are introduced, one modelling a power plant implemented with PVT modules, which has an electrical peak power of 1 MW and a theoretical thermal peak power of 2.1 MW. The other simulation models a conventional power plant composed of PV modules, also with an electrical peak power of 1 MW. The simulations of both power plants have been carried out using Matlab software. The simulation models utilize ready-made simulation models provided by MathWorks open library. These ready-made simulation models serve as a foundation for the desired simulation models; however, both have been modified to suit this research. The technical parameters of the PVT and PV modules used in the simulations are based on the data from modules manufactured by the French company DualSun. The simulations take advantage of open data provided by the Finnish Meteorological Institute (FMI) from three different weather observation points, meaning solar radiation data, as well as ambient temperature data. The weather stations are located in Turku, Ilomantsi and Sodankylä. The observation points have been selected so that they provide weather conditions that are as varied as possible.

In Chapter 3.1, the operating principle of the PVT power plant simulation model and the parameters of the PVT module are presented. In three different subsections, the results of the simulations in various locations are shown. Chapter 3.2 similarly presents a brief overview of the operating principle of the PV power plant simulation model, and the subsections detail the results of simulations in different locations. A more detailed analysis, discussion, and validation of the simulation results are presented in Chapter 4.

3.1 Simulation of PVT Power Plant

The PVT hybrid solar module simulation model is based on the photovoltaic generator simulation model made available by MathWorks, which serves as the basis for the simulation model that will be described next. It has been adjusted to ensure that it meets

the requirements of this study as precisely as possible (MathWorks Inc, n.d). The simulation model employs technical parameters based on the PVT module manufactured in France by Dualsun, and specific type of the model is SPRING4 425 TOPCon insulated PVT module. Detailed technical specifications can be found on the manufacturer's website (Dualsun, n.d.). It should be acknowledged that the manufacturer does not provide all the module parameters required for the simulation model. Consequently, the simulation model also employs assumed and estimated parameters, which may deviate from actual values.

In all simulations, open data from the FMI has been utilized, which is sourced from various observation stations and is available for download from the observation data service (FMI, n.d). The simulations have employed a one-year observation interval, starting from the first day of January and concluding on the last day of December. The simulations have utilized data from the year 2023, encompassing the environmental temperature with an accuracy of a one-hour average, as well as the total radiation with an accuracy of a one-hour average. Total radiation refers to the short-wave radiation from the sun and the atmosphere measured on a horizontal black surface (FMI, n.d). The simulation model has been implemented in such a way that it cannot utilize low levels of radiation, specifically those with an intensity below $200 \text{ W}\cdot\text{m}^{-2}$. Consequently, all original radiation data with values less than $200 \text{ W}\cdot\text{m}^{-2}$ have been converted to zero. According to research by the FMI, by orienting solar modules at a 45° facing south, the amount of utilizable radiation can be increased by 20-30 % annually compared to a horizontal installation (FMI, n.d). When the inclination angle of the modules is set at 45° , the relative increase in the amount of utilizable radiation varies between months. This variation is attributable to the tilt of the Earth's ecliptic, which is the average orbital path, in relation to the plane of the sun's equator, as well as the obliquity of the Earth's axis with respect to the orbital plane (Honey, 1921). In the simulations, an assumed increase of 20 % has been applied to the values of the usable radiation data points in accordance with the correction factor defined by the FMI (FMI, n.d).

The simulation model of a solar power plant composed of PVT modules, implemented using the graphical software environment of Matlab's Simulink, is presented in Appendix 2. The model uses as its input data the processed total solar radiation and corresponding environmental temperature data from each observation point. In the simulation model, the solar cells of the PVT modules operate in accordance with the two-diode equivalent circuit model depicted in Figure 1, where the effective current produced by the ideal current source is directly proportional to the radiation level. Within the model, the cells' temperature is proportional to both the environmental temperature and the radiation level. The system's DC-AC converter on the DC side optimizes the voltage for the most favorable electrical power level using MPP tracking technology. The optimal DC voltage levels have been defined in a voltage matrix, with the maximum reference voltage on the DC side set at 1100 V. The total voltage loss on the DC side is set to 5 %. The converter's AC side voltage is set at 20 kV. The efficiency of the converter is established at 97.1 %, which corresponds to the efficiency of a commercially available 1 MW DC-AC solar power plant converter.

In the model, the thermal power output of the PVT modules is directly modeled as proportional to both the environmental temperature and the radiation level. The simulations recognize the impact of the ratio of the PW-EG mixture on the heat transfer fluid's properties. The magnitude of the thermal power produced in the model is proportional to the difference between the environmental temperature and the temperature of the heat transfer fluid. It is assumed within the model that the system produces thermal power only concurrently with electrical power. The total thermal loss of the system is estimated to be 5 %.

3.1.1 Simulation of PVT Power Plant at the Location 1

The meteorological station locates in Artukainen, Turku, Finland (60.45275, 22.18961). The assumed lowest temperature point is -35 °C. The estimate is based on the statistical temperature observations provided by the FMI (FMI, n.d). The requisite EG-PW mixture

comprises 50 % ethylene glycol. The specific heat capacity (C_p) for 50 % EG-PW mixture is around $3473 \frac{\text{J}}{\text{kg}} \cdot \text{K}$ at 20 °C, which is approximately 17 % less than the C_p of pure water at the same temperature (Verein Deutscher Ingenieure, 2013). It is essential to recognize that within an actual system, the diminished heat capacity necessitates a compensatory increase in the circulation flow of the thermal medium. This augmentation can enhance the efficiency of heat exchange; however, it may also exacerbate heat accumulation, thereby leading to a decrease in the energy efficiency ratio (Chen, et al., 2023). Research suggests that deriving specific heat capacity values indirectly from experimental measurements of thermal conductivity should be approached with caution, due to the non-linear variation of specific heat capacity with temperature (Ignatowicz & Palm). Nonetheless, for the sake of simplicity within simulation models, it is often assumed that the specific heat capacity of the medium exhibits a linear response.

The electrical characteristics and behavior of the first location-based PVT system simulation are observed in Figure 11. The Figure displays the system's DC-side voltage, the AC-side current and power, and the temperature of the modules. In the graphically presented results provided by the simulation scope tool, the units for the displayed module temperature graph unit are °C, the unit for DC voltage is volts (V), the unit for AC peak power is watts (W), and the unit for AC current is amperes (A). When examining the AC power graph, it is essential to acknowledge the multiplier of $\cdot 10^2$ that is indicated on the left-hand side of the graph. Additionally, it is essential to note that the simulation uses seconds as the time interval. The beginning of the graph corresponds to the system's production at the start of the year, the middle represents summer, and the end part corresponds to the end of the year. It is essential to recognize that in the model, the DC-side voltage is simulated using an ideal controlled voltage source, which changes both with the current produced by the cells and with the temperature of the cells. In the real system, the voltage of the modules decreases to zero when the radiation level is sufficiently low. Due to the implementation of the model, the modules' voltage does not decrease to zero in this case and therefore appears to vary even though the system is not producing power; however, this characteristic does not have a significant impact in

this instance. Nonetheless, from Figure 11, it can be clearly seen how the system's DC-side voltage decreases as the temperature of the modules increases. Based on the data for the first location, the system's annual total electrical energy output is approximately 662 MWh.

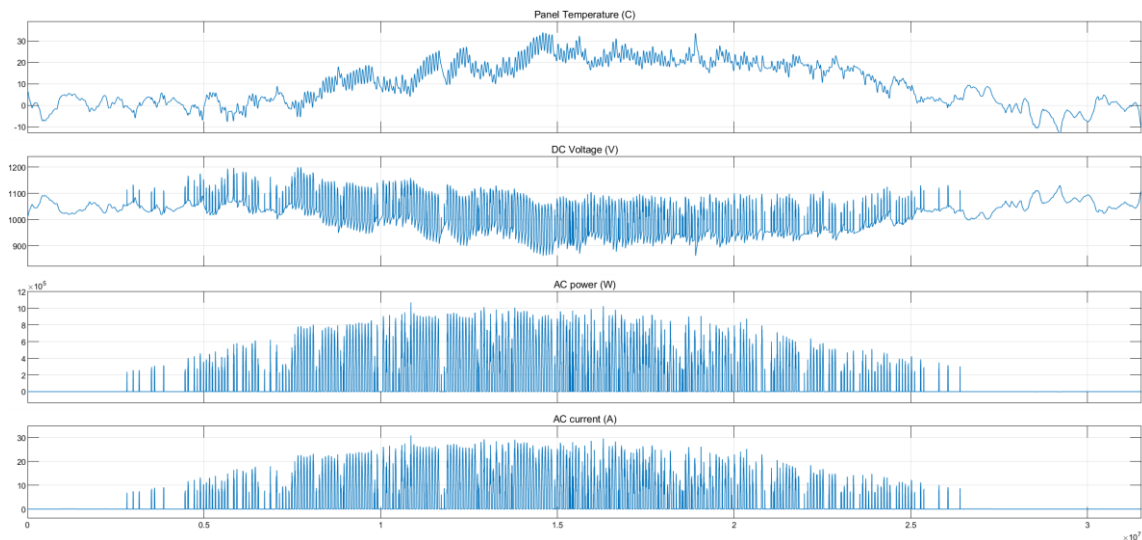


Figure 11. PVT power plant electrical parameters simulation results at location 1.

The thermal characteristics and behavior of the first location-based PVT system simulation are observed in Figure 12. The system's thermal peak power value, the temperature of the heat transfer fluid, the ambient temperature, and the temperature difference between the medium and the ambient temperature are presented in Figure 12. In the graphically presented results provided by the simulation scope tool, both the ambient and the intermediary medium's temperature graphs unit is °C. The graph illustrating the temperature difference between the intermediary medium and the ambient environment is also expressed in °C units. The unit for the system's thermal peak power graph is W. When reviewing the thermal peak power graph, it is essential to acknowledge the unit multiplier displayed in the upper left-hand corner.

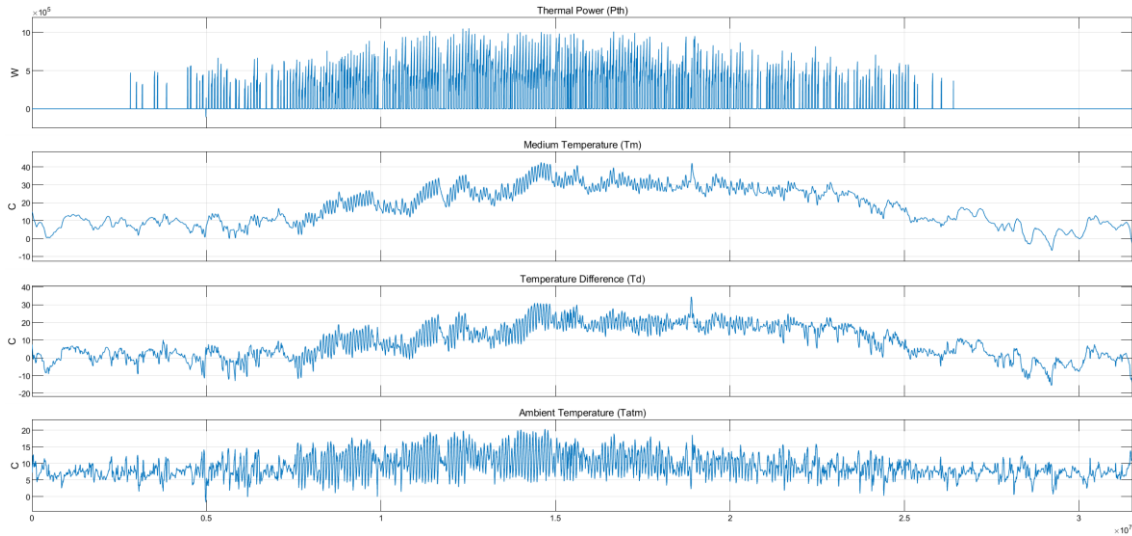


Figure 12. PVT power plant thermal parameters simulation results at location 1.

It can be observed from Figure 12 that the temperature of the medium peaks at approximately 40 °C. The temperature difference appears to average between 20-30 °C during the assumed heat power production period. Based on the results of the simulations, the system's annual total thermal energy output is approximately 729 MWh, and the total annual energy, consisting of the sum of electrical energy and thermal energy, output is approximately 1391 MWh.

3.1.2 Simulation of PVT Power Plant at the Location 2

The meteorological station locates in Mekrijärvi, Iломantsi, Finland (62.76023, 30.95225). The assumed lowest temperature point is -45 °C. The estimate is based on the statistical temperature observations provided by the FMI. The requisite EG-PW mixture comprises 60 % ethylene glycol. The specific heat capacity (C_p) for 60 % EG-PW mixture is around $3284 \frac{\text{J}}{\text{kg}} \cdot \text{K}$ at 20 °C, which is approximately 22 % less than the C_p of pure water at the same temperature (Verein Deutscher Ingenieure, 2013). It is essential to observe that the manufacturer specifies the system's operational limits, indicating that the lowest permissible temperature for the modules is -40°C (Dualsun, n.d.).

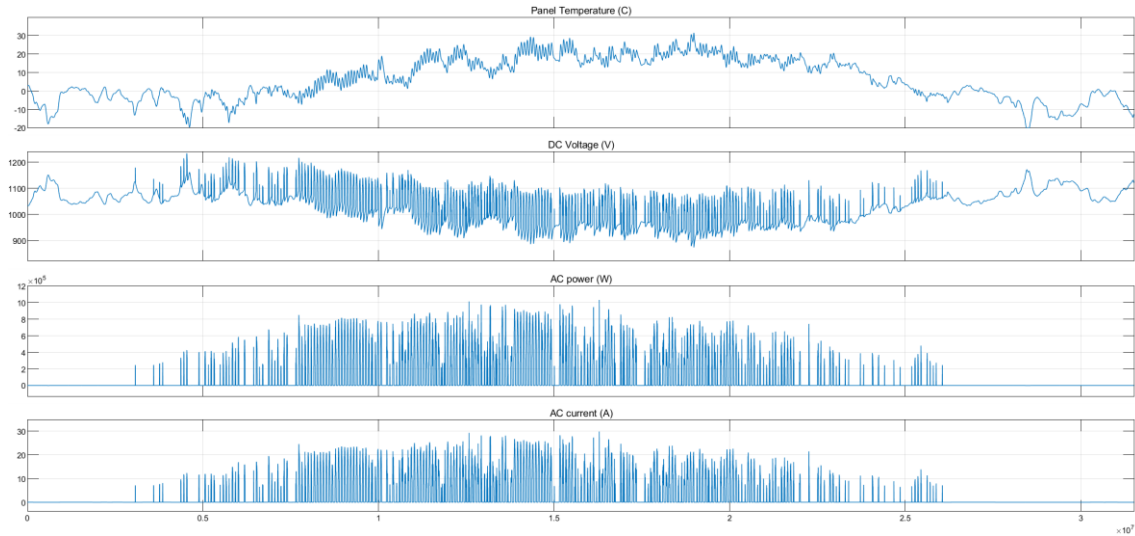


Figure 13. PVT power plant electrical parameters simulation results at location 2.

The electrical characteristics and behavior of the second location-based PVT system simulation are observed in Figure 13. Based on the data for the second location, the system's annual total electrical energy output is approximately 522 MWh.

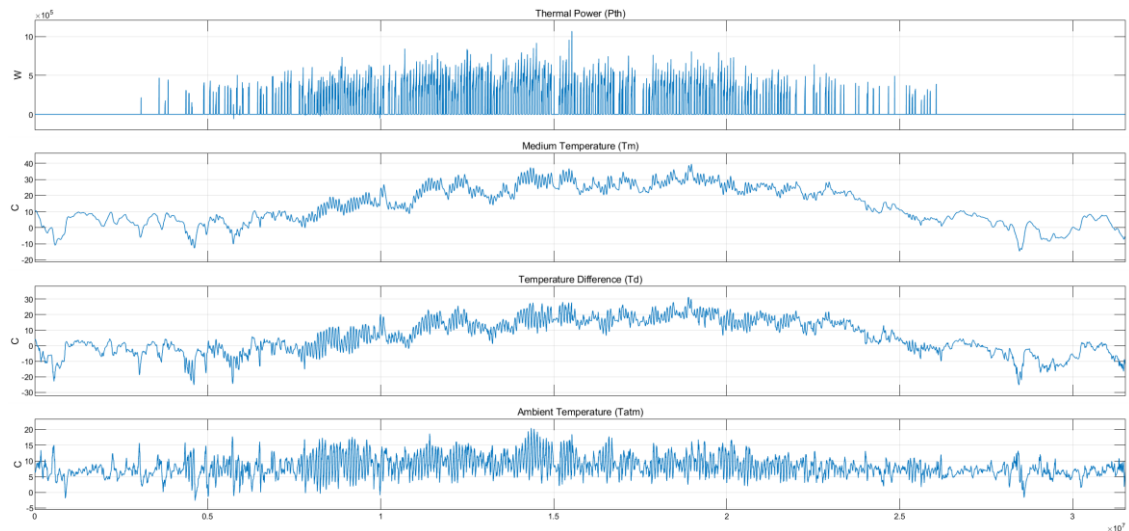


Figure 14. PVT power plant thermal parameters simulation results at location 2.

The thermal characteristics and behavior of the second location-based PVT system simulation, including the thermal peak power value, the temperature of the medium, the ambient temperature, and the temperature difference between the medium and the

ambient temperature, are observed in Figure 14. Based on the results of the simulations, the system's annual total thermal energy output is approximately 471 MWh, and the combined total annual energy is approximately 993 MWh.

3.1.3 Simulation of PVT Power Plant at the Location 3

The meteorological station locates in Tähtelä, Sodankylä, Finland (67.36718, 26.62468). The assumed lowest temperature point is -55 °C. The estimate is based on the statistical temperature observations provided by the FMI. As in the previous case, the requisite EG-PW mixture comprises 60 % ethylene glycol. The specific heat capacity (C_p) for 60 % EG-PW mixture is around $3284 \frac{\text{J}}{\text{kg}} \cdot \text{K}$ at 20 °C, which is approximately 22 % less than the C_p of pure water at the same temperature (Verein Deutscher Ingenieure, 2013).

Figure 15 shows the electrical properties and behavior of the third location-based PVT system simulation. The DC-side voltage, AC-side power and current, and module temperature are all shown in Figure 15. Based on the data for the third location, the annual electrical energy output is approximately 465 MWh.

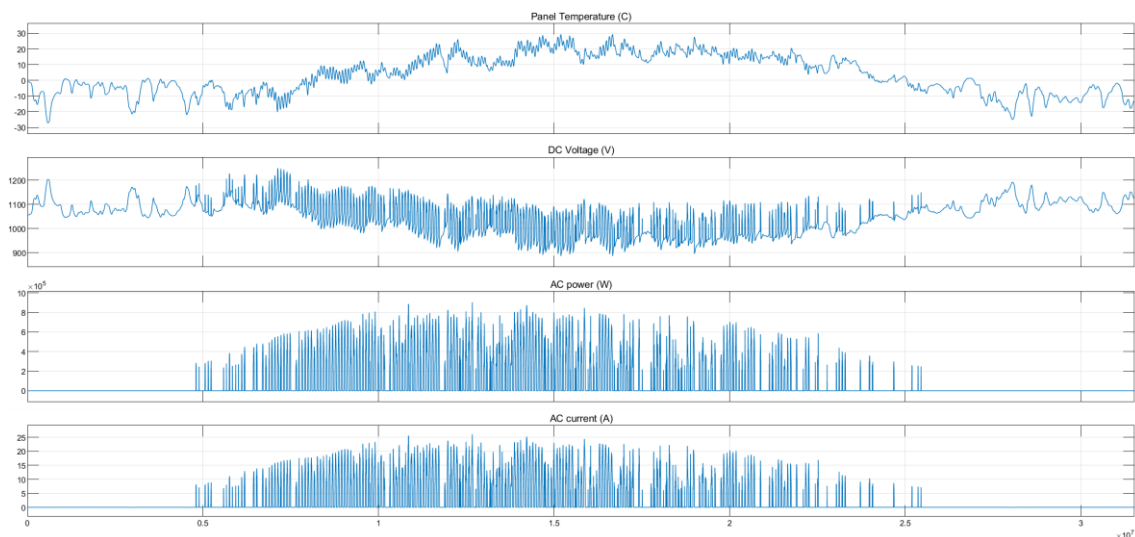


Figure 15. PVT power plant electrical parameters simulation results at location 3.

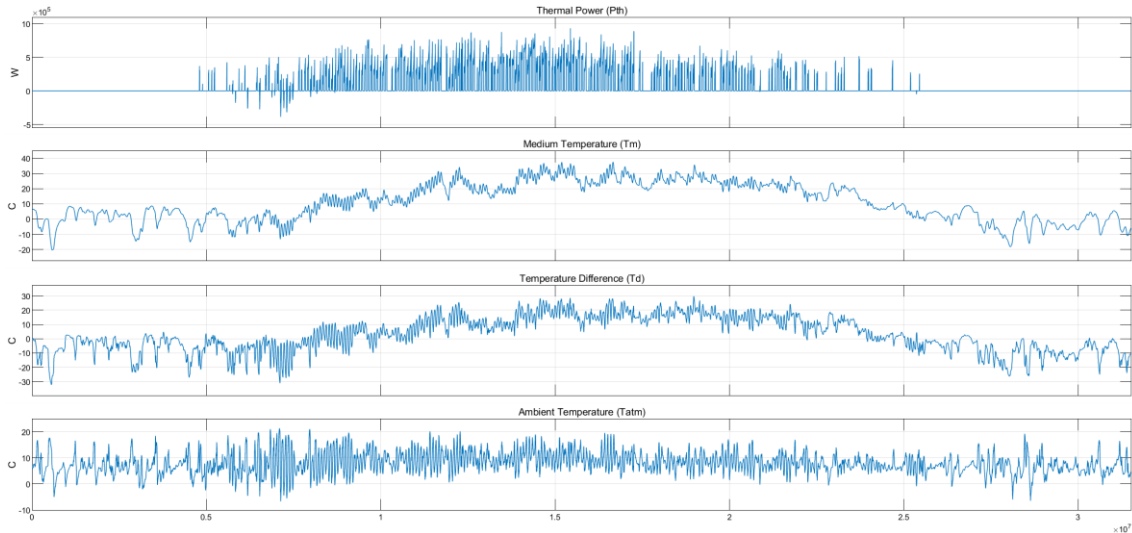


Figure 16. PVT power plant thermal parameters simulation results at location 3.

The thermal peak power value, the temperature of the medium, the ambient temperature, and the temperature difference between the medium and the ambient temperature, are observed in Figure 16. Based on the results of the simulations, the system's annual total thermal energy output is approximately 729 MWh, and the combined total annual energy is approximately 1194 MWh.

3.2 Simulation of PV Power Plant

The photovoltaic generator simulation model from MathWorks, which has been adjusted to the best reliability feasible to suit the requirements of this research, serves as the foundation for the simulation model of the PV power plant that will be presented next (MathWorks Inc, n.d). The simulation model employs technical parameters based on the PV module manufactured in France by Dualsun, and specific type of the model is FLASH 425 Half-Cut Glass-Glass TOPCon PV module. Detailed technical specifications can be found on the manufacturer's website (Dualsun, n.d.). It should be noted that not all the module parameters needed for the simulation model are supplied by the manufacturer. As a result, assumed and estimated parameters, which may differ from actual values, are also used in the simulation model.

The simulation model of a solar power plant consisting of PV modules has been developed within the graphical programming environment of MATLAB's Simulink, and is detailed in Appendix 1. This model integrates processed data on total solar irradiance and the corresponding ambient temperature measurements from each observation site as input. The PV modules' solar cells in the simulation operate based on a two-diode equivalent circuit model, as illustrated in Figure 1, where the output current from the ideal current source is directly proportional to the incident radiation intensity. Cell temperature within the model is determined by both the ambient temperature and the level of radiation. On the DC side, the system employs a DC-AC converter that utilizes MPP tracking technology to optimize voltage for maximum electrical power generation. Optimal DC voltage levels are specified within a voltage matrix, with the peak reference voltage on the DC side established at 1100 V, and the total voltage loss on the DC side maintained at 5 %. The AC side voltage of the converter is specified at 20 kV. The efficiency of the converter is set at 97.1 %, aligning with the efficiency rates of commercially available 1 MW DC-AC converters used in solar power plants.

In all simulation runs of the solar power plant consisting of PV modules, the same dataset has been utilized as the one employed in the simulations of the power plant composed of PVT modules, to facilitate reliable comparative analysis between the results.

3.2.1 Simulation of PV Power Plant at the Location 1

The electrical characteristics and behavior of the first location-based PV system simulation are observed in Figure 17. The DC-side voltage, AC-side power and current, and module temperature are all shown in the figure. In the graphically presented results provided by the simulation scope tool, the units for the displayed module temperature graph unit are °C, the unit for DC voltage is V, the unit for AC peak power is W, and the unit for AC current is A. When examining the AC power graph, it is essential to acknowledge the multiplier of $\cdot 10^2$ that is indicated on the left-hand side of the graph.

Figure 17 makes it very evident how the system's DC-side voltage decreases as the module temperatures increase. Based on the data for the first location, the system's annual total electrical energy output is approximately 656 MWh.

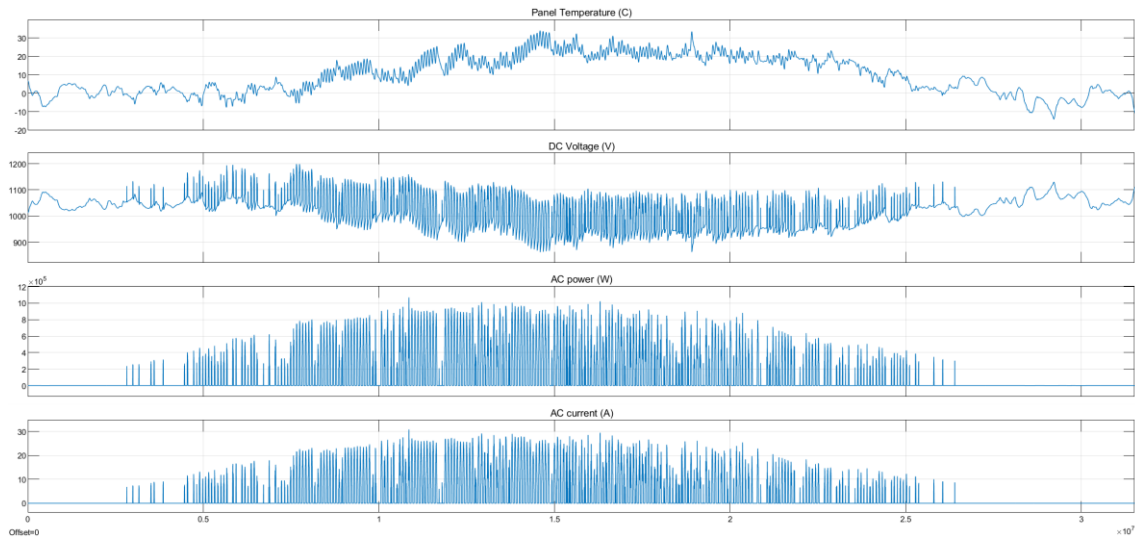


Figure 17. PV power plant simulation results at location 1.

3.2.2 Simulation of PV Power Plant at the Location 2

The electrical characteristics and behavior of the second location-based PV system simulation are observed in Figure 18. The DC-side voltage, AC-side power and current, and module temperature are all shown in the figure. The annual electrical energy output of the simulated PV system is approximately 518 MWh.

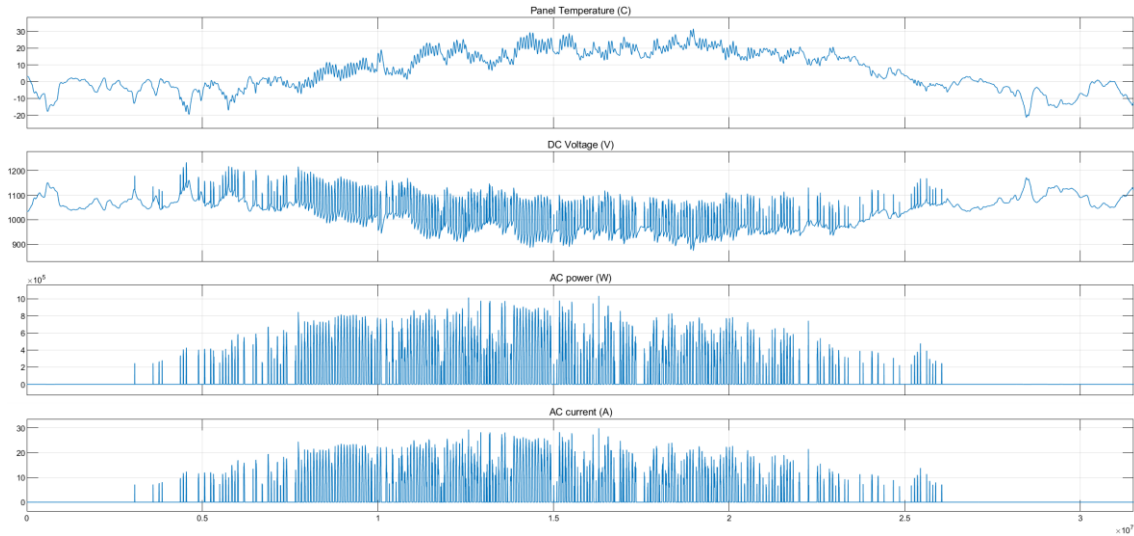


Figure 18. PV power plant simulation results at location 2.

3.2.3 Simulation of PV Power Plant at the Location 3

The electrical characteristics and behavior of the third location-based PV system simulation are observed in Figure 19, including the system's DC-side voltage, the AC-side current and power, and the temperature of the modules. The annual electrical energy output of the simulated PV system is approximately 466 MWh.

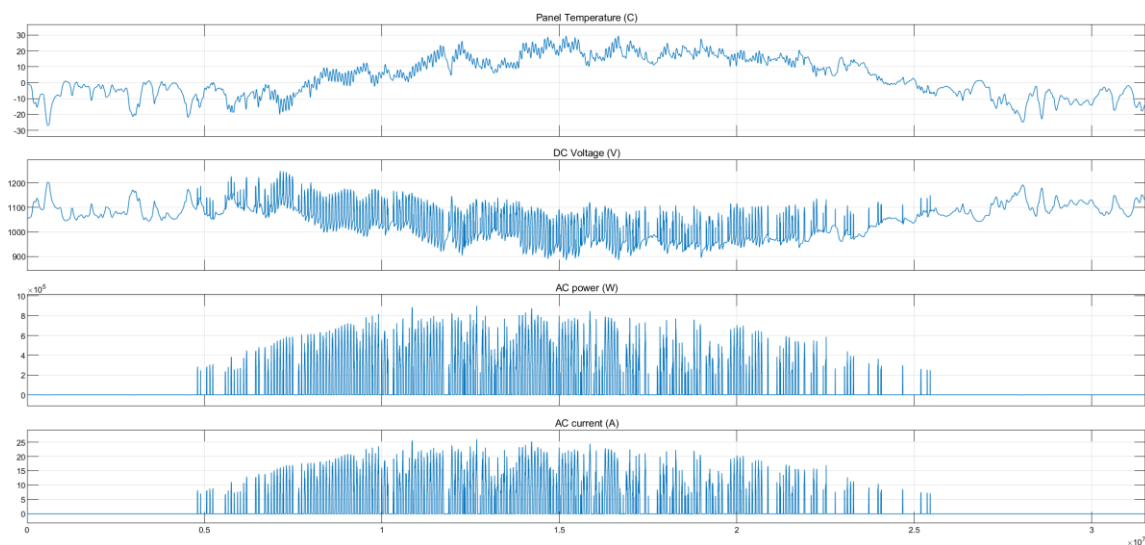


Figure 19. PV power plant simulation results at location 3.

4 Review and Analysis of Technical Results

In this chapter, the results of the simulations are analyzed. In subsection 4.1, the results obtained from simulations of power plants consisting of PVT modules are generally examined and compared with those from simulations of PV power plants. In the subsequent subsection 4.2, the reliability of the simulation results is assessed. Furthermore, the accuracy of the simulation model is intended to be validated through comparison of the obtained results with the operation of existent PVT module-based power systems, which were examined at the end of the theoretical section of the study in the form of a case study examination.

4.1 General Review and Evaluation of Simulation Results

Figure 20 presents the annual total energy yield of the simulated PV power plant in three different locations.

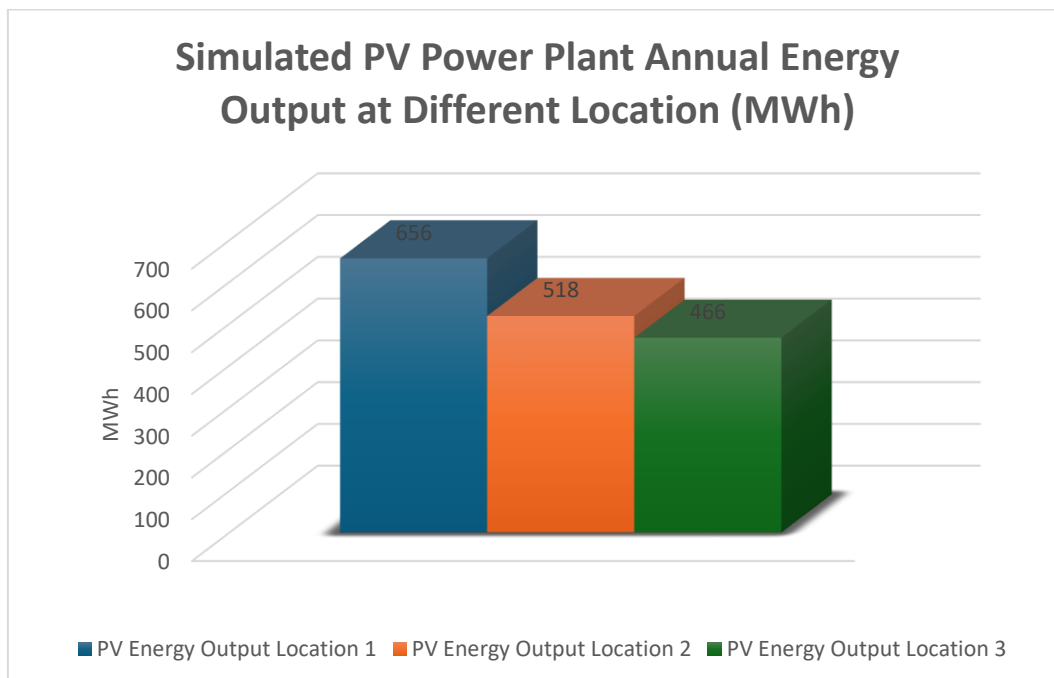


Figure 20. Simulated PV power plant annual energy output at different locations.

It is evident from the figure that the annual total energy output based on the simulation data for location 1 is the highest, while for location 3 it is the lowest. This corresponds to the expected outcome, as location 1 is the southernmost of the observation points used in the simulations, and location 3 is correspondingly the northernmost.

Figure 21 represents the annual production of electrical energy, thermal energy, and total energy of a simulated power plant composed of PVT modules, based on data collected from three different locations.

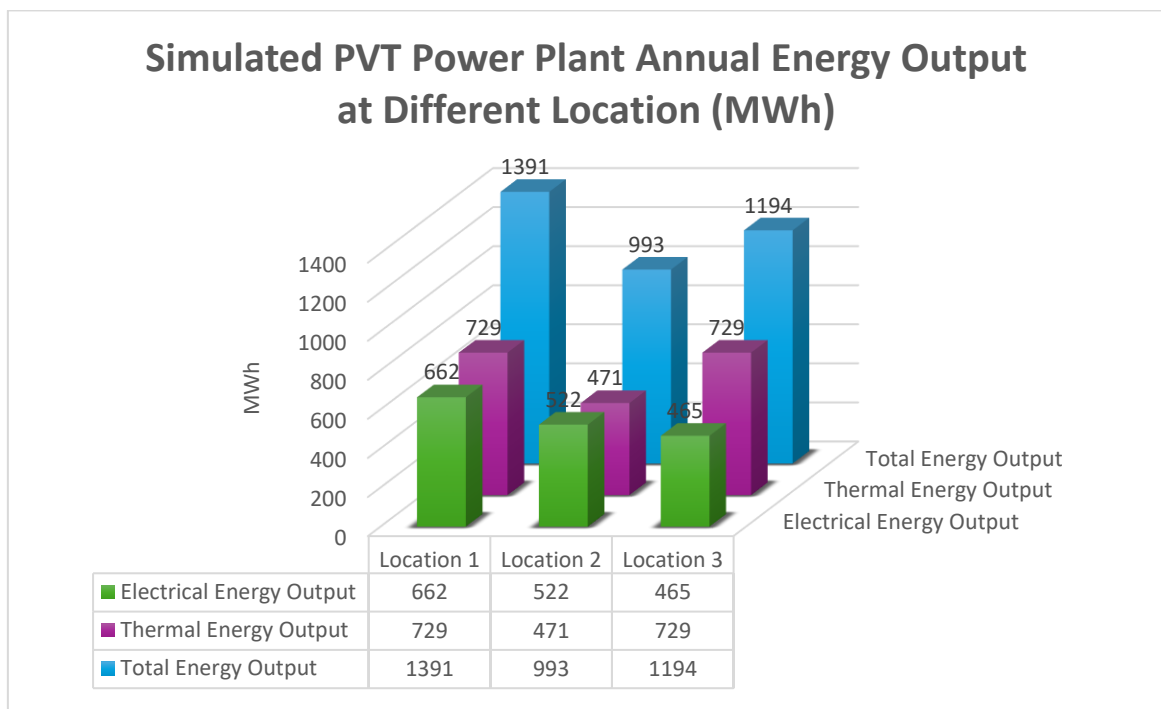


Figure 21. Simulated PVT power plant annual energy output at different locations.

The figure clearly shows that the annual amount of electrical energy from the simulation based on data from location 1 is the highest, whereas it is the lowest for location 3. This result aligns with expectations and is consistent with the simulation outcomes for the PV system. The simulation results based on data from location 1 indicate that the annual amount of electrical energy produced by the PVT system is 0.9 % greater than that of the simulated PV system. Similarly, in location 2, the annual electrical energy yield from the PVT system is 0.75 % higher in comparison to the PV system. Conversely, in location 3,

the annual electrical energy produced by the PVT system is 0.22 % less than the energy yield of the simulated PV system. The results based on data from locations 1 and 2 correspond to the expected outcomes. However, the results derived from data for location 3 deviate from the anticipated results.

The simulation results indicate that for the PVT system based on data from location 1, the amount of thermal energy produced annually is 10 % greater relative to the amount of electrical energy produced. This result matches the expected outcome. However, the simulation results for location 2 show that the amount of thermal energy produced by the PVT system is 10 % less compared to the produced electrical energy, deviating from the expected result. For location 3, the simulation results reveal that the thermal energy output of the PVT system is 57 % higher relative to the electrical energy produced, which also differs from the anticipated outcome.

The total energy produced by the PVT system is the sum of the electrical and thermal energy outputs. Therefore, only the simulation based on data from location 1 aligns with the expected results. In contrast, the total energy outcomes for locations 2 and 3 do not match the expected results due to the discrepancies in the relative proportions of thermal and electrical energy production.

4.2 Evaluation and Validation of the Reliability of Simulation Results

The simulated results for the PV solar power plant align with the expected outcomes for all locations. The simulated results of the PV power plant have been compared with those generated by the photovoltaic geographical information system (PVGIS), a tool developed by the European Commission Joint Research Centre, across all three different locations (European Commission, n.d). The PV simulation model used in the study appears to produce results that correspond sufficiently with the outcomes obtained from the PVGIS tool. However, when comparing the results, it is essential to acknowledge that the PVGIS database utilizes longer-term averaged data, whereas the simulations in this

study are based on data from only one year. This difference in data usage can account for any discrepancies between the PV simulation model and the PVGIS tool results.

In Finland, renewable energy production systems such as wind and solar power are often evaluated using the metric known as the utilization period of maximum load. This metric is determined by comparing the system's annual total energy output to its rated power capacity, with the unit of measurement being in hours. When assessing the productive capacity of solar power plants in Southern Finland, the reference value for the utilization period typically ranges between 800 to 900 hours (AF-Consult Ltd, 2016). Both the PV and PVT systems' simulation results based on data for location 1, which is in Southern Southwest Finland, indicate that the power plants' utilization period of maximum load values fall below 700 hours. This deviation from the expected value can also be explained by the quantity of data used in the simulation. Research from the FMI indicates that in Southern Southwest Finland, the coefficient of variation for the number of sunshine hours can be up to 53 % over a 29-year observation period (FMI, n.d). This variability in solar irradiance could significantly impact the predicted performance of solar power systems and thus should be acknowledged when interpreting simulation results and comparing them to long-term averages or expected values.

While developing the PVT simulation model, its behavior was initially examined by conducting simulations with constant values, including those according to the STC. Appendix 3 presents the electrical characteristics of the PVT simulation model during a test run, while Appendix 4 illustrates the thermal characteristics of the model during a test run.

When comparing the PVT simulation results to the case studies presented in the theoretical section of the study, it can be observed that the simulation results based on data for location 1 correspond well with each other, considering the locations of the case studies and the differences in the properties of the heat transfer medium used in the systems.

The amounts of thermal energy produced by the PVT system in locations 2 and 3, as per the simulations, deviate from the expected values and do not fully align with the case studies. On the other hand, one case study demonstrated that in situations where the system's heat transfer fluid temperature becomes sufficiently high, it can no longer cool the solar cells of the module effectively. As a result, the electrical power output of the modules decreases while the thermal power output increases. The simulation results based on data for locations 2 and 3 are consistent with these observations from the case study. However, deviations from the expected results may suggest that the model's performance is not entirely stable under all conditions. Alternatively, these discrepancies could be due to the data used in the simulations, and it is also possible that the results accurately reflect the conditions conveyed by the data. Nevertheless, more robust validation of the PVT simulation model requires further research and the use of a more comprehensive dataset.

5 Economic Review and Analysis

In an economic analysis of power production units, one popular tool for comparing various power generation technologies is the levelized costs of energy (LCOE), which combines all the fixed and variable costs into one specific cost measure over the life cycle of the system (Kabeyi & Olanrewaju, 2023). In the literature LCOE abbreviation also refers to the term levelized cost of electricity which is a financial metric for contrasting the lifetime expenses of producing electrical energy using different production systems (Raikar & Adamson, 2020). The LCOE for an energy-producing system is defined as the quotient of the sum of the system's lifecycle costs and the total amount of energy it produces over its lifetime. In other words, the LCOE represents the average net cost of the energy generated by the system, discounted to the present value (Kabeyi & Olanrewaju, 2023). In this chapter, the electrical and total energy generated by power plants composed of PVT modules using the LCOE analysis method is examined. As well as the electrical energy produced by power plants consisting of PV modules through the LCOE analysis are investigated. Finally, the LOCE analysis results of the PVT system and the PV system are compared with each other.

In an industrial-scale solar power system that generates electricity, the cost of the modules themselves accounts for approximately 37 % of the total lifecycle costs. The remaining expenses of the system are composed of various other components, including the design and installation, costs associated with connecting to the grid, and land-related costs. These additional costs are collectively known as the balance of system (BOS) costs. BOS includes structural and electrical components, inverters, and other elements necessary to make a functioning solar power system, excluding the solar modules. It also encompasses labor, permitting, inspection, interconnection, and any maintenance and operational costs over the lifetime of the system (VDMA, 2023). Figure 22 illustrates the allocation of total costs across various cost factors for large-scale PV power facilities, specifically those with capacities exceeding 10 MW. From the figure, it can be observed that forecasts suggest a future decrease in investment costs for both PV modules and

the overall investment of a system, which is attributable in part to the anticipated reduction in component price levels. The data presented in the figure, which corresponds to the year 2024, is utilized in the LCOE analysis for both PV and PVT power plants, assessing the overall costs of the system.

Cost elements of PV System Worldwide

For Systems > 10 MW

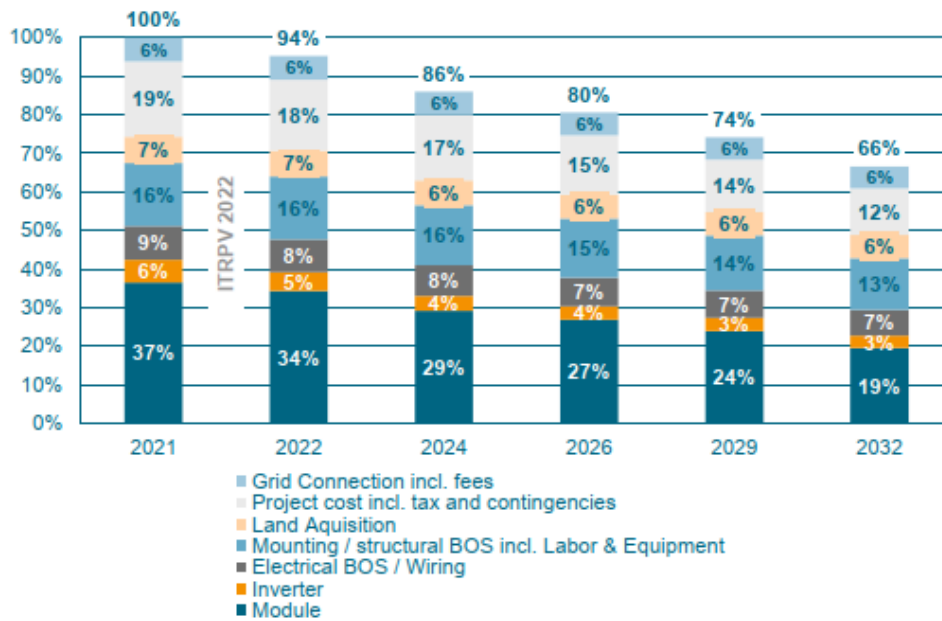


Figure 22. Cost components of large-scale PV installations (VDMA, 2023).

In LCOE analyses, the form of investment loan assumed is an annually amortizing fixed-interest annuity loan. The LCOE calculations are carried out under the assumption that the investment is fully financed through an investment loan without any invested initial capital or investment grants. This means that the entire capital cost of the energy system, including interest and principal repayments, is factored into the LCOE calculation over the system's expected life. In the LCOE analysis, the interest rate applied to the total investment loan is based on the reference rate announced by the European Central Bank for Finnish banks, which is intended as the guiding rate for new business annuity loans and stands at 5.44 % in the reference month cited (European Central Bank, 2024).

When estimating the total amount of energy produced over the lifecycle of both the PVT and PV systems, the degradation of the modules due to aging and the resulting decrease in power output have been considered. The power degradation is caused typically due to factors such temperature changes, and material fatigue as has been stated in the theoretical part of the study. Figure 23 illustrates the decline in power production of both PVT and PV modules as a function of time. The reduction in power output is assumed to decrease nearly linearly according to the manufacturer's specifications for the first 25 years. After this period, the decrease in module power production is expected to accelerate cumulatively.

However, it is essential to note that for the LCOE analyses in this study, the operational lifespan of the systems is assumed to be 25 years. This means that the LCOE calculation considers the energy production and associated costs within this timeframe, without accounting for the potentially accelerated module degradation beyond the 25-year mark. This approach is common in LCOE analyses as it aligns with the typical warranty period and expected economic life of solar modules, although the actual useful life of the modules may extend beyond this period.

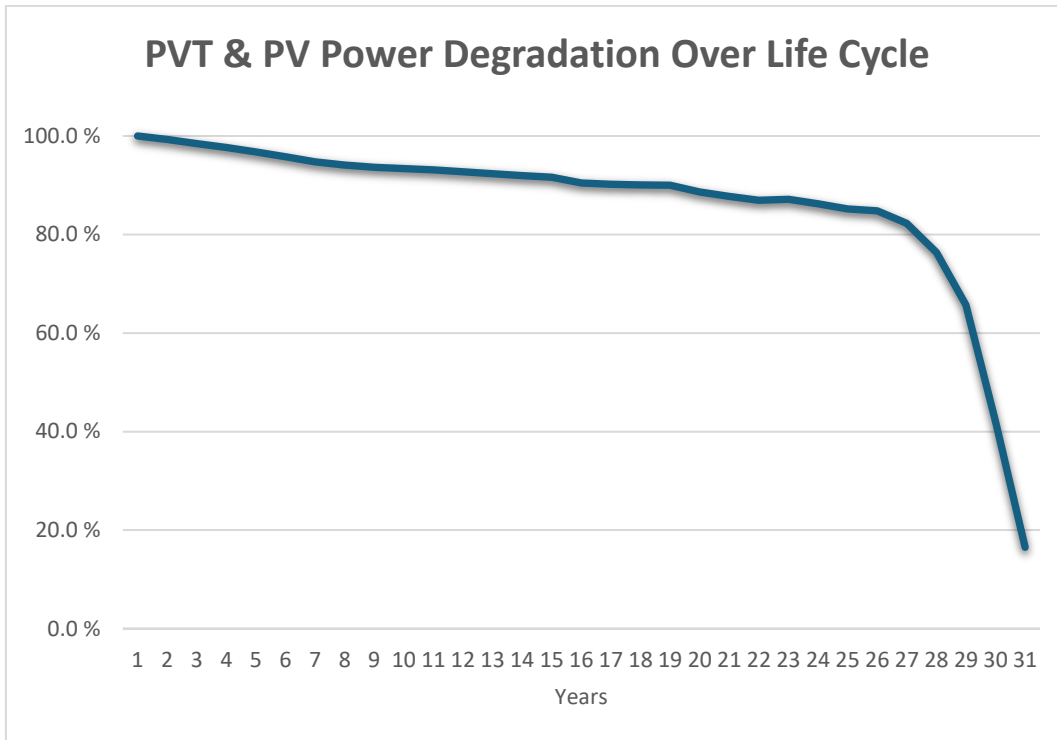


Figure 23. PVT & PV module power degradation over time.

According to a study by the FMI based on satellite measurements, there is a minor fluctuation of less than $\pm 0.1\%$ in total solar irradiance annually during the 11-year cycle of solar sunspots (Nevanlinna, 2012). While the range of variation in total solar irradiance due to solar activity fluctuations is relatively small, it is noteworthy that the amount of solar radiation reaching the Earth's surface annually can vary more significantly locally due to factors such as varying cloud cover. Therefore, when examining the energy output of installations consisting of PV modules and PVT modules over a 25-year period, the coefficient of variation is estimated to be $\pm 20.1\%$, encompassing the effects of solar activity variation. The assessment is based on observational data from the FMI, which has compared the statistics for sunshine duration and global radiation for the reference period 1991-2020 on a station-by-station basis (FMI, n.d). By including these elements in the analysis, the estimates may provide a more comprehensive understanding of the expected performance and reliability of the solar power plant over its operational lifespan.

5.1 PV Power Plants LCOE Analysis

The average electricity price in Europe was approx. 97 €/MWh in 2023 (Wasmeier, et al., 2024). In 2023, the average cost of electricity stood at 56.5 €/MWh, positioning Finland as the country with the second-lowest electricity prices in Europe (Energiateollisuus ry, 2024). In the United Kingdom, the cost of PV electricity is less than the wholesale price of electricity, at roughly 174 €/MWh for the smallest-scale systems and 59 €/MWh for large-scale systems currently (Mandys, et al., 2023). Note that the currency has been changed from GBP to EUR based on the exchange reference rates of the day before citing. The exchange reference rates (EUR vs. GBP) on 26 March 2024 was 0.85846 (European Central Bank, 2024).

The unit price of the PV module employed in the calculation of the LCOE for a PV module-based power plant is 112 €, excluding VAT. This price has been sourced from the website of a dealer based in France (Planet Soar Shop, n.d). Based on the data pertaining to module costs and the information on cost elements as presented in Figure 22, and with the estimation that the module constitutes 29 % of the total costs, the CAPEX for the PV plant with an electrical peak capacity of 1 MW is approximately 910 000 €.

Figure 24 presents estimates based on simulation results for the energy production of a PV solar power plant as a function of time in three different locations throughout the system's lifecycle. The estimates include the power degradation over time and the coefficient of variation in solar irradiance.

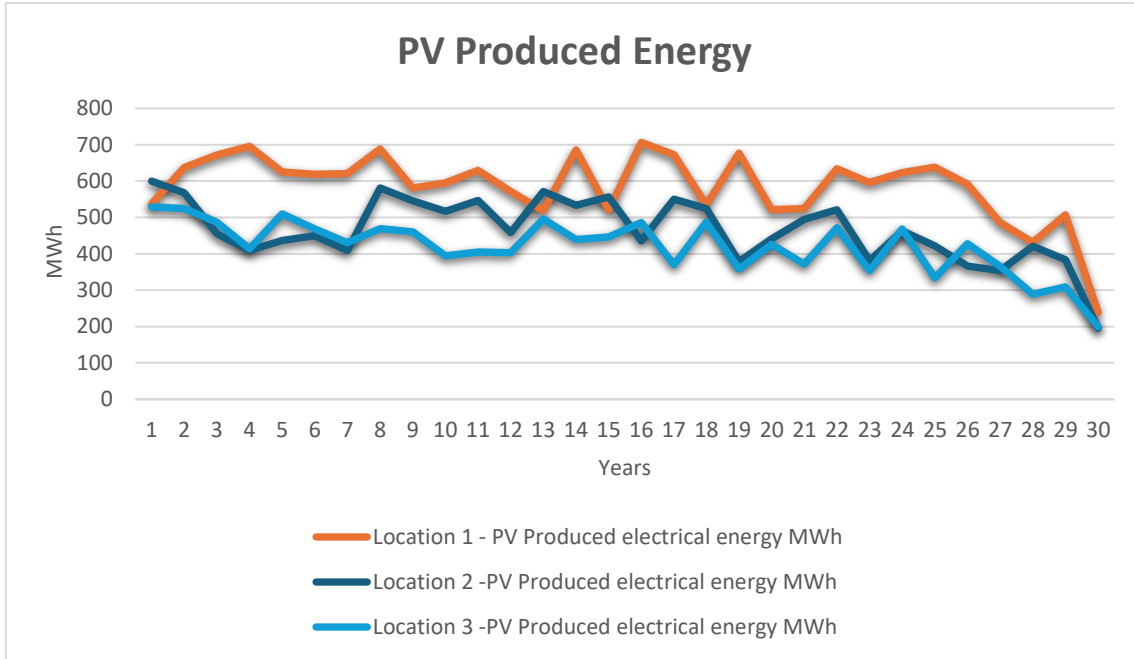


Figure 24. Energy output of simulated PV power plants over a life cycle period.

Based on the estimated lifetime energy production of the PV system and the system's cost estimates, the LCOE has been calculated for all three different locations. The LCOE values for the PV system in the three different locations are presented in Figure 25. The LCOE values for the PV systems in the three different locations presented in the figure follow the expected pattern, meaning that the net cost of energy produced by the system located at the southernmost point is the lowest, while the energy produced by the system situated at the northernmost point is the most expensive. This progression reflects the anticipated trend where the cost of energy production typically rises with decreasing solar irradiance, which is often the case as one move from lower to higher latitudes.

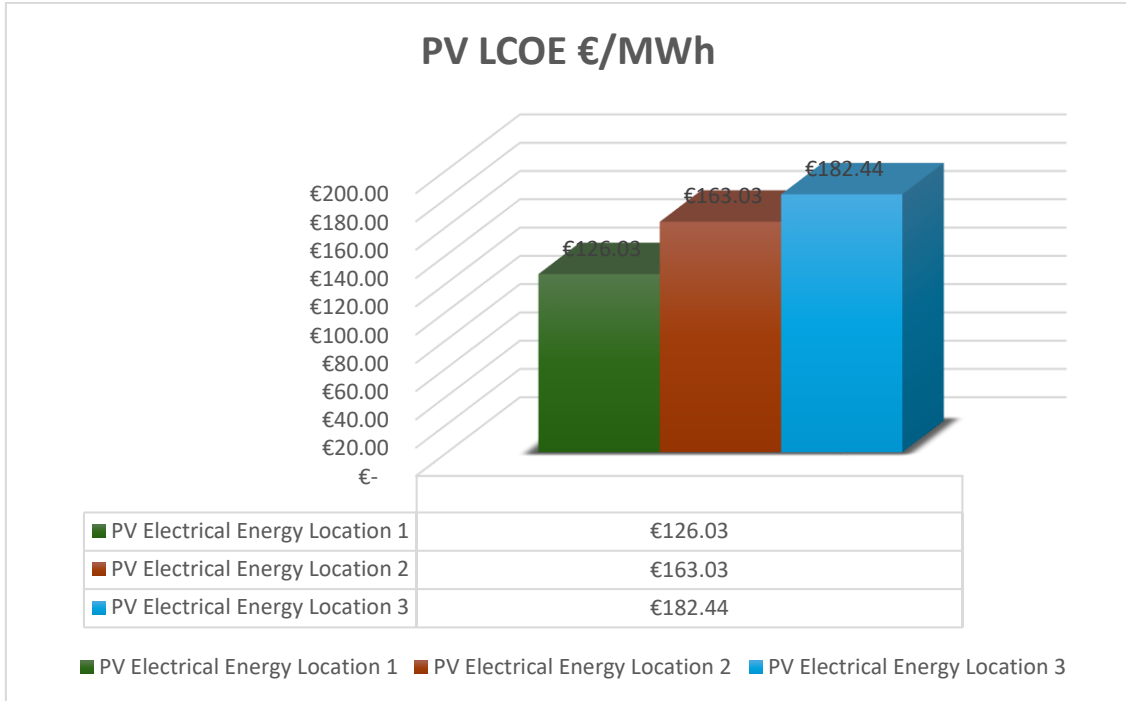


Figure 25. LCOE of simulated PV power plants.

The calculated LCOE values for PV systems located in different locations appear credible. The LCOE values correspond acceptable to the expected values in relation to the average price of electricity produced in Europe, as well as the cost of electricity generated by solar power as reported by the United Nations, considering that the cost estimates in this study do not include potential investment subsidies or payable energy tariffs.

5.2 PVT Power Plants LCOE Analysis

According to the survey statistics compiled by Energy Industry Association, in Finland, the price of energy sold into the district heating network, including taxes, and primarily produced by combined heat and power plants, has an arithmetic mean of 81.27 €/MWh and a median price of 86.44 €/MWh. The statistical data is based on information provided by approximately 100 district heating companies operating in around 170 municipalities (Energiateollisuus ry, 2024).

When assessing the total cost of a power system comprised of PVT modules, it is postulated that in addition to the investment price of the PVT modules, the investment costs consisting of all other factors are 20 % more substantial compared to a conventional power system constituted of PV modules. This estimation is grounded on research that juxtaposed the investment expenditures of PVT systems with those of PV systems (Abdul-Ganiyu, et al., 2021). Nonetheless, it should be acknowledged that the estimation is predicated on a system of limited scale, and the actual divergence in investment costs between extensive PVT and PV systems may be more pronounced or less marked. The CAPEX for the PVT plant with a 1 MW electrical peak power is estimated to be approximately 2 100 000 €, which is approximately two times greater than that of a comparable PV module-based power plant.

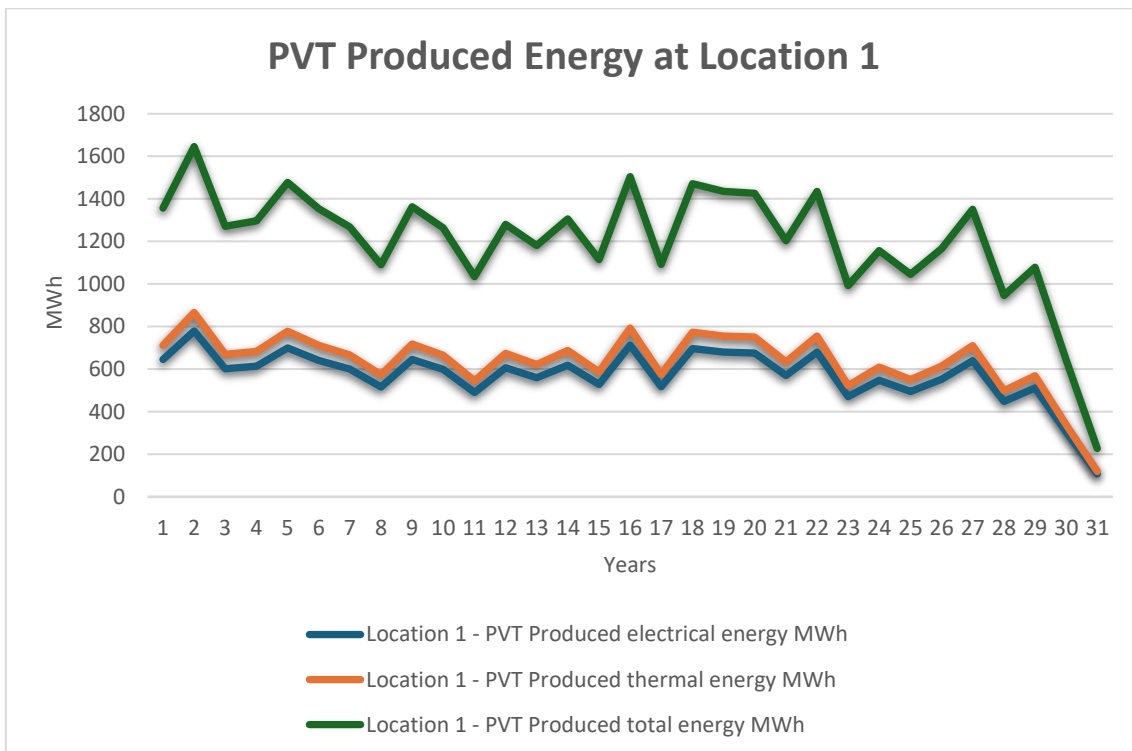


Figure 26. Energy output of the simulated PVT power plant at location 1 over a life cycle period.

Figure 26 presents estimates based on simulation results for the energy production of a PVT solar power plant as a function of time in location 1 throughout the system's lifecycle. The estimates include the power degradation over time and the coefficient of variation

in solar irradiance. In Figure 26, the electrical energy, thermal energy, and total energy produced by the PVT system are represented as a function of time throughout the system's lifecycle.

In Figure 27, the electrical energy, thermal energy, and total energy produced by the PVT system in location 2 are represented as a function of time throughout the system's lifecycle.

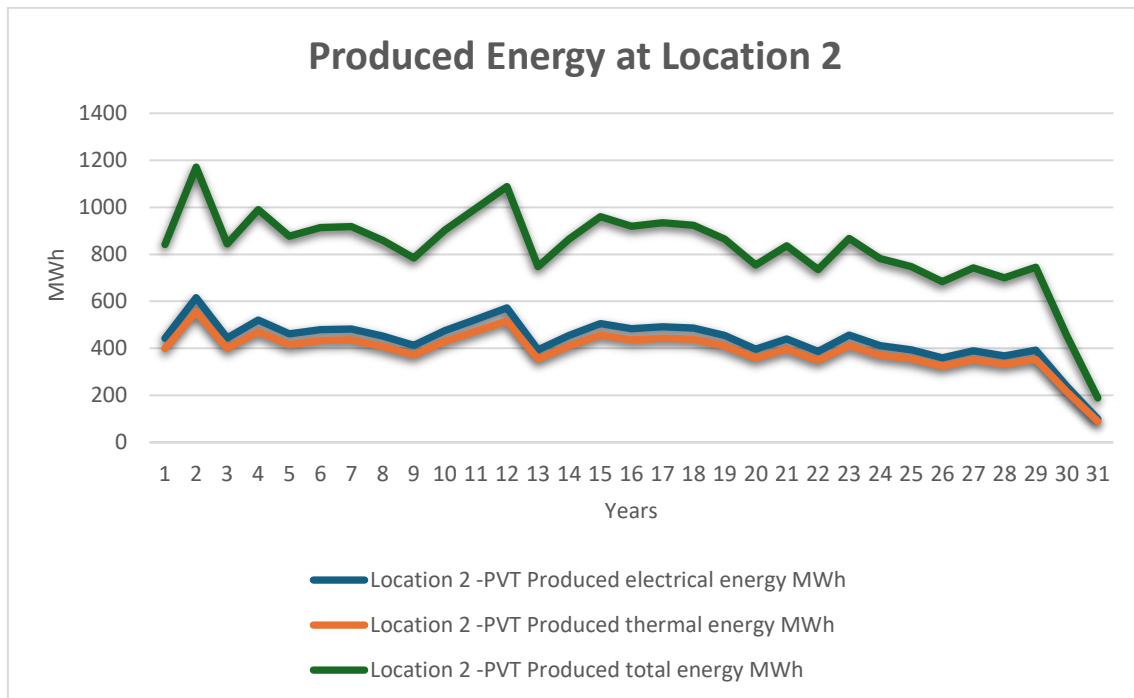


Figure 27. Energy output of the simulated PVT power plant at location 2 over a life cycle period.

Figure 28 represented the electrical energy, thermal energy, and total energy produced by the PVT system in location 3 as a function of time throughout the system's lifecycle.

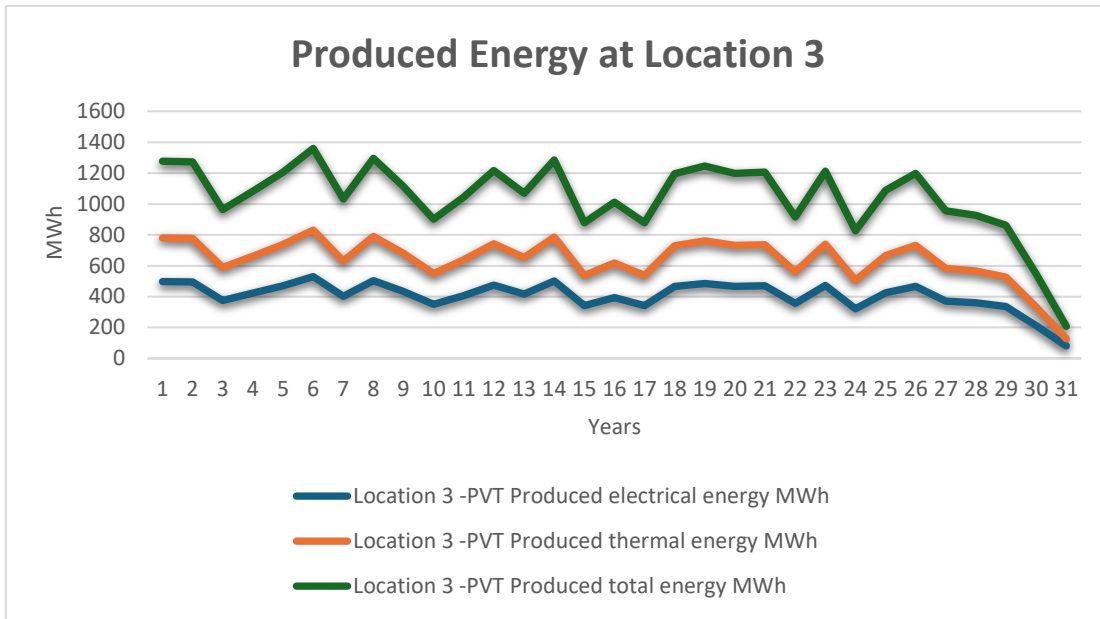


Figure 28. Energy output of the simulated PVT power plant at location 3 over a life cycle period.

In Figure 29, the LCOE for the electrical energy produced by the PVT system is presented for three distinct locations.

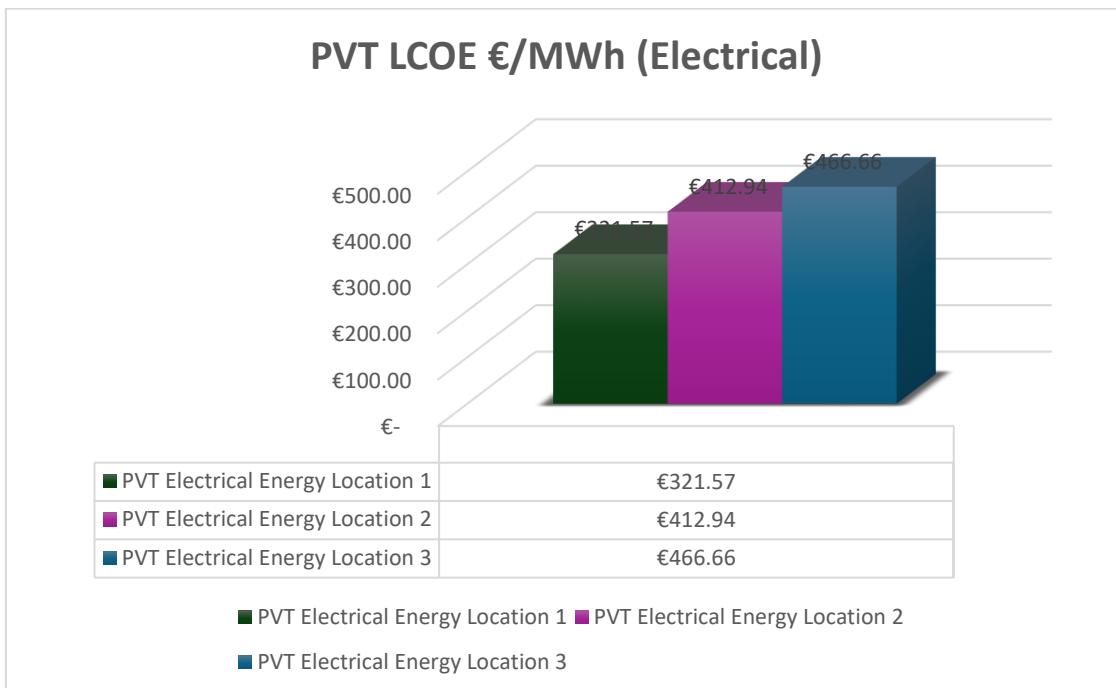


Figure 29. Electrical energy based LCOE of simulated PVT power plants.

The LCOE values presented in Figure 29 correspond to the expected values, with the LCOE increasing almost linearly from the southernmost location towards the higher LCOE value of the system located at the northernmost site.

In Figure 30, the LCOE for the thermal energy produced by the PVT system is depicted across three disparate locations. The LCOE values for the thermal energy produced by the PVT system presented in the figure align with the anticipated value for location 1. However, for the PVT systems situated in locations 2 and 3, the values deviate from the expected outcomes. These deviations can be attributed to discrepancies between the simulation results and the hypothesized results. Consequently, the LCOE value for the thermal energy at Location 3 does not appear to be a reliable result. Further investigation may be necessary to ascertain the underlying factors contributing to these discrepancies and to enhance the accuracy of the model's predictive capabilities.

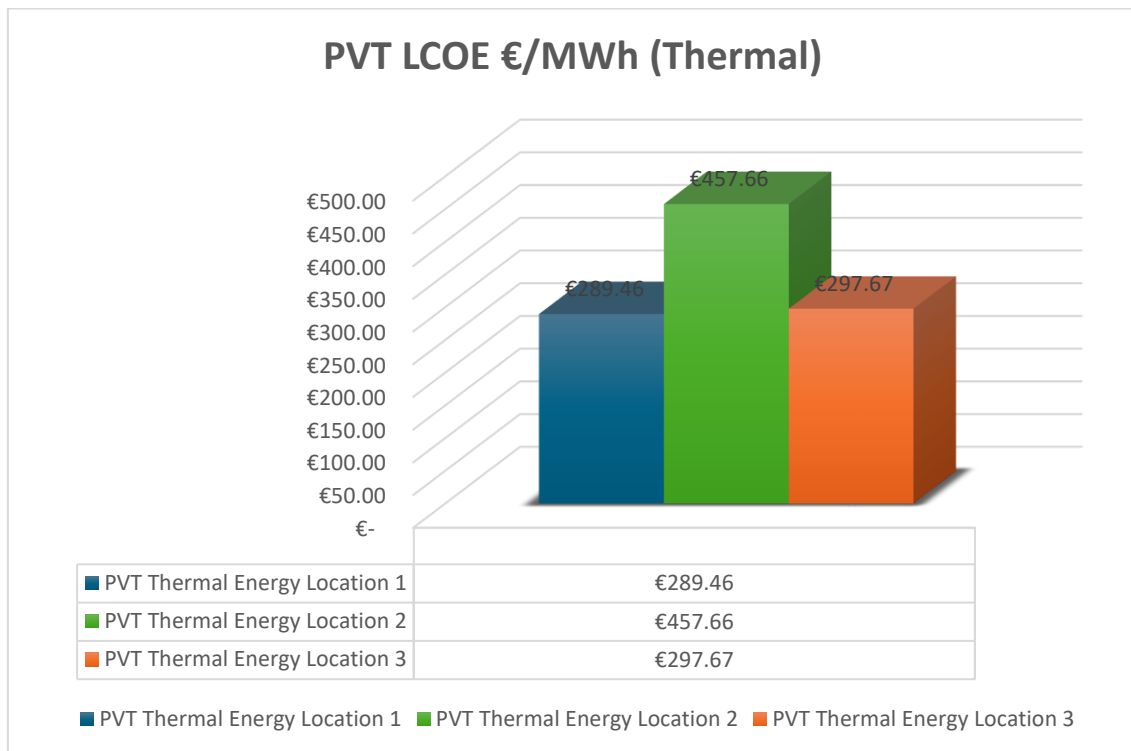


Figure 30. Thermal energy based LCOE of simulated PVT power plants.

From the results of the LCOE for the thermal energy produced by the PVT system depicted in Figure 30, it can be discerned that the cost of thermal energy generated by the PVT system is substantially higher compared to the average price of energy produced for district heating networks in Finland.

Figure 31 presents the LCOE values of the total energy produced by the PVT system across three different locations. The results for locations 1 and 2 are in line with expectations. However, the results for location 3 cannot be considered particularly reliable due to the significant deviation of the cost of thermal energy produced in location 3 from what was anticipated. This discrepancy suggests that there may be unique factors at location 3 in the simulation affecting the performance and cost-efficiency of the PVT system's thermal energy output.

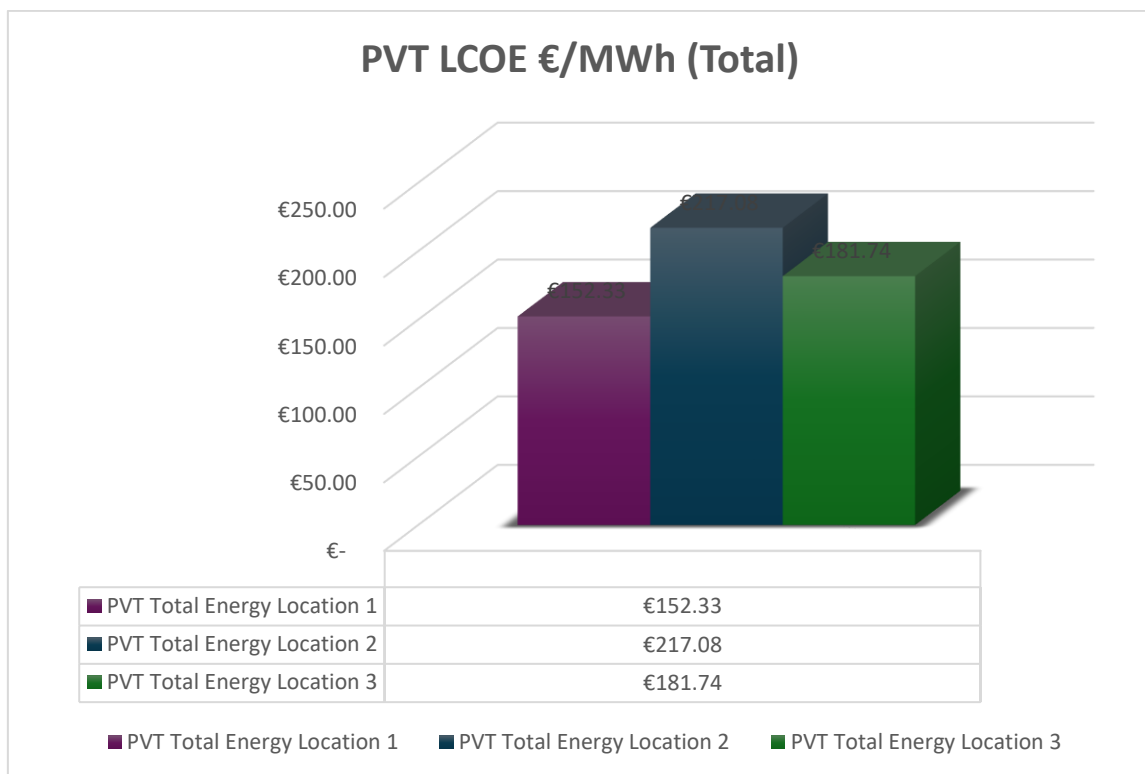


Figure 31. Total energy based LCOE of simulated PVT power plants.

5.3 Comparison of the Analysis Results

In Figure 32, a comparison is presented of the LCOE values for PV and PVT systems across three distinct locations. The graph demonstrates a predictable increase in the LCOE values for electricity generated by both systems as one moves from the southernmost location to the northernmost. The results depicted in the figure suggest that in location 1, the electricity produced by the PVT system is 150 % more expensive than that generated by a comparable PV system.

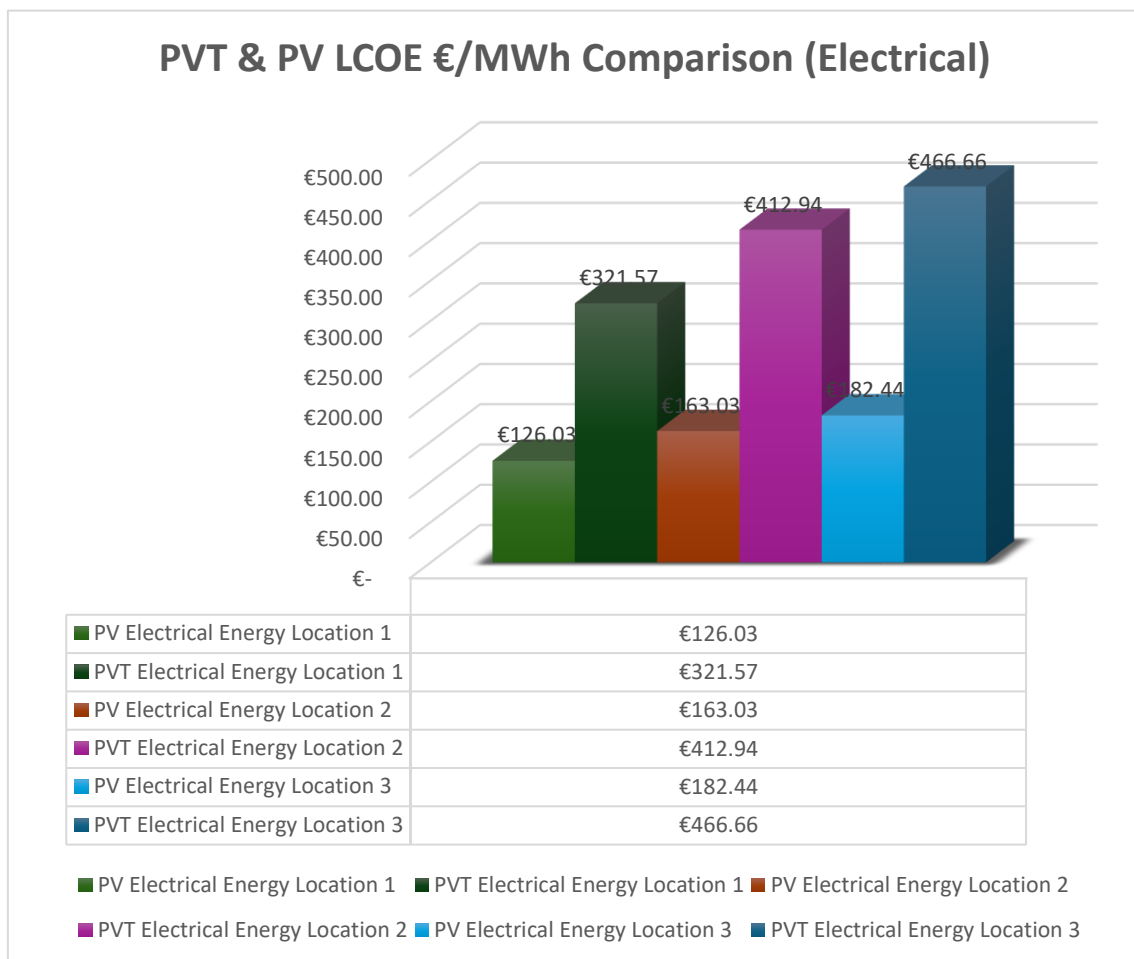


Figure 32. Comparison of simulated PVT & PV power plant LCOE based on electrical energy.

In Figure 33, the analysis focuses on how the LCOE for total energy generated by a PVT system compares to that of a similar PV system across three different locations. It is

essential to acknowledge that the LCOE value for total energy at location 3 should not be considered reliable, as mentioned in Section 5.2. Consequently, this value can be excluded from the analysis. Examining the LCOE values for total energy produced by PVT and PV systems in location 1, it is observed that the total energy produced by the PVT system is 20 % more expensive than that generated by a comparable PV system. Furthermore, as the calculations indicate, to ensure the economic viability of the total energy produced by the PVT system in relation to a similar PV system, the investment return should be at least 20 % of the initial system investment.

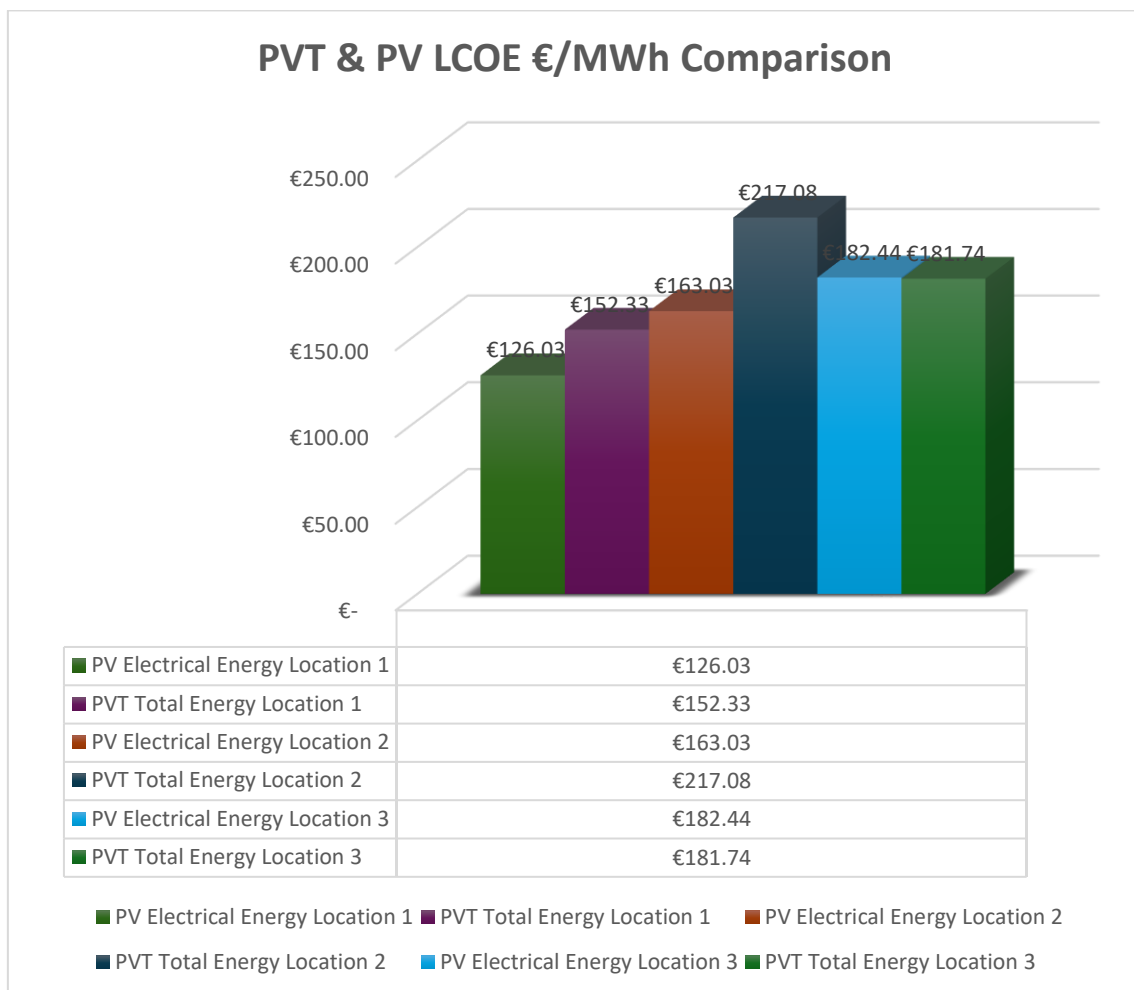


Figure 33. Comparison of simulated PVT & PV power plant LCOE based on total energy.

The results of the economic analysis suggest that, at the current level of expense, the implementation of large-scale PVT power plants is not economically viable without

investment subsidies or energy tariffs that compensate for the energy produced. In Finland, however, it is feasible to seek funding for novel projects researching and developing renewable energy sources. Financing for renewable energy development initiatives in Finland can be solicited from governmental entities such as Business Finland, which serves as the nation's official agency for trade and investment promotion, as well as innovation funding (Business Finland, 2024). Additionally, support for innovative renewable energy projects can be pursued from the Energy Authority, an expert agency within the purview of the ministry of economic affairs and employment (Energy Authority, 2022). Furthermore, assistance for new renewable energy development projects can also be sought from the European Union, which offers numerous financing tools and programs, including but not limited to the Horizon Europe-, the Innovation fund-, and the Life clean energy transition funding programs (European Commission, n.d).

6 Discussion

In this section, the research topic, and the associated challenges, as well as the need for further research and areas for development, are discussed. As the theoretical framework of the research progressed, it became apparent that although there is an extensive body of knowledge and scientific publications on the subject, most of these focus on theoretical methods. Notably, there is a paucity of empirical research based on practical measurements concerning the output of large-scale (1 MW or larger) PVT power plants. Moreover, one of the challenges in assembling the source material for the study was that most research concentrates on the performance of PVT modules in climate zones situated closer to the equator. In Finland, the Nordic countries, or regions with similar climatic conditions, there has been scarcely any research conducted previously that evaluates the use of PVT modules in large-scale power plants. Consequently, this subject necessitates more extensive research and scrutiny in the future.

During the research, it became evident that obtaining CAPEX and OPEX data for commercially available PVT modules from manufacturers is relatively challenging. Consequently, the study has utilized the available information, and it should be noted that these details may not fully correspond to the up-to-date figures.

When evaluating the use and outcomes of simulation models for PVT systems, it is important to recognize that PVT simulation is a simplified representation of the actual system. For instance, the model may not correspond to actual values in terms of losses in thermal channels with high precision, nor consider the energy consumed by circulation pumps or the losses in heat exchangers. The simulation model requires further development and must be tailored on a case-by-case basis to adequately reflect the specific requirements and unique characteristics of the system under examination. The data utilized in the simulations encompasses only a single year's worth of measured observations. Employing a more comprehensive dataset would likely yield more precise estimates of the feasibility of the system under examination. Additionally, the simulation model requires further scrutiny and validation with more extensive data. During the

development phase of the simulation models, it also became apparent that a Matlab-based simulation model might not necessarily be the optimal choice for analyzing such systems. Matlab-based simulation models may not be sufficiently user-friendly and flexible to be widely used in their current form for future design and consulting engagements.

The simulation results of the PVT system revealed that particularly the data from the northernmost observation point did not fully align with expectations. However, it is important to note that manufacturers of PVT modules specify a minimum operating temperature limit of $-40\text{ }^{\circ}\text{C}$ for their modules. To maintain the integrity of the modules' warranties, the system cannot be implemented in locations where the statistically lowest temperature falls outside this threshold. Consequently, of the locations utilized in the study, only location 1 would be a viable site for the deployment of the system.

When economic analyses are observed, it is necessary to consider that the research developed and examined a so-called generic simulation model, which did not consider factors such as energy storage or usage. Each economic analysis should be conducted on a case-by-case basis, considering all the characteristics of the power plant type being examined, including energy storage and usage profiles. When comparing the profitability of different energy production methods or energy systems, it is vital to acknowledge that the LCOE method may not always provide a factual portrayal of the economic viability of an energy system. Reviewing statistics that detail the LCOE figures for various means of energy production may not readily reveal, for example, the extent of investment support that the energy production system has received from the state or other entities. LCOE statistics also may not indicate the ratio of equity to debt financing within the energy system. Additionally, such statistics often lack mention of the impact of feed-in tariffs on the price of the produced energy. Moreover, due to these considerations, LCOE analysis in statistics in some cases assumes that the energy system's output remains constant throughout its life cycle. However, the power output of a PV or PVT plant declines over its life cycle, according to a degradation model. This model is an intermediate between the linear degradation reported by the manufacturer and the rule-based exponential

degradation, which may reflect a more elaborate understanding of the system's performance over time.

When assessing the viability of renewable energy sources and energy systems from a sustainability perspective, it is imperative to consider not only the economic dimension but also other facets that encompass ecological, social, and cultural sustainability. In examining the sustainability of energy systems from an ecological standpoint and the true environmental impacts and life cycle emissions of a system, it is crucial to consider the net energy of the system. Net energy analysis methods, such as energy return on investment (EROI), play a key role in this assessment method. The EROI indicator of an energy system represents the energy produced by the system over its lifetime relative to the energy consumed during its manufacturing, transportation, and installation phases (Müller & Chartouni, 2022).

This study evaluates the potential utilization of PVT modules in industrial-scale solar power plants. It is important to note that this research focuses primarily on examining the technical characteristics of PVT modules and does not delve into the practical implementation of a power plant composed of PVT modules in detail. The design of an actual power plant consisting of PVT modules is a comprehensive endeavor that requires expertise from various fields and close collaboration.

7 Conclusions

In this chapter, the findings and conclusions of the research are presented. Initially, the most pertinent findings and conclusions within the theoretical framework of the study are outlined. Finally, the chapter concludes with the findings based on the simulation results and the conclusions of the economic evaluation.

7.1 Theoretical Section Findings and Conclusions

Conventional PV solar modules experience a decrease in efficiency as the temperature of their cells increase. The efficiency of PV modules can potentially be improved by cooling the solar cells during operation. PVT hybrid solar modules, which concurrently produce both electrical and thermal energy, can also theoretically achieve better electrical efficiency compared to standalone PV modules. PVT hybrid modules are a combination of a conventional PV module and a flat-plate solar collector, and therefore, they adhere to the same operational principles and limitations. PVT modules can be categorized based on their technical features into three groups: liquid-based, air-based, and evacuated PVT modules, the latter utilizing vacuum tubes or chambers for thermal insulation. Commercially, only liquid-based PVT modules are currently more widely available. Typically, pure water is used as thermal medium for PVT modules. However, in colder conditions, such as those found in Finland, PW-EG mixture must be used as the thermal medium to prevent freezing. The heat absorption and conductivity capabilities of PW-EG mixture are significantly inferior to those of pure water. The thermal properties of PW-EG medium can be substantially improved by adding nanofluid, which contains metallic particles of nanometer size. Nevertheless, the use of nanofluids cannot be recommended without thorough examination due to significant environmental and health risks associated with them.

The thermal power produced by a PVT system must be fully utilized during its operation to avoid a stagnation state. A stagnation state refers to a condition where the flow rate

of the system's thermal medium is zero. Studies indicate that even a temporary stagnation state can cause significant damage to the system. The stagnation temperature for liquid-based PVT modules typically ranges between 80 and 90 °C. When considering the implementation of a PVT system on an industrial scale, the issue of stagnation must be acknowledged. In practice, this means that the system should be deployed in locations where all the generated thermal power can be continuously fed into a district heating network or an industrial process heat network.

The aging of PV and PVT modules and the power degradation due to environmental conditions may not necessarily be linear. Studies suggest that in conditions where temperature fluctuations are significant, the power degradation of modules can be considerably greater than what manufacturers claim. Research also indicates that module degradation may accumulate, particularly towards the end of the modules' lifespan. Case studies demonstrate that PVT systems can function in climatic conditions where temperatures drop below 0 °C. These case studies reveal that a water-based PVT system can generate approximately 2 % more electrical energy annually compared to a comparable PV system. Furthermore, they show that the average temperature of the thermal output produced by the PVT system is just over 40 °C. The observation intimates that in the context of Finnish climatic conditions, to facilitate the integration of PVT system into a district heating grid, there is a requisite to augment the temperature. This elevation of thermal output can be achieved through the deployment of heat pumps or alternative technological interventions.

7.2 Methodological Section Findings and Conclusions

Manufacturers of PVT hybrid modules specify a minimum operating temperature of -40 °C for their products. This implies that, within the Finnish climate, PVT systems can only be implemented in regions where the statistical lowest temperature does not exceed this threshold. Based on the data utilized in the simulations of this study, only location 1—specifically the weather observation station in Artukainen, Turku—falls within this threshold according to statistical observations. The simulation results based on the

data from location 1 suggest that the PVT system could produce approximately 0.9 % more electrical energy annually compared to a similar PV system. Furthermore, the results of the simulation indicate that the total energy output of the PVT system is approximately 112 % greater than that of an equivalent PV system on an annual basis.

The LCOE analyses reveal that the electrical energy produced by PVT system is significantly more expensive than that generated by PV system. The economic analysis indicates that substantial investment support would be required for it to be financially viable to produce electrical energy with a PVT system. The economic assessment also demonstrates that, given the current price levels of components, the thermal energy produced by a PVT system is not economically sustainable. The cost of thermal energy generated by the PVT system is substantially higher compared to the average price of energy produced for district heating networks in Finland. This observation suggests that, based on the current data and simulation parameters, the PVT system's thermal energy production may not be economically competitive with the existing district heating energy prices within the Finnish market. This comparison underscores the necessity for further optimization of PVT systems or the exploration of additional economic incentives or operational efficiencies that could render PVT-derived thermal energy more cost-competitive in similar contexts.

Despite the ability of PVT hybrid systems to produce considerably more energy per unit area compared to conventional PV systems, current price levels do not render the investment in such systems economically viable. For an industrial-scale PVT system to be financially feasible, significant investment subsidies or higher energy tariffs for the produced energy would be necessary. Current projections indicate that the cost of PV modules will continue to decline due to increased production. To ensure the economic viability of PVT systems in the future, substantial financial support will be required for research and development, as well as for the expansion of production capacity.

8 Summary

This master's thesis evaluates the potential of photovoltaic-thermal (PVT) technology in the Finnish energy sector. The thesis is a comprehensive study that combines a theoretical overview of hybrid solar modules, specifically focusing on PVT modules, with a simulation-based assessment of their performance in Finland's unique climatic conditions.

The research was conducted in collaboration with Sweco Finland Oy and aimed to enhance the company's understanding of hybrid solar modules' feasibility as part of the green transition. The study's objectives included providing a detailed theoretical background on PVT technology, developing a simulation model for an industrial-scale solar power plant using PVT modules, and conducting a techno-economic analysis to assess the viability of such plants.

The thesis is structured into two main parts: the theoretical framework and the methodological framework. The theoretical section delves into the basic principles of photovoltaic (PV) cells and modules, the impact of temperature on their efficiency, and the operation of traditional solar collectors. It then explores the technical characteristics of various types of hybrid solar modules, including liquid-circulating, air-circulating, and evacuated hybrid modules. The theoretical part concludes with case studies examining the practical application of PVT modules in power plants.

In the methodological section, the thesis presents the simulation model for a power plant consisting of PVT modules and compares it with a conventional PV module power plant. The simulations aim to scrutinize the technical performance and economic viability of PVT technology in Finnish conditions. The study also touches upon factors affecting the productivity and efficiency of a PVT power plant, such as plant topology and power electronics losses, although these are not the focus of the research.

The thesis concludes with a discussion of the findings, summarizing the potential of PVT systems in Finland. It acknowledges the challenges posed by Finland's climate and the

need for system modifications to optimize performance. The research suggests that while PVT technology can offer high-efficiency solar energy conversion, its economic viability and practical application in Finland would require careful consideration of local environmental regulations, architectural integration, and the seasonal variation in energy demand.

Overall, the thesis provides valuable insights into the role of hybrid solar modules in the transition to renewable energy in Finland, highlighting both the technological potential and the economic considerations that must be addressed for successful implementation.

References

- Abbassi, A., Mehrez, R. B., Touaiti, B., Abualigah, L., & Touti, E. (2022). Parameterization of photovoltaic solar cell double-diode model based on improved arithmetic optimization algorithm. *Optik*(253). doi:<https://doi.org/10.1016/j.ijleo.2022.168600>
- Abdul-Ganiyu, S., Quansah, D. A., Ramde, E. W., Seidu, R., & Adaramola, M. S. (2021). Techno-economic analysis of solar photovoltaic (PV) and solar photovoltaic thermal (PVT) systems using exergy analysis. *Sustainable Energy Technologies and Assessments*, 47. doi:<https://doi.org/10.1016/j.seta.2021.101520>
- Abora Energy S.L. (n.d). The Hybrid Solar Panel produces electricity and heat simultaneously. Retrieved April 4, 2024, from <https://abora-solar.com/en/>
- AF-Consult Ltd. (2016). *Energiamarkkinaskaariaiot vuosille 2020-2050*. Suomen Tuulivoimayhdistys ry. Retrieved May 3, 2024
- Aghaei, M., Fairbrother, A., Gok, A., Ahmad, S., Kazim, S., Lobato, K., Kettle, J. (2022). Review of degradation and failure phenomena in photovoltaic modules. *Renewable and Sustainable Energy Reviews*, 159. doi:<https://doi.org/10.1016/j.rser.2022.112160>
- Ahmad, T., & Zhang, D. (2020). A critical review of comparative global historical energy consumption and future demand: The story told so far. *Energy Reports*, 6, pp. 1973-1991. doi:<https://doi.org/10.1016/j.egyr.2020.07.020>
- Alam, T., Balam, N., Kulkarni, K., Siddiqui, M., Kapoor, N., Meena, C., Cozzolino, R. (2021). Performance Augmentation of the Flat Plate Solar Thermal Collector: A Review. *Energies*. doi:<https://doi.org/10.3390/en14196203>
- Al-Dousari, A., Al-Nassar, W., Al-Hemoud, A., Alsaleh, A., Ramadan, A., Al-Dousari, N., & Ahmed, M. (2019). Solar and wind energy: Challenges and solutions in desert regions. *Energy*, 176, 184-194. doi:<https://doi.org/10.1016/j.energy.2019.03.180>
- Alharbi, F. H., & Kais, S. (2015). Theoretical limits of photovoltaics efficiency and possible improvements by intuitive approaches learned from photosynthesis and quantum coherence. *Renewable and Sustainable Energy Reviews*, 1073-1089. doi:<https://doi.org/10.1016/j.rser.2014.11.101>

- Ali, A., Alhussein, M., Aurangzeb, K., & Akbar, F. (2023). The numerical analysis of Al₂O₃Cu/water hybrid nanofluid flow inside the serpentine absorber channel of a PVT; the overall efficiency intelligent forecasting. *Engineering Analysis with Boundary Elements*, 157, 82-91. doi:<https://doi.org/10.1016/j.enganabound.2023.08.041>
- Al-Sulttani, A. O., Aldlemy, M. S., Zahra, M. M., Gatea, H. A., Khedher, K. M., Scholz, M., & Yaseen, Z. M. (2022). Thermal effectiveness of solar collector using Graphene nanostructures suspended in ethylene glycol–water mixtures. *Energy Reports*, 1867-1882. doi:<https://doi.org/10.1016/j.egy.2022.01.007>
- Atia, D. M., Hassan, A. A., El-Madany, H. T., Eliwa, A. Y. & Zahran, M. B. (2023). Degradation and energy performance evaluation of mono-crystalline photovoltaic modules in Egypt. *Scientific Reports*. doi:<https://doi.org/10.1038/s41598-023-40168-8>
- Baiceanu, M., Catalina, T., & Damian, A. (2020). Experimental and simulation performance investigation of a hybrid PV/ T solar panel. *7th International Conference on Energy Efficiency and Agricultural Engineering (EE&AE)*, (pp. 1-5). doi:[10.1109/EEAE49144.2020.9279013](https://doi.org/10.1109/EEAE49144.2020.9279013)
- Bakari, R. (2018). Heat Transfer Optimization in Air Flat Plate Solar Collectors Integrated with Baffles. *Journal of Power and Energy Engineering*, 6(1), 70-84. doi:[10.4236/jpee.2018.61006](https://doi.org/10.4236/jpee.2018.61006)
- Beinert, A. J., Büchler, A., Romer, P., Haueisen, V., Rendler, L. C., Schubert, M. C., Eitner, U. (2019). Enabling the measurement of thermomechanical stress in solar cells and PV modules by confocal micro-Raman spectroscopy. *Solar Energy Materials and Solar Cells*, 193, pp. 351-360. doi:<https://doi.org/10.1016/j.solmat.2019.01.028>
- Bellos, E., & Tzivanidis, C. (2023). A detailed investigation of an evacuated flat plate solar collector. *Applied Thermal Engineering*, 234. Retrieved January 23, 2023, from <https://doi.org/10.1016/j.applthermaleng.2023.121334>
- Belyakov, N. (2019). Chapter Seventeen - Solar energy. In *Sustainable Power Generation* (p. 622). doi:<https://doi.org/10.1016/B978-0-12-817012-0.00031-1>

- Benda, V. (2018). 9 - Crystalline Silicon Solar Cell and Module Technology. A *Comprehensive Guide to Solar Energy Systems* (pp. 181-213). Academic Press. doi:<https://doi.org/10.1016/B978-0-12-811479-7.00009-9>
- Bianchini, A., Guzzini, A., Pellegrini, M., & Sacconi, C. (2017). Photovoltaic/thermal (PV/T) solar system: Experimental measurements, performance analysis and economic assessment. *Renewable Energy*, 543-555. doi:<https://doi.org/10.1016/j.renene.2017.04.051>
- Bounouar, S., Bendaoud, R., Amiry, H., Zohal, B., Chanaa, F., Baghaz, E., Benhmida, M. (2020). Assessment of Series Resistance Components of a Solar PV Module Depending on Its Temperature Under Real Operating Conditions. *International Journal of Renewable Energy Research*, 10(4). doi:<https://doi.org/10.20508/ijrer.v10i4.11240.g8040>
- Business Finland. (2024). *Energy aid*. Retrieved April 19, 2024, from <https://www.businessfinland.fi/en/for-finnish-customers/services/funding/energy-aid>
- Carmona, M., Bastos, A. P., & García, J. D. (2021). Experimental evaluation of a hybrid photovoltaic and thermal solar energy collector with integrated phase change material (PVT-PCM) in comparison with a traditional photovoltaic (PV) module. *Renewable Energy*, 680-696. doi:<https://doi.org/10.1016/j.renene.2021.03.022>
- Carrión-Chamba, W., Murillo-Torres, W., & Montero-Izquierdo, A. (2022). A review of the state-of-the-art of solar thermal collectors applied in the industry. *Ingenius*, 59-73. doi:<https://doi.org/10.17163/ings.n27.2022.01>
- Center for Sustainable Systems, University of Michigan. (2023). Photovoltaic Energy Factsheet. Retrieved March 21, 2024, from <https://css.umich.edu/publications/factsheets/energy/photovoltaic-energy-factsheet>
- Chaibi, Y., Rhafiki, T. E., Simón-Allué, R., Guedea, I., Luaces, S. C., Gajate, O. C., & Zeraouli, Y. (2021). Air-based hybrid photovoltaic/thermal systems: A review. *Journal of Cleaner Production*, 295. doi:<https://doi.org/10.1016/j.jclepro.2021.126211>

- Chander, S., Purohit, A., Sharma, A., Arvind, Nehra, S., & Dhaka, M. (2015). A study on photovoltaic parameters of mono-crystalline silicon solar cell with cell temperature. *Energy Reports*, 1, 104-109. doi:<https://doi.org/10.1016/j.egy.2015.03.004>
- Charvat, P., Ostry, M., Mauder, T., & Klimes, L. (2012). A solar air collector with integrated latent heat thermal storage. *The European Physical Journal Conferences*, 25. doi:10.1051/epjconf/20122501028
- Chen, Z., Lian, X., Tan, J., Xiao, H., Ma, Q., & Zhuang, Y. (2023). Study on heat-exchange efficiency and energy efficiency ratio of a deeply buried pipe energy pile group considering seepage and circulating-medium flow rate. *Renewable Energy*, 216. doi:<https://doi.org/10.1016/j.renene.2023.119020>
- Corkish, R., Lipiński, W., & Patterson, R. J. (2016). Solar Energy. In *World Scientific Series in Current Energy Issues : Volume 2* (p. 436). doi:https://doi.org/10.1142/9789814689502_0001
- Crane Ltd. (n.d). PVT Hybrid Module 250 Wp. Retrieved April 4, 2024 from <https://crane-bg.com/en/solar-products/pvt-hybrid-module-250-wp-photovoltaic-panel-solar-thermal-module>
- Dash, P. K., & Gupta, N. C. (2015). Effect of Temperature on Power Output from Different. *Journal of Engineering Research and Applications*, ISSN : 2248-9622, 5(1), 148-151. Retrieved March 21, 2024
- Dhimish, M., & Tyrrell, A. (2022). Power loss and hotspot analysis for photovoltaic modules affected by potential induced degradation. *npj Mater Degrad*, 6(11). doi:<https://doi.org/10.1038/s41529-022-00221-9>
- Dhimish, M., Theristis, M., & d'Alessandro, V. (2024). Photovoltaic hotspots: A mitigation technique and its thermal cycle. *Optik*. doi:<https://doi.org/10.1016/j.ijleo.2024.171627>
- Dincer, I., & Bicer, Y. (2018). 4.19.2.2.2 Flat plate collectors. In I. Dincer, & Y. Bicer, *Comprehensive Energy Systems* (pp. 762-793). Elsevier. doi:<https://doi.org/10.1016/B978-0-12-809597-3.00430-2>

- Dualsun. (n.d). Documentation technique. Retrieved April 4, 2024, from <https://dualsun.com/espace-professionnel/documentation-technique/#SPRING>
- Dunne, N. A., Liu, P., Elbarghthi, A. F., Yang, Y., Dvorak, V., & Wen, C. (2023). Performance evaluation of a solar photovoltaic-thermal (PV/T) air collector system. *Energy Conversion and Management*: X, 20. doi:<https://doi.org/10.1016/j.ecmx.2023.100466>
- El-Ahmar, M., Ahmed, A.-H., & Hemeida, A. (2016). 978-1-4673-9063-7/16/\$31.00 ©2016 IEEE Mathematical Modeling of Photovoltaic Module and Evaluate The Effect of Varoious Paramenters on its Performance. *Eighteenth International Middle East Power Systems Conference (MEPCON)*, (pp. 741-746). doi:[10.1109/MEPCON.2016.7836976](https://doi.org/10.1109/MEPCON.2016.7836976)
- Elsaid, K., Olabi, A., Wilberforce, T., Abdelkareem, M. A., & Sayed, E. T. (2021). Environmental impacts of nanofluids: A review. *Science of The Total Environment*, 763. doi:<https://doi.org/10.1016/j.scitotenv.2020.144202>
- Emmanuel, B., Yuan, Y., maxime, B., Gaudence, N., & Zhou, J. (2021). A review on the influence of the components on the performance of PVT modules. *Solar Energy*, 226, 365-388. doi:<https://doi.org/10.1016/j.solener.2021.08.042>
- Emmanuel, B., Yuan, Y., maxime, B., Gaudence, N., & Zhou, J. (2021). A review on the influence of the components on the performance of PVT modules. *Solar Energy*, 226, 365-388. doi:<https://doi.org/10.1016/j.solener.2021.08.042>
- Energiategällisus ry. (2024). Kaukolämmön hintatilasto. Retrieved March 28, 2024, from <https://energia.fi/tilastot/kaukolammon-hintatilasto/>
- Energiategällisus ry. (2024). Sähkön hintatilasto. Retrieved March 28, 2024, from <https://energia.fi/esitykset/sahkon-hintatilasto/>
- Energy Authority. (2022). *Teollisuuden sähköistämistuki*. Retrieved April 19, 2024, from <https://energiavirasto.fi/teollisuuden-sahkoistamistuki>
- European Central Bank. (2024, April 5). Bank interest rates - loans to corporations (new business) - Finland, Finland, Monthly. Retrieved April 18, 2024, from https://data.ecb.europa.eu/data/datasets/MIR/MIR.M.FI.B.A2A.A.R.A.2240.EU.R.N?chart_props=W3sibm9kZUIkljoiNTk2NTA1liwiczHJvcGVydGllcyI6W3siY29sb3

- JIZXgiOiliLCJjb2xvclR5cGUiOiliLCJjaGFydFR5cGUiOiJsaW5lY2hhcnQiLCJsaW5lU3R5bGUiOiJTb2xpZCIsImxpbmVXaWR0aCI6IjEuNS
- European Central Bank. (2024, 27 March). Pound sterling (GBP). Retrieved March 28, 2024, from https://www.ecb.europa.eu/stats/policy_and_exchange_rates/euro_reference_exchange_rates/html/eurofxref-graph-gbp.en.html
- European Commission. (n.d). *Current funding*. Retrieved April 19, 2024, from https://energy.ec.europa.eu/topics/energy-efficiency/financing/eu-programmes/current-funding_en
- European Commission. (n.d). PVGIS background information. Retrieved May 3, 2024, from https://joint-research-centre.ec.europa.eu/photovoltaic-geographical-information-system-pvgis/pvgis-background-information_en
- Farrell, C., Osman, A. I., Zhang, X., Murphy, A., Doherty, R., Morgan, K., & Shen, D. (2019). *Assessment of the energy recovery potential of waste Photovoltaic (PV) modules*. Scientific Reports. doi: 10.1038/s41598-019-41762-5
- Finnish Meteorological Institute. (2018). Lämpötilaennätyksiä. doi:<https://www.ilmatieteenlaitos.fi/lamputilaennatyksia>
- FMI. (n.d). Auringonpaiste- ja säteilytilastot. Retrieved April 24, 2024, from <https://www.ilmatieteenlaitos.fi/1991-2020-auringonpaiste-ja-sateilytilastot>
- FMI. (n.d). Energialaskennan testivuodet nykyilmastossa. Retrieved May 5, 2024, from <https://www.ilmatieteenlaitos.fi/energialaskennan-testivuodet-nyky>
- FMI. (n.d). Havaintojen lataus. Retrieved May 2, 2024, from <https://www.ilmatieteenlaitos.fi/havaintojen-lataus>
- FMI. (n.d). Kovat pakkaset ja talven kylmimmät. Retrieved March 29, 2024 from <https://www.ilmatieteenlaitos.fi/kovat-pakkaset-ja-kylmimmat-talvet>
- FMI. (n.d). Lisätietoa havaintosuureista. Retrieved May 2, 2024, from <https://www.ilmatieteenlaitos.fi/lisatietoa-havaintosuureista>
- Gorjian, S., Calise, F., Kant, K., Ahamed, M. S., Copertaro, B., Najafi, G., & Shamshiri, R. R. (2021). A review on opportunities for implementation of solar energy

- technologies in agricultural greenhouses. *Journal of Cleaner Production*, 285. doi:<https://doi.org/10.1016/j.jclepro.2020.124807>
- Gray, J. L. (2011). 3 The Physics of the Solar Cell. In A. Luque, S. Hegedus, & A. Luque, *Handbook of Photovoltaic Science and Engineering: Vol. 2nd ed. Wiley*. (pp. 83-128). Retrieved January 11, 2024, from <https://search-ebSCOhost-com.proxy.uwasa.fi/login.aspx?direct=true&db=nlebk&AN=522082&site=ehost-live>
- Gupta, M., & Prasad, R. B. (2020). Potential Use of Nanofluids in Solar Collectors: A Review. *SAMRIDDHI A Journal of Physical Sciences Engineering and Technology*, 12(01), 32-36. doi:DOI:10.18090/samriddhi.v12i01.7
- Hamed, S. B., Abid, A., Hamed, M. B., & Sbita, L. (2022). A high efficient Double diode equivalent circuit based model for triple-junction solar cells. *IEEE International Conference on Electrical Sciences and Technologies in Maghreb (CISTEM)*. IEEE. doi:10.1109/CISTEM55808.2022.10043999
- Honey, F. R. (1921). The Position of the Sun's Axis. *Popular Astronomy*, 29, pp. 327-327. Retrieved May 5, 2024, from <https://ui.adsabs.harvard.edu/abs/1921PA.....29..325H/abstract>
- Hosouli, S., Gomes, J., Loris, A., Pazmiño, I.-A., Naidoo, A., Lennermo, G., & Mohammadi, H. (2023). Evaluation of a solar photovoltaic thermal (PVT) system in a dairy farm in Germany. *Solar Energy Advances*, 3. doi:<https://doi.org/10.1016/j.seja.2023.100035>
- Hu, J., & babu, K. M. (2009). 5 - The use of smart materials in cold weather apparel. In J. Williams, *Textiles for Cold Weather Apparel* (pp. 84-112). doi:<https://doi.org/10.1533/9781845697174.1.84>
- Hu, M., Guo, C., Zhao, B., Ao, X., Suhendri, Cao, J., & Pei, G. (2021). A parametric study on the performance characteristics of an evacuated flat-plate photovoltaic/thermal (PV/T) collector. *Renewable Energy*, 884-898. doi:<https://doi.org/10.1016/j.renene.2020.12.008>
- Huang, H., Lv, J., Bao, Y., Xuan, R., Sun, S., Sneek, S., & Zhao, J. (2017). 20.8% industrial PERC solar cell: ALD Al₂O₃ rear surface passivation, efficiency loss mechanisms

- analysis and roadmap to 24%. *Solar Energy Materials and Solar Cells*, 161, pp. 14-30. doi:<https://doi.org/10.1016/j.solmat.2016.11.018>.
- Hussain, S., & Harrison, S. J. (2015). Experimental and numerical investigations of passive air cooling of a residential flat-plate solar collector under stagnation conditions. *Solar Energy*, 122, pp. 1023-1036. doi:<https://doi.org/10.1016/j.solener.2015.10.029>
- Ignatowicz, M., & Palm, B. (n.d.). Experimental investigation of thermophysical properties of ethylene glycol based secondary fluids. *International Journal of Refrigeration*, 155, pp. 137-153. doi:<https://doi.org/10.1016/j.ijrefrig.2023.08.008>
- International Electrotechnical Commission IEC. (2016, September 06). IEC 61853-2:2016. Photovoltaic (PV) module performance testing and energy rating - Part 2: Spectral responsivity, incidence angle and module operating temperature, 39. Retrieved January 16, 2024
- International Electrotechnical Commission IEC. (2022, November 23). IEC 60904-5:2011+AMD1:2022 CSV Consolidated version. Photovoltaic devices - Part 5: Determination of the equivalent cell temperature (ECT) of photovoltaic (PV) devices by the open-circuit voltage method, 2.1, 50. Retrieved January 16, 2024
- Jamil, I., Zhao, J., Zhang, L., Jamil, R., & Syed, F. (2017). Evaluation of Energy Production and Energy Yield Assessment Based on Feasibility, Design, and Execution of 3 × 50 MW Grid-Connected Solar PV Pilot Project in Nooriabad. *International Journal of Photoenergy*, pp. 1-18. doi:10.1155/2017/6429581
- Jang, J. S., Kim, H. S., Karade, V. C., Park, S. W., Kim, C.-W., & Kim, J. H. (2024). Improving the minority carrier lifetime of PERC solar cells via bi-layer rear interface passivation strategy. *Journal of Alloys and Compounds*, 970. doi:<https://doi.org/10.1016/j.jallcom.2023.172691>
- Joo, H.-J., An, Y.-S., Kim, M.-H., & Kong, M. (2023). Long-term performance evaluation of liquid-based photovoltaic thermal (PVT) modules with overheating-prevention technique. *Energy Conversion and Management*. doi:<https://doi.org/10.1016/j.enconman.2023.117682>

- Kaaya, I., Lindig, S., Weiss, K.-A., Virtuani, A., Ortin, M. S., & Moser, D. (2020). Photovoltaic lifetime forecast model based on degradation patterns. doi:<https://doi.org/10.1002/pip.3280>
- Kabeyi, M. J., & Olanrewaju, O. A. (2023). The levelized cost of energy and modifications for use in electricity generation planning. *Energy Reports*, 9(9), 495-534. doi:<https://doi.org/10.1016/j.egy.2023.06.036>
- Kabir, E., Kumar, P., Kumar, S., Adelodun, A. A., & Kim, K.-H. (2018). Solar energy: Potential and future prospects. *Renewable and Sustainable Energy Reviews*, 82(1), pp. 894-900. doi:<https://doi.org/10.1016/j.rser.2017.09.094>
- Kalogirou, S. A. (2009). Chapter three - Solar Energy Collectors. In S. A. Kalogirou, *Solar Energy Engineering* (pp. 121-217). Academic Press. doi:<https://doi.org/10.1016/B978-0-12-374501-9.00003-0>
- Karki, S., Haapala, K. R., & Fronk, B. M. (2019). Technical and economic feasibility of solar flat-plate collector thermal energy systems for small and medium manufacturers. *Applied Energy*, 254. doi:<https://doi.org/10.1016/j.apenergy.2019.113649>
- Kaya, H., Arslan, K., & Eltugral, N. (2018). Experimental investigation of thermal performance of an evacuated U-Tube solar collector with ZnO/Ethylene glycol-pure water nanofluids. *Renewable Energy*, 329-338. doi:<https://doi.org/10.1016/j.renene.2018.01.115>
- Kazemian, A., Hosseinzadeh, M., Sardarabadi, M., & Passandideh-Fard, M. (2018). Effect of glass cover and working fluid on the performance of photovoltaic thermal (PVT) system: An experimental study. *Solar Energy*, 173, 1002-1010. doi:<https://doi.org/10.1016/j.solener.2018.07.051>
- Kim, J.-H., Park, S.-H., & Kim, J.-T. (2014). Experimental Performance of a Photovoltaic-thermal Air Collector. *Energy Procedia*, 888-894. doi:<https://doi.org/10.1016/j.egypro.2014.02.102>
- Kim, J.-H., Park, S.-H., & Kim, J.-T. (2014). Experimental Performance of a Photovoltaic-thermal Air Collector. *Energy Procedia*, 48, pp. 888-894. doi:<https://doi.org/10.1016/j.egypro.2014.02.102>

- Kober, T., Schiffer, H.-W., Densing, M., & Panos, E. (2020). Global energy perspectives to 2060 – WEC's World Energy Scenarios 2019. *Energy Strategy Reviews*, 31. doi:<https://doi.org/10.1016/j.esr.2020.100523>
- Krügenger, J., & Harder, N.-P. (2013). Weak Light Performance of PERC, PERT and Standard Industrial Solar Cells. *Energy Procedia*, 38, pp. 108-113. doi:<https://doi.org/10.1016/j.egypro.2013.07.256>
- Kumar, L. H., Kazi, S., Masjuki, H., Zubir, M., Jahan, A., & Bhinitha, C. (2021). Energy, exergy and economic analysis of liquid flat-plate solar collector using green covalent functionalized graphene nanoplatelets. *Applied Thermal Engineering*, 192. doi:<https://doi.org/10.1016/j.applthermaleng.2021.116916>
- Kutlu, C., Li, J., Su, Y., Wang, Y., Pei, G., & Riffat, S. (2020). Investigation of an innovative PV/T-ORC system using amorphous silicon cells and evacuated flat plate solar collectors. *Energy*, 203. doi:<https://doi.org/10.1016/j.energy.2020.11787>
- Libra, M., Mrázek, D., Tyukhov, I., Severová, L., Poulek, V., Mach, J., Šubrt, T., Beránek, V., Svoboda, R., & Sedláček, J. (2023). Reduced real lifetime of PV panels – Economic consequences. *Solar Energy*, 259, pp. 229-234. doi:<https://doi.org/10.1016/j.solener.2023.04.063>.
- Liu, Z., Fu, R., & Yuying, Y. (2022). Chapter 2 - Preparation and evaluation of stable nanofluids for heat transfer application. In A. H. Muhammad, *Advances in Nanofluid Heat Transfer* (pp. 25-57). Elsevier. doi:<https://doi.org/10.1016/B978-0-323-88656-7.00013-1>.
- López, L. H., Monzonís, L. M., Vicente, L. B., Kaur, J., & H. Buschman, M. (2019). *Report about nanofluids health, safety and environmental impact*. Nanouptake COST Action. doi:<http://dx.doi.org/10.6035/CA15119.2019.02>
- Luca, D. D., Caldarelli, A., Gaudino, E., Gennaro, E. D., Musto, M., & Russo, R. (2023). Modeling of energy and exergy efficiencies in high vacuum flat plate photovoltaic-thermal (PV-T) collectors. *Energy Reports*, 1044-1055. doi:<https://doi.org/10.1016/j.egypr.2022.11.152>
- Luca, D. D., Strazzullo, P., Gennaro, E. D., Caldarelli, A., Gaudino, E., Musto, M., & Russo, R. (2023). High vacuum flat plate photovoltaic-thermal (HV PV-T) collectors:

- Efficiency analysis. *Applied Energy*, 352.
doi:<https://doi.org/10.1016/j.apenergy.2023.121895>
- Lunardi, M. M., Alvarez-Gaitan, J., Chang, N. L., & Corkish, R. (2018). Life cycle assessment on PERC solar modules. *Solar Energy Materials and Solar Cells*(187), 154-159. doi:<https://doi.org/10.1016/j.solmat.2018.08.004>
- Lupu, A. G., Homutescu, V. M., Balanescu, D. T., & Popescu, A. (2018). Efficiency of solar collectors – a review. *The 8th International Conference on Advanced Concepts in Mechanical Engineering*. IOP. doi:[doi:10.1088/1757-899X/444/8/082015](https://doi.org/10.1088/1757-899X/444/8/082015)
- Luzzi, A., & Lovegrove, K. (2004). Solar Thermal Power Generation. In C. J. Cleveland, *Encyclopedia of Energy* (pp. 669-683). Elsevier. doi:<https://doi.org/10.1016/B0-12-176480-X/00531-3>
- Ma, Y., Tao, Y., Wang, Y., & Tu, J. (2024). Performance investigation and evaluation of a low-temperature solar thermal energy storage system under dynamic weather conditions. *Energy and Buildings*, 304.
doi:<https://doi.org/10.1016/j.enbuild.2023.113868>
- Maka, A. O., & Chaudhary, T. N. (2024). Performance investigation of solar photovoltaic systems integrated with battery energy storage. *Journal of Energy Storage*, 84.
doi:<https://doi.org/10.1016/j.est.2024.110784>
- Mandys, F., Chitnis, M., & Silva, S. R. (2023). Levelized cost estimates of solar photovoltaic electricity in the United Kingdom until 2035. *Patterns*, 4(5).
doi:<https://doi.org/10.1016/j.patter.2023.100735>
- Mao, Y., Robinson, J., & Binner, E. (2023). Understanding heat and mass transfer processes during microwave-assisted and conventional solvent extraction. *Chemical Engineering Science*, 233(116418).
doi:<https://doi.org/10.1016/j.ces.2020.116418>
- Markvart, T., & Castañer, L. (2003). Ila-1 - Principles of Solar Cell Operation. In T. Markvart, & L. Castañer, *Practical Handbook of Photovoltaics* (pp. 71-93).
doi:<https://doi.org/10.1016/B978-185617390-2/50005-2>
- MathWorks Inc. (n.d). Photovoltaic Generator. Retrieved February 2, 2024, from <https://se.mathworks.com/help/sps/ug/photovoltaic-generator.html>

- Mechanical Engineering Industry Association (VDMA). (2023). International Technology Roadmap for Photovoltaic (ITRPV) 2022. Retrieved April 17, 2024, from <https://www.vdma.org/international->
- Menon, G. S., a, S. M., Elias, J., Delfiya, D. A., Alfiya, P., & Samuel, M. P. (2022). Experimental investigations on unglazed photovoltaic-thermal (PVT) system using water and nanofluid cooling medium. *Renewable Energy*, *188*, pp. 986-996. doi:<https://doi.org/10.1016/j.renene.2022.02.080>
- Mintairov, M. A., Evstropov, V. V., Mintairov, S. A., Nakhimovich, M. V., Salii, R. A., Shvarts, M. Z., & Kalyuzhnyy, N. A. (2024). Current invariant as fundamental relation between saturation currents and band gaps for semiconductor solar cells. *Solar Energy Materials and Solar Cells*(264). doi:<https://doi.org/10.1016/j.solmat.2023.112619>
- Mishra, R., Tripathi, R., Gupta, V., & Dwivedi, V. (2021). Expression for the electrical efficiency of photovoltaic modules in different photovoltaic thermal (PVT) configurations. *Materials Today: Proceedings*, *47*(13), 3754-3760. doi:<https://doi.org/10.1016/j.matpr.2021.02.426>
- Motiva Oy. (2024). Auringonsäteilyn määrä Suomessa. Retrieved April 10, 2024, from https://www.motiva.fi/ratkaisut/uusiutuva_energia/aurinkosahko/aurinkosahko_n_perusteet/auringonsateilyn_maara_suomessa
- Müller, D., & Chartouni, D. (2022). Implications on EROI and climate change of introducing Li-ion batteries to residential PV systems. *Applied Energy*, *326*. doi:<https://doi.org/10.1016/j.apenergy.2022.119958>
- Naked Energy. (n.d.). Virtu Spec Sheets. Retrieved April 12, 2024, from <https://nakedenergy.com/products>
- Navarro, M. A., Oliva, D., Ramos-Michel, A., & Haro, E. H. (2023). An analysis on the performance of metaheuristic algorithms for the estimation of parameters in solar cell models. *Energy Conversion and Management*, *276*. doi:<https://doi.org/10.1016/j.enconman.2022.116523>
- Nazri, N. S., Fudholi, A., Bakhtyar, B., Yen, C. H., Ibrahim, A., Ruslan, M. H., & Sopian, K. (2018). Energy economic analysis of photovoltaic–thermal–thermoelectric (PVT-

- TE) air collectors. *Renewable and Sustainable Energy Reviews*, 187-197. doi:<https://doi.org/10.1016/j.rser.2018.04.061>
- Nevanlinna, H. (2012). *Auringon aktiivisuus ja ilmastonmuutos*. Finnish Meteorological Institute. Retrieved March 30, 2024, from <https://helda.helsinki.fi/server/api/core/bitstreams/e880403e-36a0-4f14-b004-1f36de15e553/content>
- Nguyen-Duc, T., Nguyen-Duc, H., Le-Viet, T., & Takano, H. (2020). Single-Diode Models of PV Modules: A Comparison of Conventional Approaches and Proposal of a Novel Model. *Energies*(13(6):1296). doi:<https://doi.org/10.3390/en13061296>
- Nieto, L. M., Rodríguez, J. P., Campos, R. M., & Higuera, P. J. (2024). Multi-junction solar cell measurements at ultra-high irradiances for different temperatures and spectra. *Solar Energy Materials and Solar Cells*. doi:<https://doi.org/10.1016/j.solmat.2023.112651>
- Niewelt, T., Maischner, F., Kwapil, W., Khorani, E., S.L. Pain, Y. J., Hopkins, E., & Murphy, J. (2024). Stability of industrial gallium-doped Czochralski silicon PERC cells and wafers. *Solar Energy Materials and Solar Cells*. doi:<https://doi.org/10.1016/j.solmat.2023.112645>
- Ocaya, R. (2006). An experiment to profile the voltage, current and temperature behaviour of a P-N diode. *European Journal of Physics*(27 625). doi:10.1088/0143-0807/27/3/015
- Odeh, S. (2018). Analysis of the Performance Indicators of the PV Power System. *Journal of Power and Energy Engineering*(06), 59-75. doi:10.4236/jpee.2018.66005.
- Ouédraogo, A., Zouma, B., Ouédraogo, E., Guissou, L., & Bathiébo, D. J. (2021). Individual efficiencies of a polycrystalline silicon PV cell versus temperature. *Results in Optics*, 4. doi:<https://doi.org/10.1016/j.rio.2021.100101>
- Paudyal, B. R., & Imenes, A. G. (2021). Investigation of temperature coefficients of PV modules through field measured data. *Solar Energy*, 224, pp. 425-439. doi:<https://doi.org/10.1016/j.solener.2021.06.013>

- Peng, Z., Herfatmanesh, M. R., & Liu, Y. (2017). Cooled solar PV panels for output energy efficiency optimisation. *Energy Conversion and Management*, 150, pp. 949-955. doi:<https://doi.org/10.1016/j.enconman.2017.07.007>
- Pindado, S., Cubas, J., & Manuel, C. (2014). Explicit Expressions for Solar Panel Equivalent Circuit Parameters Based on Analytical Formulation and the Lambert W-Function. *Energies*(7), 4098-4115. doi:[doi:10.3390/en7074098](https://doi.org/10.3390/en7074098)
- Planet Soar Shop. (n.d). *Dualsun FLASH 425 W Half-Cut Glass-Glass Topcon solar panel*. Retrieved April 11, 2024 from <https://www.planetsoarshop.com/en/products/dualsun-flash-425-w-half-cut-glass-glass-topcon-solar-panel>
- Poredoš, P., Tomc, U., Petelin, N., Vidrih, B., Flisar, U., & Kitanovski, A. (2020). Numerical and experimental investigation of the energy and exergy performance of solar thermal, photovoltaic and photovoltaic-thermal modules based on roll-bond heat exchangers. *Energy Conversion and Management*, 210. doi:<https://doi.org/10.1016/j.enconman.2020.112674>
- Pourasl, H. H., Barenji, R. V., & Khojastehnezhad, V. M. (2023). Solar energy status in the world: A comprehensive review. *Energy Reports*, pp. 3474-3493. doi:<https://doi.org/10.1016/j.egy.2023.10.022>
- Prakash, A., Kumar, M., Manchanda, H., & Grewal, R. (2022). A review on solar flat plate air collector with different design modifications. *International multidisciplinary conference-2021*. Retrieved January 29, 2024
- Rahman, T., Mansur, A., Hossain Lipu, M., Rahman, M., Ashique, R., Houran, M., Hossain, E. (2023). Investigation of Degradation of Solar Photovoltaics: A Review of Aging Factors, Impacts, and Future Directions toward Sustainable Energy Management. *Energies*, 16(3706). doi:<https://doi.org/10.3390/en16093706>
- Rahman, T., Mansur, A., Hossain Lipu, M., Rahman, M., Ashique, R., Houran, M., & Hossain, E. (2023). Investigation of Degradation of Solar Photovoltaics: A Review of Aging Factors, Impacts, and Future Directions toward Sustainable Energy Management. *Energies*, 16(3706). doi:<https://doi.org/10.3390/en16093706>

- Raikar, S., & Adamson, S. (2020). 13 - Renewable energy finance in the international context. In S. Raikar, & S. Adamson, *Renewable Energy Finance* (pp. 185-220). Academic Press. doi:<https://doi.org/10.1016/B978-0-12-816441-9.00013-1>
- Ramos, C. A., Alcaso, A. N., & Cardoso, A. J. (2019). Photovoltaic-thermal (PVT) technology: Review and case study. *IOP Conference Series: Earth and Environmental Science*. 354. 012048. doi:[doi:10.1088/1755-1315/354/1/012048](https://doi.org/10.1088/1755-1315/354/1/012048)
- Ramos, C. A., Alcaso, A. N., & Cardoso, A. J. (2019). Photovoltaic-thermal (PVT) technology: Review and case study. *International Conference on New Energy and Future Energy System*. IOP. doi:[10.1088/1755-1315/354/1/012048](https://doi.org/10.1088/1755-1315/354/1/012048)
- Rehm, B., Consultant, D., Haghshenas, A., Paknejad, A. S., & Schubert, J. (2008). CHAPTER TWO - Situational Problems in MPD. In B. Rehm, J. Schubert, A. Haghshenas, A. S. Paknejad, J. Hughes, & E. Inc (Ed.), *Managed Pressure Drilling* (pp. 39-80). Gulf Publishing Company. doi:<https://doi.org/10.1016/B978-1-933762-24-1.50008-5>
- Rimar, M., Fedak, M., Vahovsky, J., Kulikov, A., Oravec, P., Kulikova, O., & Kana, M. (2020). Performance Evaluation of Elimination of Stagnation of Solar Thermal Systems. *Processes*, 8(5). doi:<https://doi.org/10.3390/pr8050621>
- Rodríguez-Hidalgo, M., Rodríguez-Aumente, P., Lecuona, A., Gutiérrez-Urueta, G., & Ventas, R. (2011). Flat plate thermal solar collector efficiency: Transient behavior under working conditions. Part I: Model description and experimental validation. *Applied Thermal Engineering*, 31(14–15), 2394-2404. doi:<https://doi.org/10.1016/j.applthermaleng.2011.04.003>
- Rosales-Pérez, J. F., Villarruel-Jaramillo, A., Pérez-García, M., Cardemil, J. M., & Escobar, R. (2024). Techno-economic analysis of hybrid solar thermal systems with flat plate and parabolic trough collectors in industrial applications. *Alexandria Engineering Journal*, 98-119. doi:<https://doi.org/10.1016/j.aej.2023.11.056>
- Rosen, M., & Farsi, A. (2022). CHAPTER EIGHT - Seawater desalination systems using sustainable energy technologies. In M. Rosen, & A. Farsi (Eds.), *Sustainable Energy Technologies for Seawater Desalination* (pp. 277-360). Academic Press. doi:<https://doi.org/10.1016/B978-0-323-99872-7.00010-3>

- Said, Z., Iqbal, M., Mehmood, A., Le, T. T., Ali, H. M., Cao, D. N., & Pham, N. D. (2023). Nanofluids-based solar collectors as sustainable energy technology towards net-zero goal: Recent advances, environmental impact, challenges, and perspectives. *Chemical Engineering and Processing - Process Intensification*, 191. doi:<https://doi.org/10.1016/j.cep.2023.109477>
- Salcantay OU. (n.d). Hybrid solar panel 250W hot water and electricity. Retrieved April 4, 2024, from <https://www.todoensolar.com/Hybrid-solar-panel-250W-hot-water-and-electricity>
- Saleh, G., Faraji, M., & Dalili, A. (2018). A New Explanation for the Color Variety of Photons. *MATEC Web of Conferences* 186. 01003. doi:10.1051/mateconf/201818601003
- Satpathy, R., & Pamuru, V. (2021). Chapter 5 - Manufacturing of crystalline silicon solar PV modules. In *Solar PV Power* (pp. 135-241). Academic Press. doi:<https://doi.org/10.1016/B978-0-12-817626-9.00005-8>
- Segev, G., Dotan, H., Ellis, D. S., Piekner, Y., Klotz, D., Beeman, J. W., & Rothschild, A. (2018). The Spatial Collection Efficiency of Charge Carriers in Photovoltaic and Photoelectrochemical Cells. *Joule*, pp. 210-224. doi:<https://doi.org/10.1016/j.joule.2017.12.007>
- Sforza, P. M. (2016). Chapter 9 - Thermal Protection Systems. In P. M. Sforza, *Manned Spacecraft Design Principles* (pp. 391-452). doi:<https://doi.org/10.1016/B978-0-12-804425-4.00009-X>
- Sharma, C. (2014, May). Solar Panel Mathematical Modeling Using Simulink. *International Journal of Engineering and Research Applications*, ISSN : 2248-9622, 4(5), 67-72. Retrieved January 11, 2024
- Sharma, N. K., Gaur, M., & Malvi, C. (2021). Application of phase change materials for cooling of solar photovoltaic panels: A review. *Materials Today: Proceedings*, 47(19), pp. 6759-6765. doi:<https://doi.org/10.1016/j.matpr.2021.05.127>
- Shen, L., Li, Z., & Ma, T. (2020). Analysis of the power loss and quantification of the energy distribution in PV module. *Applied Energy*, 260. doi:<https://doi.org/10.1016/j.apenergy.2019.114333>

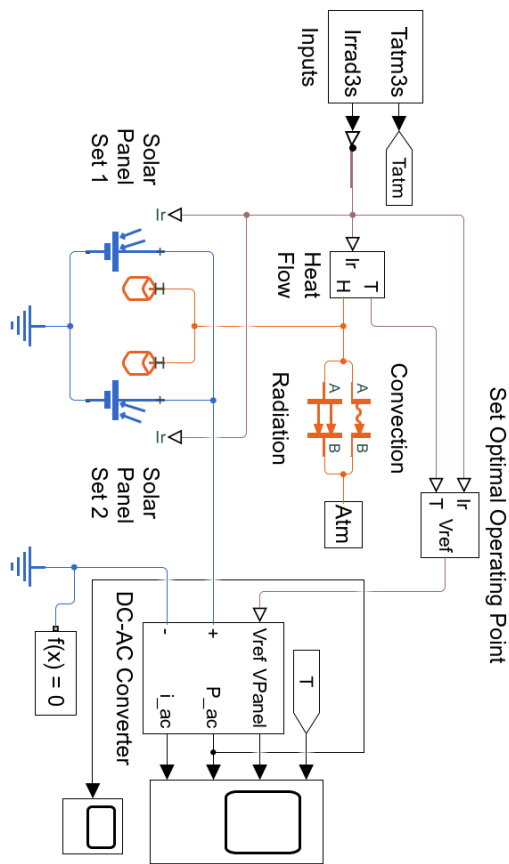
- Shimura, S., Herrero, R., Zuffo, M. K., & Grimoni, J. A. (2016). Production costs estimation in photovoltaic power plants using reliability. *Solar Energy*, *133*, pp. 294-304. doi:<https://doi.org/10.1016/j.solener.2016.03.070>
- Singh, A., Umakanth, V., Tyagi, N., Baghel, A. K., & Kumar, S. (2023). Comparative study of commercial crystalline solar cells. *Results in Optics*, *11*. doi:<https://doi.org/10.1016/j.rio.2023.100379>
- Soga, T. (2006). Chapter 1 - Fundamentals of Solar Cell. In T. Soga, *Nanostructured Materials for Solar Energy Conversion* (pp. 3-43). doi:<https://doi.org/10.1016/B978-044452844-5/50002-0>
- Streicher, W. (2001). Minimising the risk of water hammer and other problems at the beginning of stagnation of solar thermal plants — a theoretical approach. *Solar Energy*, *69*(6), pp. 187-196. doi:[https://doi.org/10.1016/S0038-092X\(01\)00018-4](https://doi.org/10.1016/S0038-092X(01)00018-4)
- Summ, T., Oyinlola, M., Khattak, S., Trinkl, C., & Zörner, W. (2024). Statistical analysis of solar thermal collectors in the Solar Keymark Database. *Sustainable Energy Technologies and Assessments*, *61*. doi:<https://doi.org/10.1016/j.seta.2023.103581>
- Sun, V., Asanakham, A., Deethayat, T., & Kiatsiriroat, T. (2020). A new method for evaluating nominal operating cell temperature (NOCT) of unglazed photovoltaic thermal module. *Energy Reports*, *6*, 1029-1042. doi:<https://doi.org/10.1016/j.egy.2020.04.026>
- Sweco AB. (2024). *About us*. Retrieved January 8, 2024, from <https://www.swecogroup.com/about-us/>
- Tackley, P. (2015). 7.12 - Mantle Geochemical Geodynamics. In G. Schubert, *Treatise on Geophysics* (pp. 521-585). Elsevier. doi:<https://doi.org/10.1016/B978-0-444-53802-4.00134-2>
- Terashima, K., Sato, H., & Ikaga, T. (2020). Development of an environmentally friendly PV/T solar panel. *Solar Energy*, *199*, 510-520. doi:<https://doi.org/10.1016/j.solener.2020.02.051>

- U.S. Energy Information Administration. (2023). Energy Institute - Statistical Review of World Energy (2023). Retrieved January 8, 2024, from <https://ourworldindata.org/energy-production-consumption>
- United Nations. (2023). First global stocktake. *Conference of the Parties serving as the meeting, Fifth session*, (p. 21). Retrieved January 4, 2024, from <https://unfccc.int/news/cop28-agreement-signals-beginning-of-the-end-of-the-fossil-fuel-era>
- Venkateswari, R., & Sreejith, S. (2019). Factors influencing the efficiency of photovoltaic system. *Renewable and Sustainable Energy Reviews*, 101, 376-394. doi:<https://doi.org/10.1016/j.rser.2018.11.012>
- Verein Deutscher Ingenieure. (2013). *VDI-Wärmeatlas*. Springer Vieweg Berlin, Heidelberg. doi:<https://doi.org/10.1007/978-3-642-19981-3>
- Vutukuru, R., Pegallapati, A. S., & Maddali, R. (2019). Suitability of various heat transfer fluids for high temperature solar thermal systems. *Applied Thermal Engineering*, 159. doi:<https://doi.org/10.1016/j.applthermaleng.2019.113973>
- Wasmeier, M. S., Roon, D.-I. S., & Kern, D.-I. T. (2024). European day-ahead electricity prices in 2023. FfE Munich. Retrieved March 28, 2024, from <https://www.ffe.de/en/publications/europaeische-day-ahead-strompreise-im-jahr-2023/>
- Wu, H., Grabarnik, S., Emadi, A., Graaf, G. d., & Wolffenbuttel, R. F. (2009). Characterization of thermal cross-talk in a MEMS-based thermopile detector array. *Journal of Micromechanics and Microengineering*, 7. doi:10.1088/0960-1317/19/7/074022
- Xi, Q., Long, W., & Ma, Q. (2021). Research of flat plate solar air collector in drying. *E3S Web of Conferences*. doi:10.1051/e3sconf/202124802015
- Yağan, Y., Vardar, K., & Ebeoğlu, M. (2018). Modeling and Simulation of PV Systems. *IOSR Journal of Electrical and Electronics Engineering (IOSR-JEEE)*, 01-11. doi:10.9790/1676-1302030111
- Yao, J., Liu, W., Zhao, Y., Dai, Y., Zhu, J., & Novakovic, V. (2021). Two-phase flow investigation in channel design of the roll-bond cooling component for solar

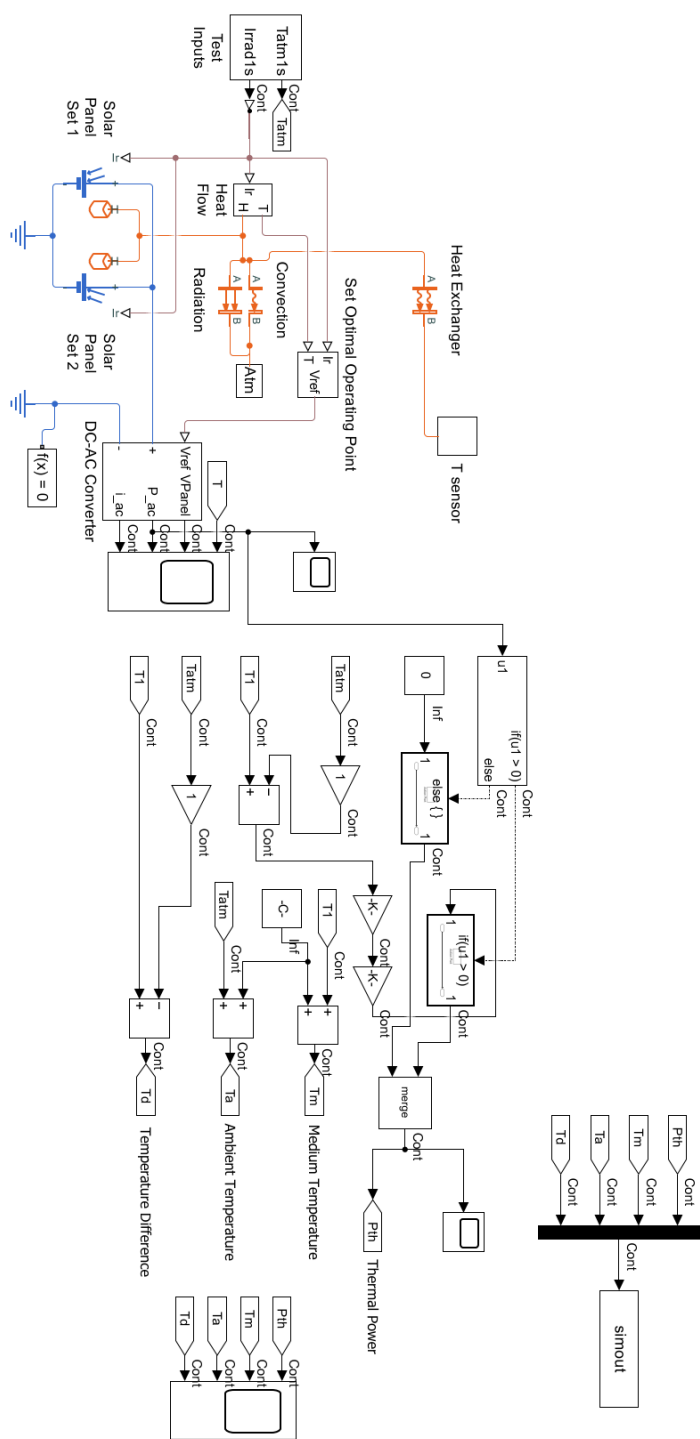
- assisted PVT heat pump application. *Energy Conversion and Management*, 235.
doi:<https://doi.org/10.1016/j.enconman.2021.113988>
- Zainal, N. A., man, A., & Yusoff, A. R. (2016). Modelling of Photovoltaic Module Using Matlab. *IOP Conference Series: Materials Science and Engineering* 114 (2016) 012137. IOP. doi:[doi:10.1088/1757-899X/114/1/012137](https://doi.org/10.1088/1757-899X/114/1/012137)
- Zhang, J., & Zhu, T. (2022). Systematic review of solar air collector technologies: Performance evaluation, structure design and application analysis. *Sustainable Energy Technologies and Assessments*, 54.
doi:<https://doi.org/10.1016/j.seta.2022.102885>
- Zongxiang, L., Haibo, L., Ying, Q., Le, X., & Chanan, S. (2024). Chapter 18 - Multitemporal-spatial-scale flexibility to improve renewable energy accommodation. In L. Zongxiang, L. Haibo, Q. Ying, X. Le, & S. Chanan, *Power System Flexibility* (pp. 251-261). Academic Press. doi:<https://doi.org/10.1016/B978-0-323-99517-7.00024-5>

Appendices

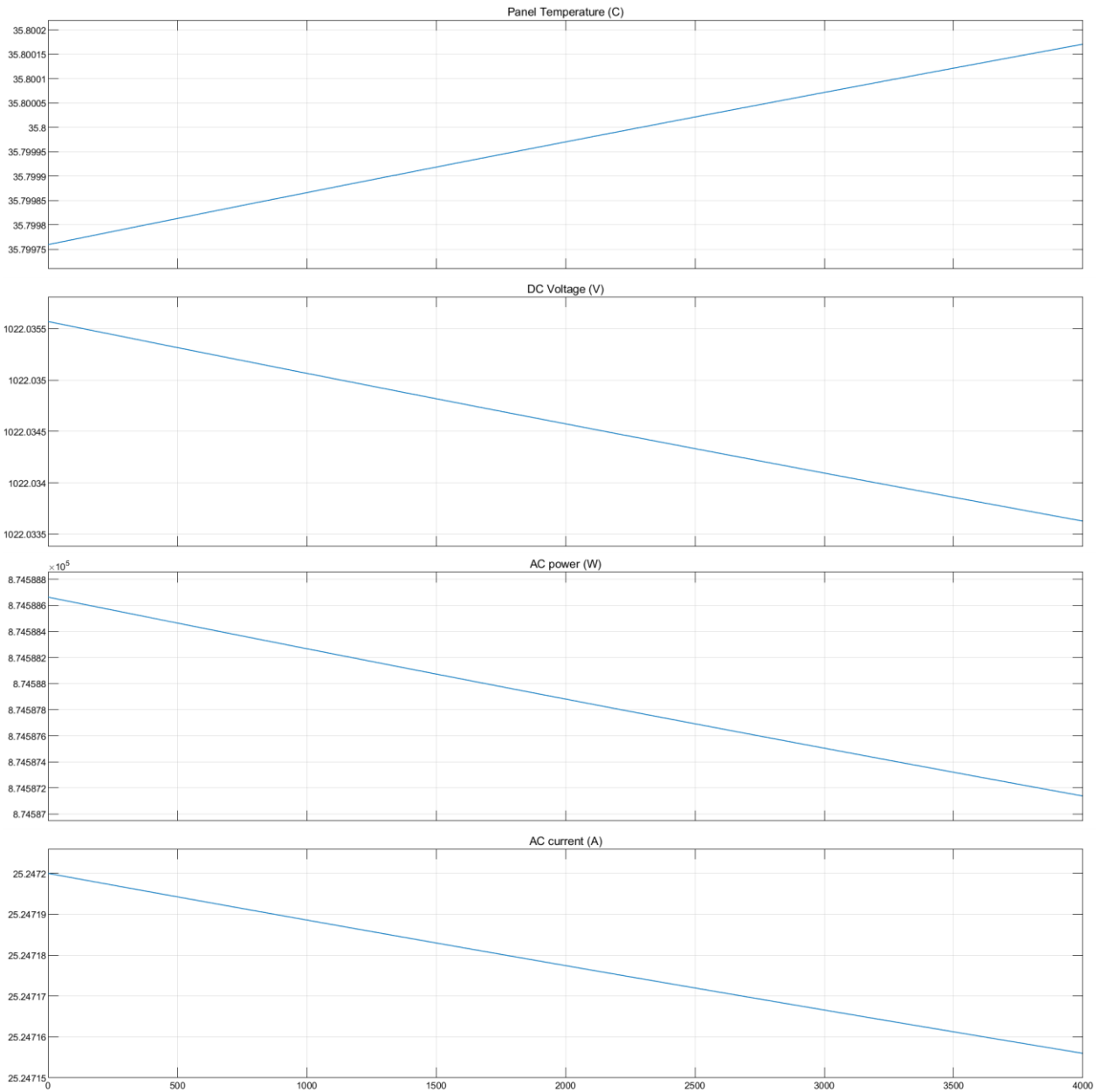
Appendix 1. PV Simulation Model



Appendix 2. PVT Simulation Model



Appendix 3. PVT Simulation Electrical Power Test Results



Appendix 4. PVT Simulation Thermal Power and Quantities Test Results

